

AN APPLICATION OF CLIMATOLOGICAL WATER BALANCE
MODELING TO DENDROCLIMATOLOGY
IN THE BLACK HILLS OF SOUTH DAKOTA

by
Wanmei Ni

A Thesis Submitted to the Faculty of the
SCHOOL OF RENEWABLE NATURAL RESOURCES
In Partial Fulfillment of the Requirements
For the Degree of
MASTER OF SCIENCE
WITH MAJOR IN WATERSHED MANAGEMENT
In the Graduate College
THE UNIVERSITY OF ARIZONA

1 9 9 3

STATEMENT BY AUTHOR

This thesis has been submitted in partial fulfillment of requirements for an advanced degree at The University of Arizona and is deposited in the University Library to be made available to borrowers under rules of the Library.

Brief quotations from this thesis are allowable without special permission, provided that accurate acknowledgement of source is made. Request for permission for extended quotation from or reproduction of this manuscript in whole or in part may be granted by the head of the major department or the Dean of the Graduate College when in his judgment the proposed use of the material is in the interests of scholarship. In all other instance, however, permission must be obtained from the author.

SIGNED: 

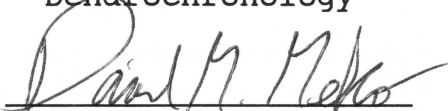
APPROVAL BY THESIS DIRECTOR

This thesis has been approved on the date shown below:



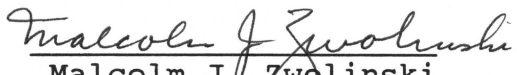
Thomas W. Swetnam
Assistant Professor
Dendrochronology

Aug. 31, 1993
Date



David M. Meko
Adjunct Assistant Professor
Dendrohydrology

Aug 31, 1993
Date



Malcolm J. Zwolinski
Professor of Renewable
Natural Resources

Aug. 31, 1993
Date

ACKNOWLEDGEMENTS

The author wishes to thank his thesis advisor Dr. David M. Meko for his very helpful directions and advice throughout this project. Part of funding for this thesis was provided by the National Science Foundation, Division of Atmospheric Sciences, under Grant ATM 9017155.

During the course of the project, Mr. Thomas P. Harlan very kindly taught dendrochronological methods and helped on sample cross-dating. Thanks to Mr. Richard Holmes for providing computer programs and to Mr. Robert G. Lofgren, who helped greatly in climatic data retrieval and computer programming. Thanks to Dr. Akio Tsuchiya for the advice on water balance modeling. Thanks to fellow students Mr. Nabil Shbouki, Mr. Anthony C. Caprio, Miss Shao Xuemei and Mr. Henri Grissino-Mayer, who gave a lot of valuable help and provided information and advice during the study.

Committee members Dr. Thomas W. Swetnam and Dr. Malcolm J. Zwolinski are acknowledged for their advice and help in the preparation of the final draft of this thesis. I am very indebted to Mr. William R. Boggess for his extremely valuable guidance and editorial advice.

Thanks to Carolyn Hull Sieg and Shelly Deisch, of the Rocky Mountain Forest and Range Experiment Station, for the field collection of tree-ring specimens.

The main climatic data was collected with the help of Mr. Matthew J. Bunkers and Mr. James R. Miller Jr. of the South Dakota School of Mines.

The author also wishes to thank Prof. Malcolm K. Hughes, Prof. Charles W. Stockton and the L. L. Foundation, who provided the chance for starting this research in dendroclimatology and dendrohydrology.

TABLE OF CONTENTS

LIST OF TABLES	6
LIST OF ILLUSTRATIONS	9
ABSTRACT	10
1. INTRODUCTION	11
2. DESCRIPTION OF PROJECT	18
§2.1 Physiography	
§2.2 Climate	
§2.3 Vegetation	
3. DATA COLLECTION AND TREATMENT	26
§3.1 Climatic and environmental data	
A. Estimating missing records	
B. Testing homogeneity	
C. Comparing data from different sources	
§3.2 Developing tree-ring chronologies	
4. STATISTICAL PROPERTIES OF THE RELATIONSHIP BETWEEN TREE GROWTH AND TRADITIONAL CLIMATE VARIABLES	47
§4.1 Correlation analysis	
§4.2 Outlier analysis	
§4.3 Factor analysis and data grouping	
§4.4 Running correlation analysis	

5. SOIL MOISTURE SIMULATION AND SEARCH FOR BEST CANDIDATE FOR CLIMATE RECONSTRUCTION	79
§5.1 SNWBAL model	
§5.2 Characteristics analysis of the model	
A. Sensitivity analysis of PENSEL and SNWBAL models	
B. Correlation field analysis of \bar{w}	
§5.3 Running correlation analysis of \bar{w}	
§5.4 Coherence analysis	
§5.5 Response function analysis	
§5.6 Conclusions and suggestions	
APPENDIX I Penman Formula Calculation	127
APPENDIX II Tree-ring Sample Site Name List	133
LIST OF REFERENCES	134

LIST OF TABLES

3.1	Climate Stations -- Original Data	28
3.2	Climate Records -- HCN Data	29
3.3	Climate Records -- NDA Data	29
3.4	Normal Period for Climate Data	34
3.5	Information on Tree-Ring Sites	37
3.6	Cross-Dating and Measuring Statistics (List of COFECHA Results)	39
3.7	Summary of Chronology Statistics (List of ARSTAN Results)	43
3.8	Comparison of COFECHA Statistics for New Chronology REN with Statistics for earlier chronologies	45
3.9	Correlation Coefficients of New Pine Chronologies with Earlier Collections	46
4.1	Correlation of Monthly Precipitation with Tree-ring Chronologies	49
4.2	Correlation Coefficients of Chronologies with PPT for previous September Through Current August	52
4.3	Outlier-Year Numbers	63
4.4	Chronology Group by Factor Analysis	71
4.5	PPT Group by Factor Analysis	72
4.6	Correlation Coefficients Among DQUART Rotation Factors	72
5.1	Process of PENSEL and SNWBAL modeling	80
5.2	Sensitivity Test for Main Input Factors of model PENSEL	91
5.3	Sensitivity Test of SNWBAL Model	94

5.4	Low-pass Filter Weights	106
5.5	Correlation Coefficients of Tree-ring Chronologies with Seasonal PDSI (April -- July)	113
5.6	Correlation Coefficients of Two Chronologies with Climate Parameters	114
5.7	Comparison of Variable Selection in Response Function (grouped)	119
5.8	Comparison of Variable Selection in Response Function (separated)	121

LIST OF ILLUSTRATIONS

2-1.	Map of Northern Great Plains Showing Location of Study Area	19
2-2.	Monthly Temperature Departure at Rapid City, During 1900-1990	22
2-3.	Monthly Precipitation at Rapid City	24
3-1.	Climate Stations in the Study Area	27
3-2.	Comparison of Different Data Sources	32
3-3.	Tree-ring Sample Sites in the Black Hills Area	36
3-4.	Tree-ring Chronologies Used in the Study	44
4-1.	Correlation Analysis of Tree-Ring Chronologies and Temperature Departures(April-July)	54
4-2.	Correlation Analysis of Tree-Ring Chronology and Precipitation Departures(April-July)	55
4-3.	Scatter Plot of Tree-ring Chronologies with Temperature and Precipitation	64
4-4.	Number of Outlier-years Counted from All Linear Correlation Analysis In the Black Hills Area Using All Available Tree-ring Chronologies and Climatic Records	64
4-5.	Comparison of Outlier-year Numbers	65
4-6.	Climate Pattern In Favorable Growth Year 1935	65
4-7.	Climate Pattern In Severe Dry Year 1934 ..	66
4-8.	Climate Pattern In Severe Dry Year 1939 ..	66
4-9.	Climate Pattern In Outlier Year 1932	67

4-10.	Climate Pattern In Outlier Year 1985	67
4-11.	Monthly Climate Variables In Key Years ...	68
4-12.	Running Correlation Between Pine and Oak at the Same Sample Site	77
4-13.	Running Standard Deviation of Oak and Pine, with 5-year Window	77
4-14.	Running Standard Deviation of Oak and Pine, with 23-year Window	77
5-1.	Precipitation Distribution at Rapid City and Hot Springs	88
5-2.	Correlation Field of Soil Moisture \bar{w} with Precipitation, at Rapid City	100
5-3.	Correlation Field of Soil Moisture \bar{w} with Temperature, at Rapid City	100
5-4.	Running Correlation of \bar{w} with Oak and pine Tree-ring Chronologies (Four plots)	102
5-5.	Frequency Response of Designed Filters ...	107
5-6.	Coherence Analysis of Oak-Pine on the Base of Factor Score and Site Chronology ..	107
5-7.	Cross-spectral Analysis of Tree-ring Chronologies with PPT and TMP	108
5-8.	Cross-spectral Analysis of Tree-ring Chronologies with \bar{w}	110
5-9.	Comparison of Response Function Analysis on Different Variable Combinations (P_a) ..	116
5-10.	Comparison of Response Functions for Different Variable Combinations (GCE)	117
5-11.	Comparison of Response Functions for Different Variable Combinations (REN)	118
5-12.	Response Function Results of MRL	123

ABSTRACT

Tree-ring data from bur oak (Quercus macrocarpa) and ponderosa pine (Pinus ponderosa) were used to investigate the relationship between annual ring width and soil moisture in the Black Hills area of western South Dakota and eastern Wyoming. Soil moisture values were developed from a water balance model (SNWBAL), using climate data from weather stations in the area.

The response between the tree-ring chronologies and climate and water-balance variables shows a strong relation between annual ring growth and precipitation and soil moisture. The best variable combinations for reconstructing the local drought history were identified from this analysis.

Several statistical approaches were used to check the internal consistency of the data and to determine the relationship between the various data sets.

A scenario for further study, especially for the reconstruction of past climate variables was drawn based on the results of response analysis.

Chapter I.

INTRODUCTION

Development in the Great Plains of the United States, from the present into next century is related to the availability of water from both surface and groundwater systems. As population grows, water demand will increase dramatically. As in many places of the world today, reasonable management and use of available water resources is a vital issue for the Great Plains.

Tree rings indicate that from 1750 to 1964 the Great Plains experienced extensive droughts near 1756, 1820, 1862, 1934 and 1956 (Meko, 1992). The climatic and historical records for Rapid City, South Dakota, show that the Black Hills area has shared similar drought events (Miller, 1986). Are these droughts a periodic event in the Great Plains, or are they related only to random climate variation? What is the probability of drought occurrence during the past hundred years? How often do droughts occur, and what is the probability of severe drought in the future? Based on our present knowledge, it is difficult to provide a clear answer to these questions.

Many paleoclimatic approaches have been used to investigate the occurrence and effect of drought on earth's ecosystem. These include analysis of tree rings, ice cores, pollen profiles, and geomorphology. Some methods, such as pollen analysis and geomorphologic analog, are less precise than others because they focus on time scales of decades to thousands of years or more. While these methods can detect trends of environmental change measured in hundreds or thousands of years, they lack high resolution for decadal, annual, or seasonal variations. Despite accurate dating and precise chemical analysis, ice core studies are confined to high elevation and high latitude locations. Also, the expense involved in such studies generally limits their wide use. In contrast, dendrochronological methods provide an efficient way to study climate and environmental variations with high resolution and reasonable cost. The time period covered by tree-ring studies is considerably shorter than that by the methods discussed above and tree-ring studies are best done in areas where the environmental factors of interest limit tree growth (Fritts, 1976; Fritts and Swetnam, 1989, Baumgartner et al, 1989).

Until quite recently, only limited dendrochronological work had been done in the Black Hills. Records from the International Tree-Ring Data Bank (ITRDB) show that from the

late 1950s to the late 1960s, H.E. Weakly developed five juniper (Juniperus, spp) chronologies collected in the Missouri River Basin of South Dakota. In the early 1960's, Harold C. Fritts (HCF) worked on ponderosa pine chronologies from the boundary of South Dakota and Nebraska. In the early 1980's the research group led by Charles W. Stockton (CWS) developed two ponderosa pine chronologies near the Black Hills.

The Black Hills are part of the Great Plains region and considerably more work has been done in that large region using some of the methods mentioned above. Some of the more significant studies are those of Thomas (1962), Borchert (1971), and Perry (1980), who analyzed climatic records and found a rhythmic return of drought in the Great Plains at about 20-year intervals. Mitchell, Stockton and Meko (1979) discussed the evidence for a 22-year cycle in drought area from tree-ring chronologies in the western United states, and found a weak phase link between reconstructed drought and the Hale solar cycle.

Oladipo (1987) studied the power spectra and coherence of precipitation from 407 climate stations and concluded that there is no evidence of periodicity in drought in the Great Plains. Currie (1981,1989) found that there are 18.6-year

and 11-year drought rhythms in the Great Plains and claimed out that Oladipo's failure to find periodicity was due to inappropriate methodology. Using tree-ring chronologies developed from 58 sites from the fringes of the Great Plains, Meko (1992) found no clear evidence for a 22-year or 18.6 drought cycle. Also the historic 'dust bowl' drought in the early 1930s, which is unique in the long-term history, was less persistent over several years than some earlier droughts. Thus, based on Meko's results, which included a much wider data base than previous studies, there is no tree-ring evidence for a rhythmic occurrence of drought in the Great Plains during the period of 1750-1964.

The lack of periodicity in drought does not mean that knowledge of drought history is unimportant. Since the first settlement of the Black Hills in 1870s, the local environment has shifted from forest land to pasture and farms. Even a moderate drought may bring a huge loss to the farmers and local economy. Studying drought and understanding the history of drought in the Great Plains remains a vital issue for both scientific research and local economic development of the Black Hills area.

The main objective of this paper is to use newly developed tree-ring chronologies of bur oak (Quercus

macrocarpa) and ponderosa pine (Pinus ponderosa) from the Black Hills to investigate the relationship of tree-ring growth to the water balance, and to find the appropriate candidate variables for reconstructing local drought history from the tree-ring chronologies.

Since the 1950s, following the pioneering research of A.E. Douglass (1914) and Edmund Schulman (1951), a number of studies have successfully used tree-ring chronologies, along with environmental information, to analyze the relationship between tree-ring growth and climatic variables, such as precipitation and temperature (Fritts, 1976; Hughes et al, 1982, Schweigruher, 1988; Fritts, 1991). The conventional methods for dealing with tree-ring growth and climate variation have largely focused on the relations between these variables, or combined variables such as Palmer Drought Severity Index (PDSI) (Palmer, 1965). Many researchers have pointed out that tree-ring growth responds to various environmental, physiological, and genetic factors acting on trees at different stages of the growing season. Therefore, there is no simple way to explain tree-ring growth based on a single factor. Even the most successful climate reconstructions have many 'unexplained variations', which may not be just a noise component but worthwhile environmental signals that probably could be restored by some appropriate

techniques.

One goal of this study is to investigate the value of climatological water balance modeling for reducing the unexplained variation in tree rings from the Black Hills by more concisely expressing the drought signal in tree rings. To achieve this goal, the strength of the relationship between tree-rings and traditional climate variables (e.g., precipitation, temperature) will be compared with the strength of the relationship between tree-rings and secondary drought variables (e.g., soil moisture) output from a climatological water balance model.

Previous dendrochronological studies in the Black Hills area concentrated on ponderosa pine and its growth dependence on local climate. Schulman (1956) studied the relationship of chronologies from Douglas-fir (Pseudotsuga menziesii) and limber pine (Pinus flexilis) to precipitation records in the Missouri River Basin and found a very high correlation with annual precipitation. For the period 1896 to 1950, the correlation coefficient was as high as 0.45 to 0.67. Partial- correlation analysis of ponderosa pine chronologies from the western Great Plains shows that growth in ponderosa pine is well related to total annual precipitation (Stockton and Meko, 1983).

Bur oak has not been previously used as a sample species for dendrochronological work in the Black Hills. Research in North America and Europe has shown that various oak species have considerable potential for dendroclimatological studies. The growth response of oak species to climate is generally strong and the growth pattern is relatively stable with few missing rings (Eckstein,1982; Cook,1982). Will (1946) reported a relationship between major drought and growth variations of bur oak from near Bismarck, North Dakota. Lawson (1978) found that bur oak from eastern Nebraska cross-dated and that growth variation was highly correlated with local climate data. Blasing and Duvick (1981) found a strong signal for annual precipitation in white oak (Quercus alba) chronologies from Iowa.

The study uses various statistical methods, such as general correlation analysis, correlation field analysis, factor analysis, spectra analysis and response function analysis, to examine the drought signal in a newly developed set of bur oak and ponderosa pine chronologies from the Black Hills. From these analysis the best combination of tree-ring chronologies and climate variables is identified for the further study.

CHAPTER 2 DESCRIPTION OF PROJECT

§2.1 Physiography

The Black Hills are located in the northwestern quarter of the Great Plains, within the boundaries of 101°W to 104°W longitude and 43°N to 45°N latitude. Most of the region is in the western part of South Dakota with a smaller portion in the northeastern corner of Wyoming (Fig.2-1). The area is characterized by its high mountains. The highest elevation, 7,595 ft above sea level, is in northern part of the Black Hills, about 35 miles south of Spearfish.

Rising from the eastern edge of the rolling plains, the Black Hills form a unique physiographic feature between the Rocky Mountains and the Great Plains.

The high mountains are composed of igneous rocks and the lower elevations of limestone with smooth topography. Valleys are filled with Quaternary alluvium and weathering debris from ridges.

The parent soil material of the Black Hills area was laid down in past ages by glaciers, water and wind. The more

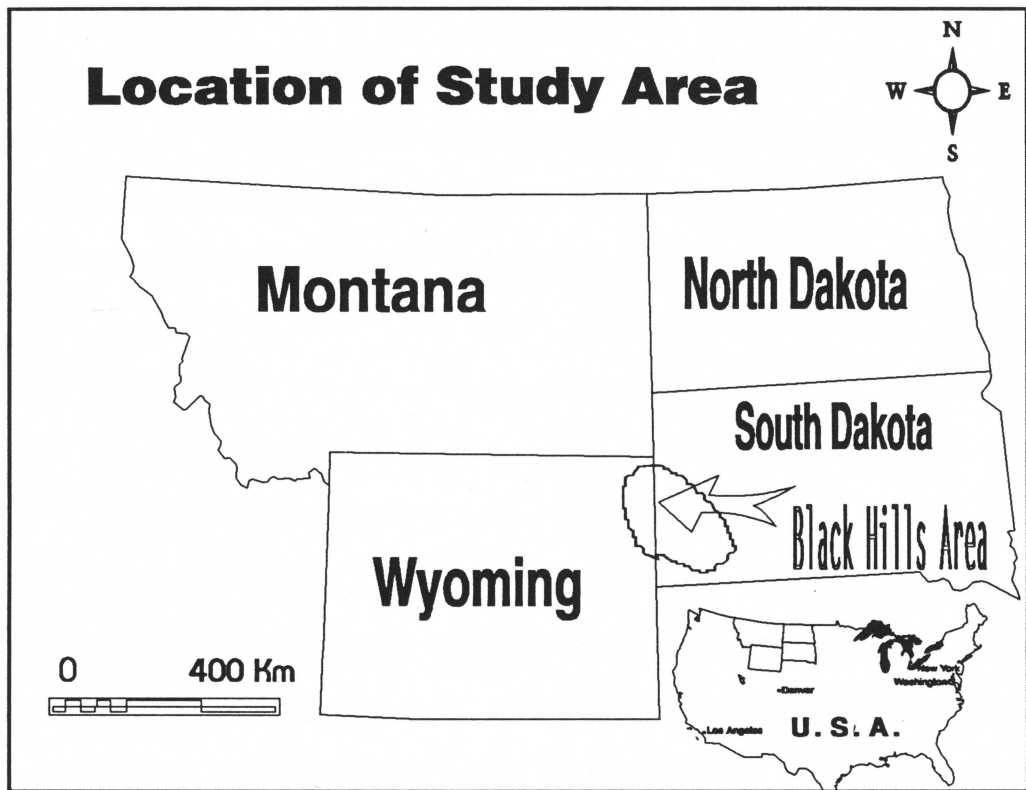


Figure 2-1. Map of Northern Great Plains showing location of study area

rugged terrain has been developed for livestock grazing. The lower elevations with relatively gentle topography have been used for irrigated agriculture for more than a hundred years.

The northern part of the Black Hills has more abundant annual rainfall and better growth conditions than the southern part. Like other parts of the Great Plains, the Black Hills suffered severe drought and great dust storms in the 1930s 'Dust Bowl' (Lawson & Baker, 1981).

§2.2 Climate

The Black Hills share some of the climatic characteristics of the much larger semi-arid to arid region of the Great Plains. There are, however, differences because the Black Hills are higher than surrounding parts of the Great Plains. Climate records show that sunshine is abundant, with the percentage of maximum annual sunshine hours at Rapid City averaging 54% in winter and 60-73.5% over most other months of the year. The long term average relative humidity oscillates around 40% in May, July, August and September. In other months it is much higher, around 50-70%. The spring-summer combination of low relative humidity and abundant sunshine results in a high potential

evapotranspiration rate. These details will be discussed later in the Penman model calculation of Appendix I.

Monthly mean temperature in the Black Hills area ranges from 6°F in winter to 73°F in summer as measured at Rapid City, and the monthly temperature departure varies greatly in winter-spring during 1900-1990 (Fig 2-2). There is an obvious seasonal variation, but the regional variation is not great. From climate records of 31 stations, it seems that the whole Black Hills area has had the same climate variation trend throughout the period of record. The average correlation among all stations is 0.80 for monthly mean temperature and about 0.60 for monthly precipitation.

Precipitation in the Black Hills is unevenly distributed in space and time. The highest precipitation is concentrated in the north near Spearfish with another center near Edgemont and Oelrichs in the south. The wet center shifts toward the northeast during the winter. Precipitation is also very unevenly distributed within the year: in the spring-summer season (Apr-Aug), the percentage of annual precipitation is 71.3% for Rapid City and 68.9% for Hot Springs. According to Miller (1986), the regional climate regime is characterized by summer thunderstorms which produce a large portion of the summer precipitation. From April to August, moist air moves



Fig 2-2. Monthly temperature departure at Rapid City during 1900-1990. The top line in the box in the position for 1991 represents normal conditions.

from the southeast towards the Rocky Mountains. Moisture condenses from the ascending current at the higher elevations of the Black Hills and reaches the ground as rainfall. The monthly precipitation from 1900 to 1990 is plotted in Figure 2-3.

Historical records show that many of the main droughts in the Black Hills occurred during spring and summer, and were characterized by low soil moisture in the growing season. The plots for 1934 and 1936 illustrate failure of spring and summer precipitation.

The climate conditions of the Black Hills in winter result from arctic air masses moving from north to south over the area. Snowfall is normally light; the highest mean monthly snowfall on record was 2.69 inches in March. On the average, total snowfall is only about 14.3% of the annual precipitation. A mid-winter warming forms the so called 'banana belt' on the eastern slopes of the Black Hills (Miller, 1986). In the spring, temperatures are generally unsettled; spring snows may occur in May or even in June.

Summer in the Black Hills is usually warm, and most summer precipitation comes from thunderstorms. There is very little rainfall in the autumn, and snow may occur as early as

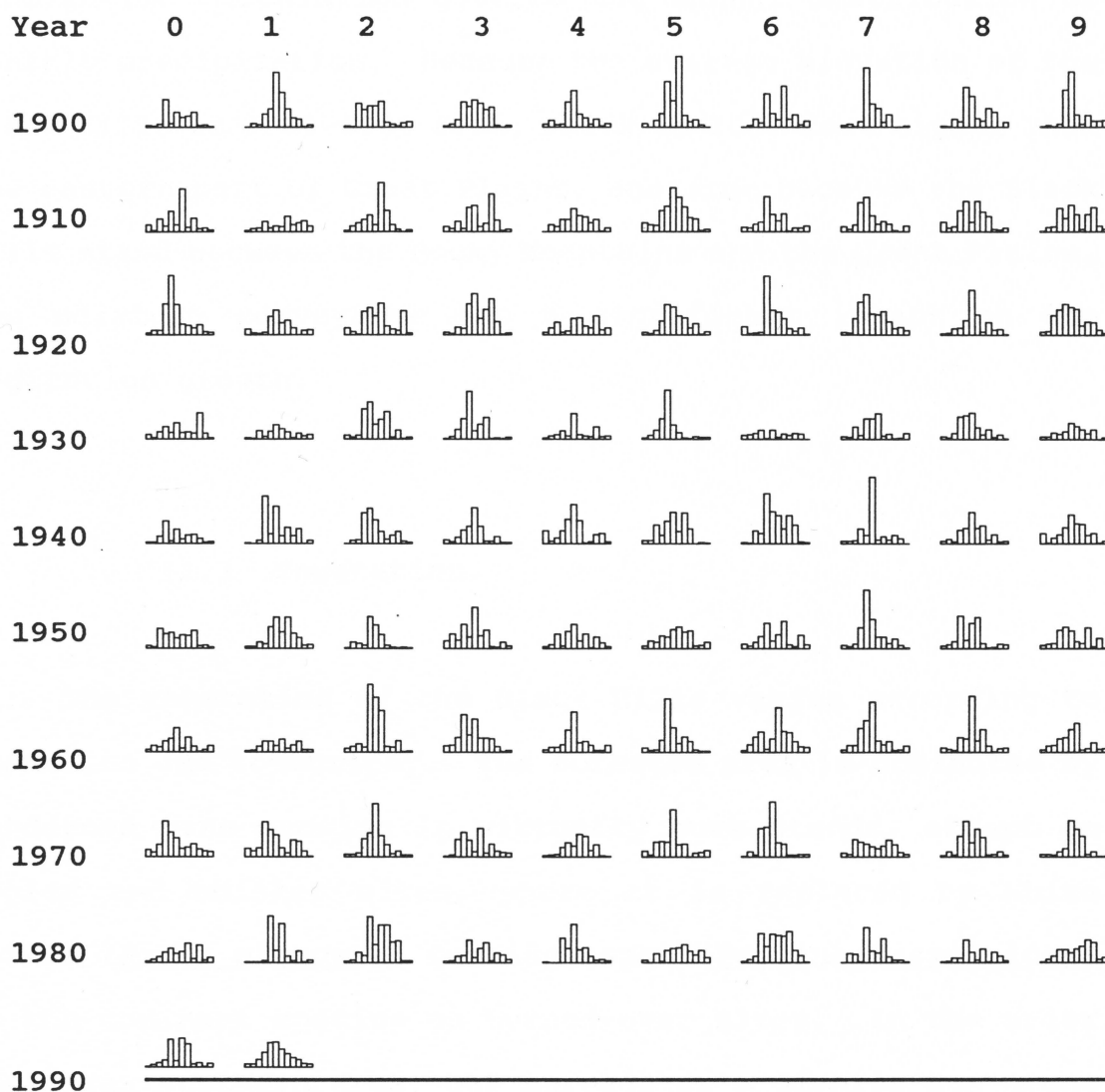


Fig 2-3. Monthly precipitation at Rapid City

Total record is from 1900 to 1990. The 50-year mean monthly precipitation is plotted on the position of 1991. Apr-Aug is the main season of ppt. The lowest monthly ppt occurrences in the Apr-Aug season are: Apr 1984: 0.04; May 1936: 0.09.

The highest occurrences are: Apr 1941: 6.47; May 1962: 9.21.

Driest year was 1936: 7.51; wettest year was 1962: 28.89.

The highest monthly ppt occurred in July 1905: 9.66 inches.

September. During spring and summer, a south to north atmospheric circulation governs the annual distribution of monthly precipitation. Because the average elevation of the Black Hills is 5000-6000 feet, which is 2000 feet higher than the eastern part of Great Plains, and also because the Black Hills stand between the Rocky Mountains and the Great Plains, the moisture conveyance has a significant impact on the vegetation growth.

§2.3 Vegetation

The vegetation of the Black Hills varies according to elevation and topography. The forested area is dominated by ponderosa pine growing in virtually pure stands, except on cooler and moister sites, where it is replaced by White Spruce (Picea glauca). Quaking Aspen (Populus tremuloides) is the dominant species on burned-over sites. In the drier and lower southern area, oak spreads as a diverse age group or as isolated trees. Most tree-ring samples from this study were collected from sites at high elevations.

Chapter 3. DATA COLLECTION AND TREATMENT

§3.1. Climate data

Climate data for this study were obtained from various sources. Monthly precipitation and temperature data for numerous stations were provided by Matthew J. Bunkers at the Department of Meteorology of the South Dakota School of Mines, Rapid City, South Dakota. This data is referred to as the "original" data. Two subsets of monthly precipitation and temperature data adjusted specifically for application to historical studies were also used. The first is the Historical Climate Network (HCN) data set (Karl et al 1990), obtained from computer files at the Tree-ring Laboratory (TRL) at the University of Arizona. The second is the National Drought Atlas (NDA) data set (Willeke et al, 1991), obtained also from files at TRL. Palmer Drought Severity Index (PDSI) was also included in the NDA data set.

Monthly wind speed, relative humidity, and other data needed for the Penman-method computation of potential evapotranspiration were obtained from Miller (1986) and other wind speed records from the publication "Monthly Local Climatological Data" (NOAA). All climate stations used in this study are plotted in Figure 3-1.

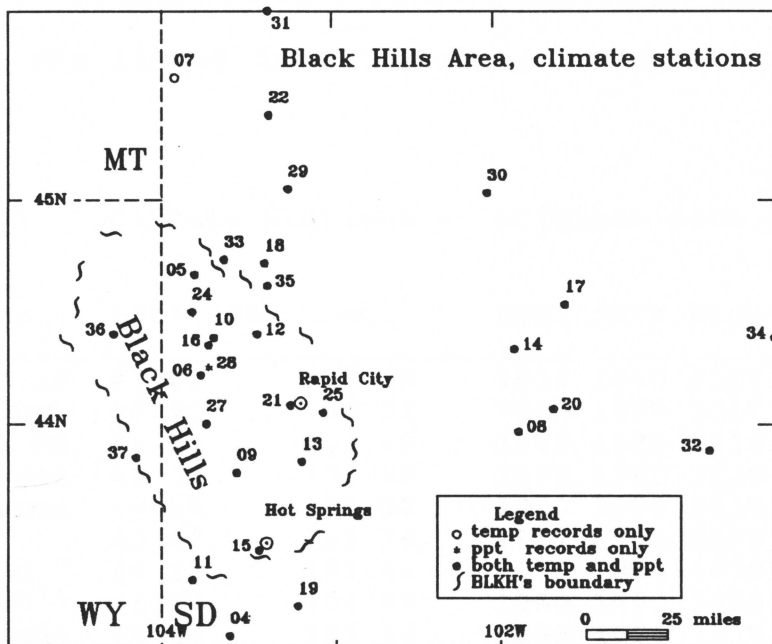


Figure 3-1. Climate stations in study area.

Identifying information on the stations in the 'original', HCN and NDA data sets is listed in Table 3.1, 3.2 and 3.3. The listed data include years with some missing data.

Table 3.1 Climate Stations -- original data

ID	St. Name	Latitude	Long.	BgYr	EdYr	Elev	CID#
04	Ardmore 2N	43 03	103 39	1914	1990	3550	39023605
05	Bell Four.	44 40	103 51	1909	1990	3017	39055901
06	Buskala Ra.	44 13	103 49	1948	1982	6110	39124604
07	Camp Crook	45 33	103 58	1896	1990	3120	39129401
08	Cottonwood	43 58	101 52	1910	1990	2414	39197205
09	Custer	43 47	103 36	1912	1990	5480	39208704
10	Deadwood	44 23	103 44	1910	1990	4670	39220704
11	Edgemont	43 18	104 49	1980	1990	3460	39255705
12	Fort Meade	44 24	103 28	1898	1990	3330	39306905
13	Hermosa	43 50	103 12	1906	1990	3291	39377504
14	Hill Land	44 20	101 53	1949	1990	2530	39385705
15	Hot Springs	43 26	103 28	1908	1990	3560	39400704
16	Lead	44 21	103 46	1909	1990	5350	39483404
17	Milesvill	44 32	101 34	1949	1990	2220	39554401
18	Newell	44 43	103 25	1908	1990	2860	39605401
19	Oelrichs	43 11	103 14	1891	1990	3340	39621205
20	Phillip 2N	44 04	101 39	1948	1990	2241	39655205
22	Redig	45 23	103 23	1915	1990	3070	39706201
24	Spearfish	44 30	103 52	1898	1990	3640	39788204
25	Rapid City	44 03	103 04	1888	1990	3165	39694705
27	Deer Field	44 00	103 47	1931	1990	6060	39223104
28	Dumont 2 EN	44 15	103 46	1910	1969	6140	39240904
29	Dupree	45 03	103 16	1922	1990	2370	39242901
30	Faith	45 02	102 02	1927	1990	2570	39285201
31	Ludlow	45 51	103 23	1924	1990	3050	39504801
32	Murdo	43 53	100 42	1908	1990	2320	39580106
33	Orman Dam	44 44	103 40	1907	1974	2933	39635701
34	Pierre	44 23	100 17	1893	1990	1726	39659706
35	Vale	44 37	103 24	1909	1978	2773	39855201
36	Sundance WY	44 24	104 21	1916	1990	1800	
37	Newcastl WY	43 51	104 13	1907	1990	4315	

Table 3.2 Climate Records -- HCN Data

ID	Sta. Name	Latitude	Longitude	Years	Elev.
4007	HOT SPRINGS	43 26	103 28	1897-1987	3535
6947	RAPID CITY	44 5	103 16	1888-1987	3370
1905	COLONY WY	44 56	104 12	1914-1987	3570
5830	LUSK, WY	42 46	104 28	1889-1987	5020
6660	NEWCASTLE, WY	43 51	104 13	1906-1987	4315

Table 3.3 Climate Records -- NDA Data

ID	Sta. Name	Latitude	Longitude	Years	Elev.
39044007	Hot Springs	43:26	103:28	1908-1990	3535
39056947	Rapid City	44:05	103:16	1897-1990	3370
39065891	Murdo	43:53	100:43	1908-1990	2300
39066597	Pierre FAA AP	44:23	100:17	1900-1990	1726
39051872	Cottonwood	43:58	101:52	1910-1990	2414

To use the most reliable data set and at the same time provide as much information as possible, it is necessary to examine the quality of each data set. The procedure used includes handling missing records, checking homogeneity over time, and specifying the better or best data set for use in subsequent data processing.

A. Estimating the missing records

There are 24 stations whose monthly climate records have missing data. The computer program CLIFILL, written in August, 1981, by M.K. Cleaveland and then modified by Robert

Lofgren of the Tree Ring Laboratory, University of Arizona, has been used to estimate the missing monthly climate records. The main principle used in calculating the missing monthly values is to set the missing station as the predictand and the nearby stations which satisfy a pre-determined correlation threshold as the predictors in a simple regression equation. Because of the characteristics of the Black Hills, the stations in the north and south regions are grouped and estimated separately. Both groups use the same criterion for their estimations. The correlation coefficient (r) between the estimated station and another nearby station is used as the threshold for entry of variables in the regression. For temperature, the threshold was set to $r \geq 0.750$, for precipitation, to $r \geq 0.450$.

B. Homogeneity test

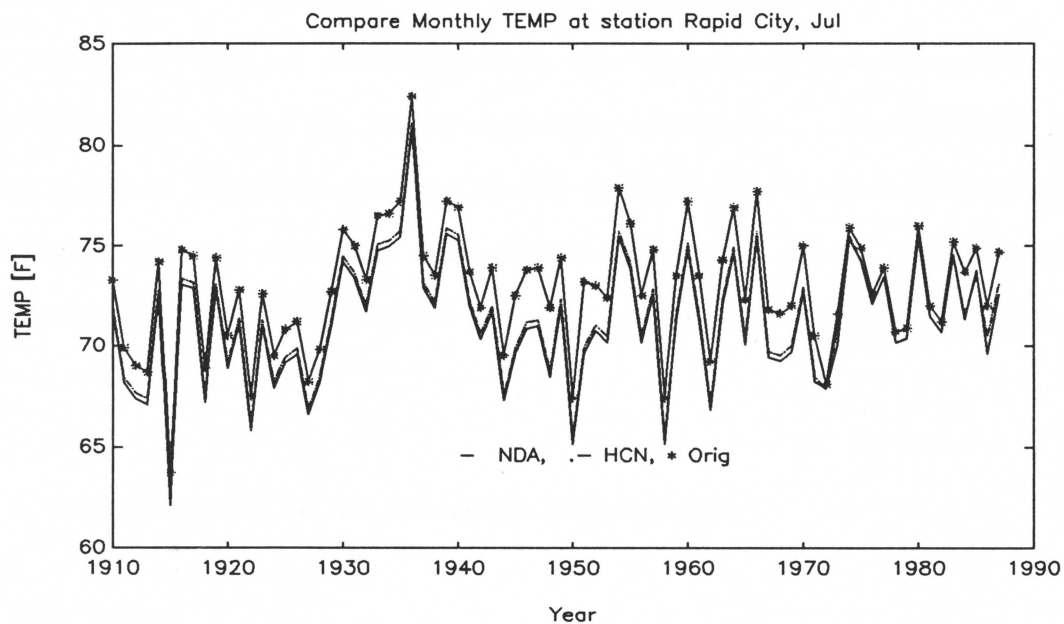
Because some climate stations changed their locations during the period of observation, it was necessary to check the homogeneity of the data set in order to reduce any artificial bias introduced into the climate time series. The double mass plot has been applied to perform the data examination.

The double mass plot is based on the assumption that under the same climate regime, if the two adjacent stations are kept in the same observation routines throughout their

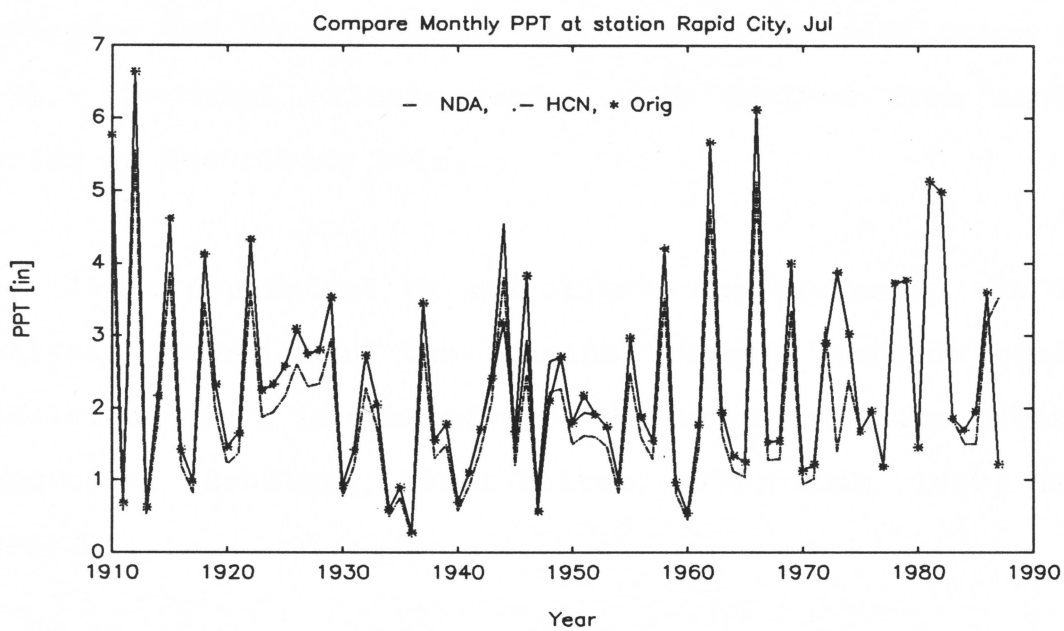
history, the accumulative values of one plotted against another will form a straight line. Some stations did not show homogeneity, such as station #13, where the location had been changed often. For other stations, such as station #11, the record was too short to be used. All other stations with problems of this kind were discarded, leaving 25 stations for use in later analysis.

C. Comparing data from different sources

Some stations have climate data in two or more networks, each of which was originally processed in different ways to handle missing data and inhomogeneity. It is important, therefore, to find the best or 'most suitable' data set for the analysis. Time series plots for July temperature and precipitation at Rapid City, which is in all three networks (original, HCN and NDA), are shown in Figure 3-2. The plots show that the HCN precipitation is lower than the original precipitation especially in 1924-1930, the early 1950s and most high-precipitation years before 1970. For temperature, both HCN and NDA data are lower than the original. The differences among these three data sets are not quite parallel through time. The comparison points out the inherent uncertainty in climate as measured by instrumental records. The differences in the plot in Fig 3.2 suggest that choice of data set might have a large bearing on results of statistical analysis (e.g.,



(a)



(b)

Figure 3-2. Comparison data in NDA, HCN and original networks.

correlation) relating tree rings to climate.

For the sake of convenience, the original data processed by CLIFILL were used in the following analysis. These data have the longest records and maintain relatively high variations in extreme values of low precipitation and high temperature, while the other data sets tended to smooth these variations.

4 Calculation of climate departures

The high elevation of the Black Hills makes the seasonal temperature change sharp. The instrumental records also emphasize the large seasonal variations in precipitation (Fig 2-3). Seasonal climate series were derived from monthly series as describing below.

It is convenient to use climate departures in the data analysis rather than the original climate records because tree-ring growth is sensitive to the departures from ordinary conditions (Schulman, 1956; Fritts, 1976; Cook, 1990; Meko, 1992).

Departures of precipitation were calculated by dividing the monthly observations by the average value for the month for a 'normal period'. The 'normal period' is defined as a

long time span during which there are few extreme anomalies. The normal period selected for the Black Hills is 1940-1990. Monthly temperature departures were derived by subtracting the 1940-1990 mean from the observations. The seasonal departure for precipitation has computed by dividing seasonal-total precipitation by the 'normal' value for the season. The seasonal departure of temperature was computed as the average of monthly departures for the season. For stations whose records did not cover the normal period, a slight adjustment was made to define the normal period (Table 3.4).

Table 3.4 Normal Period for Climate Data

Station ID #	Begin Yr	End Yr
#14,20	1950	1990
#28,33,35	1940	1969
others	1940	1990

For comparison with other seasonal methods (Graumlich, 1987, Fritts, 1976) taking into consideration the tree-growth season, an annual precipitation series for each station was formed by summing precipitation data for January to August of the current year and the previous September to December.

§3.2. DEVELOPING TREE-RING CHRONOLOGIES

Tree-ring chronologies used in this study were developed from samples collected as part of a National Science Foundation supported project, " A Dendroclimatic Study of Drought in the Northern Great Plains" (Grant No. ATM 9017155). Principal Investigators on the grant are David Meko, from the Laboratory of Tree Ring Research, University of Arizona, Carolyn Hull Sieg, from the Rocky Mountain Forest and Range Experiment Station, and Arthur DeGaetano, of the South Dakota School of Mines. Tree-ring samples were collected under the direction of Dr. Sieg.

A total of 23 chronologies have been used to build a local tree-ring data set: 16 are bur oak and the remainder are ponderosa pine. Sample locations are shown on Figure 3-3, and the site information is given in Table 3.5.

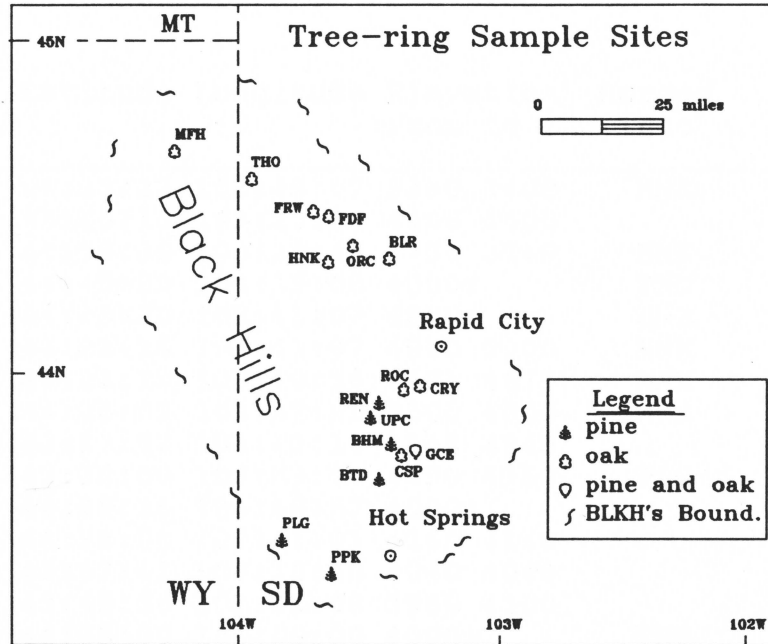


Figure 3-3. Tree-ring sample sites. MFH is merged into site THO; HNK is the combination of sites HNK, ORD, ORC, WIL, SNY and CRW. Symbols for ORD, SNY, CRW, and WIL are omitted because the sites are too close together for plotting.

Table 3.5 Information on Tree-Ring Sites

No	ID	Sp.	Latitude	Longitude	Elevation from to		Merged into ¹
01	CRW	Q	44:35:27	103:43:07	3380	3400	HNK
02	CSP	Q	43:45:15	103:23:30	4400	4400	
03	SNY	Q	44:18:30	103:26:45	3730	3740	HNK
04	MFH	Q	44:40:00	104:19:00	4000±		THO
05	HNK	Q	44:20:00	103:41:07	4800±		HNK
06	ORD	Q	44:22:15	103:41:07	4920	5000	HNK
07	ORC	Q	44:23:18	103:40:36	4671	4671	HNK
09	WIL	Q	44:26:52	103:37:55	3800	4000	HNK
10	PPK	P	43:23:52	103:41:13	4848	4848	
11	PLG	P	43:30:00	103:53:00	4450	4780	PLG
12	FDF	Q	44:28:16	104:40:57	4000±		
13	FRW	Q	44:29:06	103:41:01	4160	4160	
16	CRY	Q	43:57:41	103:18:40	4040	4040	
17	GCE	Q	43:45:56	103:21:08	3960	4100	
18	THO	Q	44:35:00	104:00:00	4000±		THO
25	ROC	Q	43:56:60	103:22:45	4200	4800	
26	BHM	P	43:47:15	103:26:00	5800	5800	
27	BLR	Q	44:20:35	103:26:00	3600	3600	
28	VET	P	44:05:00	103:30:15	4600	4600	UPC
29	REN	P	43:54:39	103:28:50	5440	5440	
30	HTL	P	43:53:38	103:28:50	5000	5000	UPC
31	BTD	P	43:41:00	103:26:30	4560	4560	PLG
38	UPC	P	43:52:30	103:31:00	5800	5900	UPC

Note:

No --- serial number for cross-referencing with larger Great Plains collection.

SP --- species, P for ponderosa pine, Q for bur oak.

1 : The ID specified in this column is the merged ID, as in Figure 3-3, elevation unit is ft.

Station names are listed in APPENDIX II.

According to conventional methods, each site should have at least 20 trees, with 2 cores taken from each tree. This requirement was not reached for several sites because there were not enough trees available and some cores were seriously

rotted toward the center of the tree. The sample size is sufficiently large, however, to satisfy the requirements of statistical analysis. Later in the data analysis, several adjacent sites which have close loadings in their first principal component were merged into one site. Examples are HNK, PLG and THO; their chronologies are combinations of several neighboring samples in order to guarantee a large sample size and enhance the climatic signal.

1. Developing site chronology

After field collection, cores were transported to the Laboratory of Tree Ring Research at the University of Arizona. Standard procedures were used in mounting, surfacing, cross-dating and measuring the samples (Stokes and Smiley, 1968; Fritts, 1976; Holmes et al, 1986).

To affirm the cross-dating results, the computer program COFECHA was used to flag possible dating and measuring errors (Holmes 1983, 1986). The COFECHA results are listed in Table 3.6.

Table 3.6 shows that pine generally has higher serial correlation and higher mean sensitivity than oak; sites UPC and FRW are exceptions. The high correlation within each site

indicates that the cross-dating is reliable and that the samples for a given site are under the same environmental regime.

Table 3.6 Cross-Dating and Measuring Statistics
(List of COFECHA Results)

Site ID	Sp ¹	Lc ²	Chronol. Byr ³	Eyr ⁴	Ser. Corr ⁵	Avg Ms ⁶	Sample Sz ⁷	Yr ⁸
BHM	P	s	1660	1990	0.717	0.337	33	9106
GCP	P	s	1703	1990	0.736	0.410	25	3750
REN	P	s	1281	1991	0.616	0.355	32	9036
UPC	P	s	1543	1991	0.455	0.306	17	5229
PLG	P	s	1646	1991	0.606	0.386	9	2192
PPK	P	s	1654	1991	0.591	0.458	16	3380
THO	Q	n	1747	1990	0.516	0.265	10	1212
FRW	Q	n	1858	1990	0.631	0.342	12	984
FDF	Q	n	1807	1990	0.692	0.257	14	1527
HNK	Q	n	1733	1991	0.444	0.226	12	1501
BLR	Q	n	1751	1990	0.608	0.232	13	1988
CRY	Q	s	1883	1991	0.571	0.280	28	2391
CSP	Q	s	1775	1990	0.538	0.221	10	1169
GCE	Q	s	1767	1991	0.619	0.260	40	5110
ROC	Q	s	1717	1990	0.581	0.218	10	1780

Note: 1--- species. P is pine, Q is oak;
 2--- sample location on the Black Hills area, s for south region, n for north region;
 3--- beginning year of the chronology;
 4--- ending year of the chronology;
 5--- serial correlation;
 6--- average mean-sensitivity;
 7--- sample size (number of cores);
 8--- total number of measured rings (years) used to build the chronology.

Table 3.6 also lists the sample ages for each site. The oldest sample is from REN, which begins in 1281; the youngest sample is from CRY, which begins in year 1883.

Tree-ring chronologies for each site were formed by using program ARSTAN, developed by Cook (1985) and modified by Holmes et al (1986). The program describes the 'age trend' and produces the necessary standardization (Fritts, 1976,1991; Graybill, 1982). Tree-ring data commonly possess two components which are unrelated to climatic variation and need to be removed from the time series before such data are analyzed with climate data. Those two unwanted components are: i) a quasi-deterministic component related to the changing geometry of the growing tree and ii) a stochastic component related to the persistence of climatic effects of one year on physiological status of the tree in ensuing years, and also related to forest stand dynamics. The first component was removed by fitting a negative exponential or spline curve to the ring-width series. Trends shared in common at the site are not removed because they are thought to be generated by large-scale variation of climate (Fritts, 1976). The second portion of unwanted component was removed by fitting the tree-ring chronology to an autoregressive or moving-average model (Box & Jenkins, 1976, Fritts, 1976, Meko, 1981; Biondi, 1987, Cook, 1990). With program ARSTAN, the 'age trend' and other non-climatic variations unique to individual trees and sites were removed by fitting a cubic-spline function. By using a spline length of 70 years, a large part of climatic variation common to trees in this

region was preserved. For removing the autoregressive component, an AR(1) model was used for most chronologies; some chronologies required an AR(2) or more higher order model. The model order was automatically chosen by the AIC (Akaike Information Criterion) [Holmes et al, 1986].

As a result of running the ARSTAN program, three versions of each chronologies were developed for future analysis: ARStan, STanDard and RESidue.

The RES version is the residuals from autoregressive modeling. This 'prewhitened' series is more suitable than the STD or ARS series for later analysis. Table 3.7 lists the basic statistics for each chronology after running ARSTAN. Statistics are based on the common period 1916-1990. From this table, we can see the following:

- 1) Pine generally has a higher standard deviation than oak. The higher variance in pine chronologies may be related to higher sensitivity of pine to environmental variation.

- 2) The skew coefficients indicate that pine-chronologies are generally closer to a normal distribution than oak chronologies.

- 3) The high value of V_{at} (variance due to autoregression) indicates that both pine and oak are very strongly affected by the previous year's growth, except for sites BHM, CRY, FRW and

BLR.

4) Except for site UPC, all tree-ring sites have a high percentage of the variance explained by the first eigenvector. This means that within each site, most samples have a strong common signal.

5) Generally, the standard deviations decrease from the whole interval -- column 4-5 in Table 3.6 -- to the common period. Sites REN, FRW, THO and CRY have the highest percentage of reduction, which ranges from 13% to almost 20%. Only GCE shows a slight increase (3%) of standard deviation in common period. The decrease may be caused by the larger sample size in the common period. In most sites, the small decrease (less than 10%) of the standard deviation demonstrates a consistent growth behavior at those sites through time. Hence the entire chronology is reliable to be used in the analysis.

Table 3.7 Summary of Chronology Statistics (List of ARSTAN Results)

ID	Stdv	Skew	Kurt	V _{at} (%)	AR	Vleg	Cd %
BHM	0.241	-0.448	0.670	17.2	3	51.37	0.830
GCP	0.307	0.160	0.623	32.7	1	56.23	0.326
REN	0.254	-0.066	2.578	28.9	4	41.99	18.898
UPC	0.159	-0.220	0.311	41.8	2	29.27	0.000
PLG	0.265	-0.196	0.467	23.7	5	45.39	6.038
PPK	0.297	0.178	0.134	35.2	4	47.87	8.081
THO	0.246	0.218	0.820	22.1	1	49.01	19.919
FRW	0.300	0.276	-0.221	8.9	1	54.94	15.667
FDF	0.219	0.328	-0.445	26.4	1	53.93	5.936
HNK	0.169	0.533	1.088	20.7	1	43.35	5.325
BLR	0.186	0.300	0.966	18.7	2	51.17	8.602
CRY	0.203	0.196	-0.298	15.4	3	49.55	13.300
CSP	0.187	0.849	1.212	56.8	1	56.89	6.952
GCE	0.188	0.342	-0.388	28.7	1	43.36	-3.191
ROC	0.182	0.736	1.273	25.5	1	53.71	9.890

Stdv --- Standard deviation for whole interval;
 Skew --- Skewness coefficient;
 Kurt --- Kourtosis coefficient;
 V_{at}(%) --- Variance due to autoregression;
 AR --- Order of autoregression;
 Vleg --- Percentage of variance explained by 1st eigenvector;
 Cd (%) --- Decrease of Standard deviation from total period to common period.

Nine bur oak and six ponderosa pine chronologies are plotted for the common period 1916 to 1990 in Figure 3-4. The plots show that the high growth in 1932 and 1986 is prominent in all oak chronologies and low growth in 1939 and 1985 is prominent in pine chronologies. The plot also shows that the pine and oak have a distinct difference: pine chronologies have much less variance during the 1940s-1960s and much higher

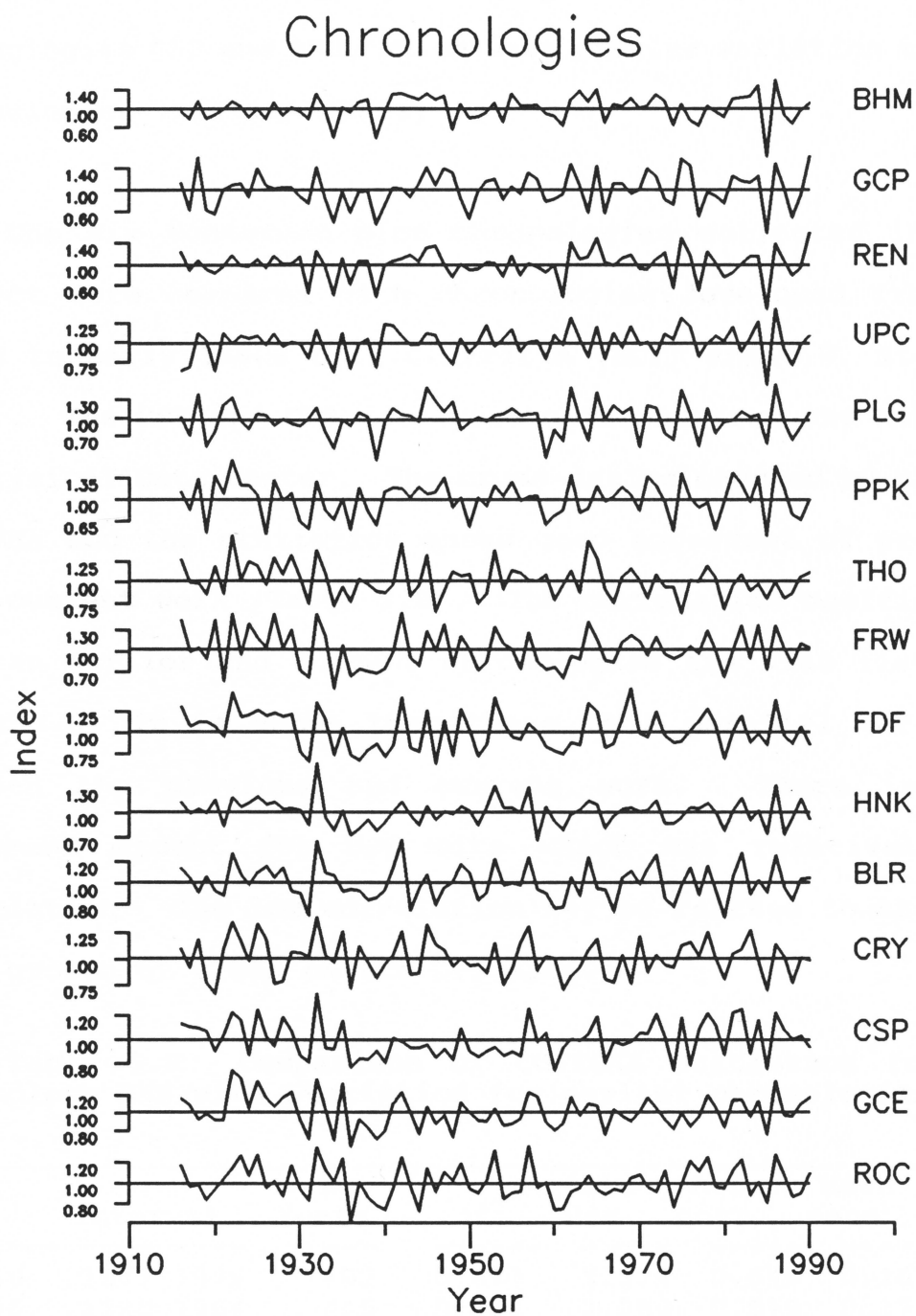


Figure 3-4. Chronologies used in the study. BHM to PPK are pine, the rest are oak.

in the 1980s than oak chronologies. Exceptions are oak chronologies CSP and HNK, which have similar variation to pine chronologies in 1940s-1960s.

The six Ponderosa pine chronologies collected in this project were compared with chronologies developed from the 1960s to early 1980s by H.C. Fritts (HCF) and C.W. Stockton (CWS). The HCF and CWS data were obtained from the National Geophysical Data Center. The cross-dating checked by program COFECHA and the statistics shows good agreement of previous with current work (Table 3.8). The correlation coefficients between earlier and current chronologies are also listed in Table 3.9, it is shown that there is a parallel variation between the previous and current work. There is good agreement except for UPC site which has relatively low correlation. The low correlation may be related to the very fast growth of trees on the UPC site.

Table 3.8 Comparison of COFECHA Statistics for New Chronology REN with Statistics for earlier chronologies

ID ^a	Interval	No. Years	r ^b	Std dev	Auto corr	Mean sens ^c
CUS640	1577 1979	403	0.677	3.314	0.594	0.267
144596	1520 1964	445	0.831	3.257	0.579	0.273
146649	1520 1964	445	0.801	3.942	0.608	0.326
REN	1285 1991	707	0.646	2.531	0.727	0.273
Mean			0.739	3.164	0.415	0.284

- a --- ID is the same in NGDC data set.
 CUS640 and 545640 are from CWS;
 144596 and 146649 are from HCF.
- b --- Correlation Coefficient with Master.
- c --- Mean sensitivity.

Table 3.9 Correlation Coefficients^a of New Pine Chronologies with Earlier Collections

ID	BHM	GCP	REN	UPC	PLG	PPK
CUS640	0.710	0.505	0.638	0.325	0.423	0.394
545640	0.255	0.550	0.501	0.209	0.448	0.422
144596	0.350	0.559	0.494	0.228	0.568	0.586
146649	0.339	0.530	0.469	0.186	0.550	0.625

^a --- period for analysis is 1916-1990.

**Chapter 4. STATISTICAL PROPERTIES OF THE RELATIONSHIP
BETWEEN TREE GROWTH AND TRADITIONAL
CLIMATE VARIABLES**

An important step in tree-ring studies of climate is to identify seasons and temporal characteristics of the climate signal. In this chapter, the precipitation and temperature signal in the chronologies is examined by four methods. The first method is correlation analysis -- to delineate a climate 'season' most strongly related to tree growth, and to evaluate site-to-site differences in strength of the climate signal. The second method is outlier analysis -- case study of climate conditions in years that tree-growth is poorly related to the 'seasonal' climate. The third method is factor analysis to identify the spatial clusters of precipitation, temperature, and tree-growth anomalies. The fourth method is running correlation analysis to study the stability of the correlation between oak and pine chronologies through time.

§4.1. Correlation analysis

Correlation analysis is a commonly used method to examine the linear relationship between two variables. Simple correlation analysis has long been used to probe for potential connections between tree-ring indices and climate variables.

Three correlation analyses were used to inspect the relationship between tree-ring growth and climate variables.

A. Monthly correlation analysis

A simple correlation analysis of monthly climate series with tree-ring chronologies showed that April-July precipitation for all stations is significantly positively correlated with tree growth. The months of September, November, and December have negative correlations for stations 08,19,20,32,34. For most stations, March and December precipitation has a negative relationship with tree-ring growth. A similar relationship holds for stations 05,12,18,22 and 27. Most of the negative correlation coefficients are small, however, and do not reach significant levels.

Table 4.1 lists the correlations between each chronology and monthly precipitation and temperature at Hot Springs (#15), Oelrichs (#19), and Rapid City (#25). The period for the analysis is 1916 to 1990. The months cover from January to December of the growth year. Consistent positive correlations for all station-chronology pairs are restricted to the months April through July. Some evidence for a March precipitation signal shows in the positive correlation for Hot Springs (#15), but the relationship turns to negative and insignificant for other stations. Correlation between chronologies and monthly temperature (not shown) has a similar

pattern, with the sign of correlation reversed.

Table 4.1 Correlation of Monthly Precipitation
with Tree-ring Chronologies

Climate Station #15: Hot Springs

site	Jan	Feb	Mar	Apr	May	Jun
BHM	0.07	0.05	0.18	0.21	0.31	0.30
GCP	0.18	0.07	0.12	0.11	0.32	0.34
REN	0.06	0.13	0.21	0.16	0.33	0.24
THO	-0.03	0.11	0.16	0.13	0.18	-0.07
FRW	0.09	0.10	0.19	0.35	0.36	0.24
FDF	0.14	0.12	0.10	0.11	0.13	0.08
BLR	0.06	0.17	0.19	0.20	0.15	0.04
CRY	0.18	-0.05	0.29	0.09	0.19	0.05
CSP	0.11	-0.03	0.24	0.12	0.27	0.07
GCE	0.11	-0.01	0.26	0.22	0.36	0.15
HNK	0.18	0.06	0.26	0.22	0.27	0.22
ROC	0.12	0.05	0.33	0.18	0.32	0.19

site	Jul	Aug	Sep	Oct	Nov	Dec
BHM	0.13	-0.08	0.09	-0.06	-0.01	-0.06
BLR	0.04	0.06	-0.12	-0.06	0.12	-0.10
CRY	0.03	0.13	-0.06	-0.07	0.16	-0.12
CSP	0.10	0.12	-0.11	-0.11	0.02	-0.11
FDF	0.08	0.11	-0.10	-0.03	0.17	-0.02
FRW	0.20	0.04	-0.07	-0.04	0.09	-0.08
GCE	0.17	0.08	-0.07	-0.05	0.18	-0.10
GCP	0.31	-0.03	0.03	-0.09	-0.03	-0.13
HNK	0.00	0.13	-0.05	0.01	0.05	-0.11
REN	0.12	-0.04	0.04	-0.07	-0.01	-0.05
ROC	0.08	0.19	-0.05	-0.02	0.02	-0.14
THO	0.08	0.15	-0.05	-0.14	0.13	-0.05

Climate station #19 Oelrichs						
site	Jan	Feb	Mar	Apr	May	Jun
BHM	0.15	0.02	-0.02	0.19	0.26	0.31
BLR	0.22	-0.13	0.01	0.03	0.10	0.14
CRY	0.12	-0.16	0.03	0.01	0.12	0.22
CSP	0.24	-0.15	-0.02	0.05	0.21	0.26
FDF	0.25	-0.05	0.05	0.09	0.05	0.19
FRW	0.21	0.00	0.01	0.26	0.23	0.30
GCE	0.20	-0.07	-0.01	0.15	0.25	0.39
GCP	0.22	0.11	0.01	0.12	0.29	0.33
HNK	0.20	-0.19	-0.02	0.11	0.21	0.30
REN	0.16	0.11	0.05	0.19	0.27	0.23
ROC	0.11	-0.10	0.05	0.12	0.20	0.32
THO	0.03	-0.09	-0.07	-0.01	0.16	0.09

site	Jul	Aug	Sep	Oct	Nov	Dec
BHM	0.23	-0.08	0.11	-0.08	-0.21	0.06
BLR	0.18	-0.18	-0.14	0.10	-0.02	-0.10
CRY	0.01	-0.03	-0.05	0.10	-0.10	0.09
CSP	0.18	-0.13	-0.07	0.12	-0.06	0.02
FDF	0.22	-0.05	-0.15	0.02	0.07	-0.05
FRW	0.29	-0.09	-0.04	0.01	-0.02	0.03
GCE	0.25	-0.10	-0.05	0.14	0.00	-0.04
GCP	0.28	-0.09	0.10	-0.03	-0.13	0.14
HNK	0.19	-0.13	-0.06	0.18	-0.07	-0.07
REN	0.22	-0.11	0.08	-0.05	-0.12	0.06
ROC	0.18	-0.10	-0.05	0.18	-0.12	-0.07
THO	0.21	-0.04	-0.14	-0.05	0.01	-0.06

Climate station #25 Rapid City						
site	Jan	Feb	Mar	Apr	May	Jun
BHM	0.10	0.15	-0.03	0.26	0.34	0.30
BLR	0.01	0.09	-0.04	0.25	0.22	0.23
CRY	0.06	0.00	-0.04	0.03	0.33	0.09
CSP	0.01	-0.05	-0.08	0.15	0.37	0.09
FDF	0.09	0.10	0.03	0.16	0.24	0.18
FRW	0.09	0.16	-0.02	0.35	0.45	0.32
GCE	-0.02	-0.01	-0.05	0.18	0.48	0.17
GCP	0.18	0.17	-0.09	0.14	0.41	0.34
HNK	0.07	0.14	-0.06	0.23	0.38	0.19
REN	0.11	0.18	0.07	0.16	0.37	0.32
ROC	-0.01	0.12	0.01	0.21	0.38	0.12
THO	-0.06	0.01	-0.08	0.09	0.32	0.01

site	Jul	Aug	Sep	Oct	Nov	Dec
BHM	0.22	0.15	0.10	-0.09	-0.22	-0.05
BLR	0.15	0.01	-0.01	-0.04	0.00	-0.12
CRY	-0.01	0.26	-0.02	-0.07	-0.06	0.02
CSP	0.27	0.10	0.00	-0.04	-0.09	-0.11
FDF	0.02	0.12	0.00	-0.06	0.08	-0.10
FRW	0.29	0.18	-0.03	-0.06	-0.06	-0.09
GCE	0.22	0.17	0.05	0.02	-0.04	-0.06
GCP	0.37	0.20	-0.03	-0.15	-0.23	-0.12
HNK	0.09	0.20	0.03	-0.01	-0.04	-0.11
REN	0.26	0.17	0.09	-0.15	-0.22	-0.07
ROC	0.16	0.22	-0.01	-0.05	-0.14	-0.11
THO	0.14	0.04	0.00	-0.07	0.07	0.00

B. Growth year correlation analysis

The correlation analyses using growth-year (Sep-Aug) precipitation and tree growth data is listed in Table 4.2. The results show a significant relationship between these two variables, but the correlations for some stations are not stable. The reason for this is that negative and positive monthly responses offset one another in the annual climate variable. In order to develop a consistent relationship for most of the stations, a seasonalized series is preferred to an annual series. Correlation between tree growth and monthly climate series indicates that a "season" defined as Apr-Jul is special for the tree-ring data.

Table 4.2 Correlation Coefficients of Chronologies
with PPT for previous September Through
Current August

ID	04	05	08	09	12	14	15	16
BHM	0.417	0.336	0.480	0.587	0.464	0.423	0.427	0.540
GCP	0.362	0.328	0.457	0.480	0.493	0.233	0.458	0.501
REN	0.378	0.361	0.405	0.520	0.516	0.362	0.415	0.565
UPC	0.195	0.150	0.351	0.305	0.269	0.107	0.246	0.339
PLG	0.314	0.273	0.363	0.393	0.513	0.414	0.372	0.417
PPK	0.414	0.463	0.503	0.537	0.603	0.438	0.546	0.469
THO	0.189	0.231	0.267	0.285	0.264	0.347	0.344	0.307
FRW	0.455	0.554	0.559	0.551	0.636	0.530	0.541	0.583
FDF	0.253	0.270	0.364	0.374	0.276	0.554	0.309	0.364
HNK	0.224	0.239	0.449	0.399	0.328	0.384	0.355	0.380
BLR	0.289	0.373	0.364	0.252	0.360	0.523	0.271	0.312
CRY	0.169	0.209	0.290	0.257	0.243	0.281	0.352	0.351
CSP	0.278	0.267	0.406	0.370	0.300	0.448	0.388	0.380
GCE	0.455	0.384	0.535	0.479	0.454	0.465	0.542	0.431
ROC	0.320	0.324	0.461	0.399	0.363	0.394	0.468	0.307

ID	18	19	20	21	22	24	25	27
BHM	0.455	0.398	0.348	0.595	0.290	0.498	0.525	0.417
GCP	0.381	0.371	0.342	0.590	0.318	0.411	0.616	0.361
REN	0.476	0.382	0.249	0.560	0.367	0.488	0.605	0.460
UPC	0.204	0.249	0.163	0.345	0.191	0.295	0.367	0.285
PLG	0.393	0.317	0.380	0.697	0.334	0.417	0.545	0.228
PPK	0.575	0.408	0.369	0.598	0.403	0.541	0.577	0.241
THO	0.387	0.301	0.032	0.074	0.340	0.417	0.323	0.296
FRW	0.619	0.454	0.461	0.572	0.512	0.716	0.723	0.396
FDF	0.330	0.360	0.294	0.270	0.353	0.394	0.413	0.416
HNK	0.351	0.326	0.319	0.283	0.377	0.451	0.480	0.352
BLR	0.391	0.192	0.369	0.391	0.310	0.448	0.387	0.192
CRY	0.245	0.220	0.292	0.331	0.323	0.366	0.319	0.278
CSP	0.285	0.291	0.419	0.401	0.317	0.304	0.379	0.480
GCE	0.438	0.510	0.502	0.545	0.343	0.478	0.556	0.440
ROC	0.348	0.348	0.378	0.377	0.322	0.407	0.468	0.380

ID	29	30	31	32	33	34	35	36
BHM	0.334	0.516	0.364	0.269	0.535	0.410	0.478	0.454
GCP	0.408	0.527	0.290	0.221	0.429	0.334	0.361	0.338
REN	0.378	0.546	0.383	0.288	0.535	0.389	0.536	0.463
UPC	0.234	0.363	0.251	0.196	0.259	0.233	0.241	0.260
PLG	0.396	0.520	0.269	0.255	0.419	0.298	0.361	0.327
PPK	0.525	0.542	0.354	0.406	0.658	0.462	0.581	0.489
THO	0.327	0.313	0.250	0.315	0.377	0.248	0.369	0.377
FRW	0.574	0.618	0.510	0.443	0.676	0.531	0.610	0.583

Table 4.2 (continue)

ID	29	30	31	32	33	34	35	36
FDF	0.413	0.382	0.357	0.258	0.321	0.310	0.278	0.372
HNK	0.396	0.416	0.320	0.300	0.410	0.392	0.353	0.353
BLR	0.463	0.467	0.353	0.342	0.383	0.368	0.321	0.306
CRY	0.330	0.399	0.245	0.128	0.188	0.209	0.185	0.274
CSP	0.385	0.390	0.343	0.272	0.284	0.335	0.258	0.355
GCE	0.478	0.420	0.296	0.366	0.427	0.389	0.424	0.536
ROC	0.480	0.363	0.206	0.259	0.291	0.292	0.350	0.280

C. Seasonal correlation analysis

To determine how strongly a climate record is associated with each chronology for a chosen season, a simple correlation analysis was applied to chronology-precipitation and chronology-temperature pairs for April-July data. Pairwise scatter plots summarizing the correlation analysis are shown in Fig 4-1 and Fig 4-2.

The climate data for each station is on the X-axis, and the chronology data on Y-axis. The order for both the chronologies and climate data is based on the factor analysis, results, which will be discussed later in this chapter. The top six chronologies along the left axis are pine; the bottom nine are oak. In Fig 4-1 and Fig 4-2, the first upper row and the first left column are the histograms showing the distribution of each variable. For each scatterplot, an ellipse is drawn at the 85% Gaussian bivariate confidence

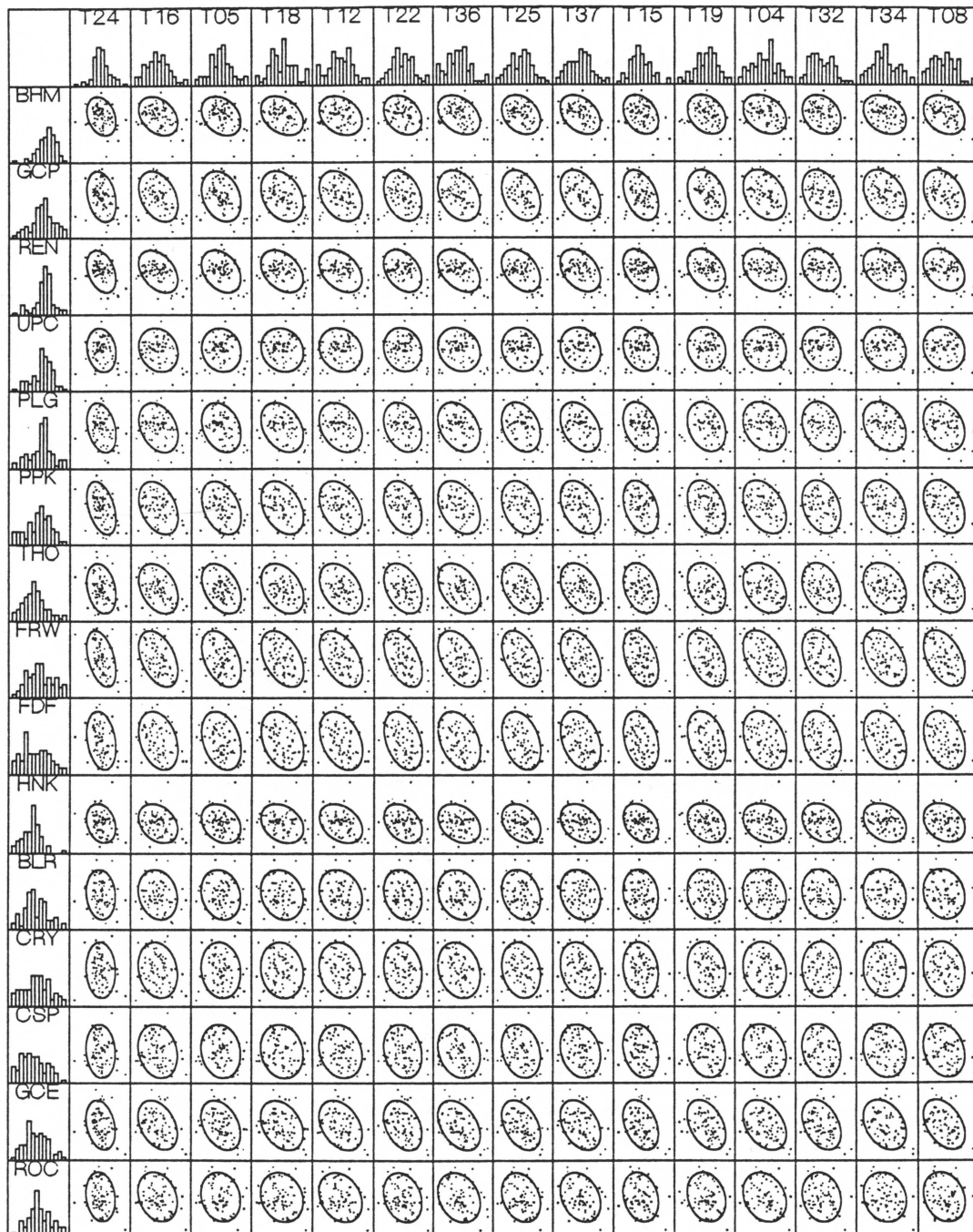


Figure 4-1. Correlation Analysis of Tree-ring Chronology and Temperature Departure (Apr-Jul). X-axis is climate station, Y-axis is tree-ring site. Upper part from BHM to PPK is pine; the lower part is oak. Histograms are distributions for each data set.

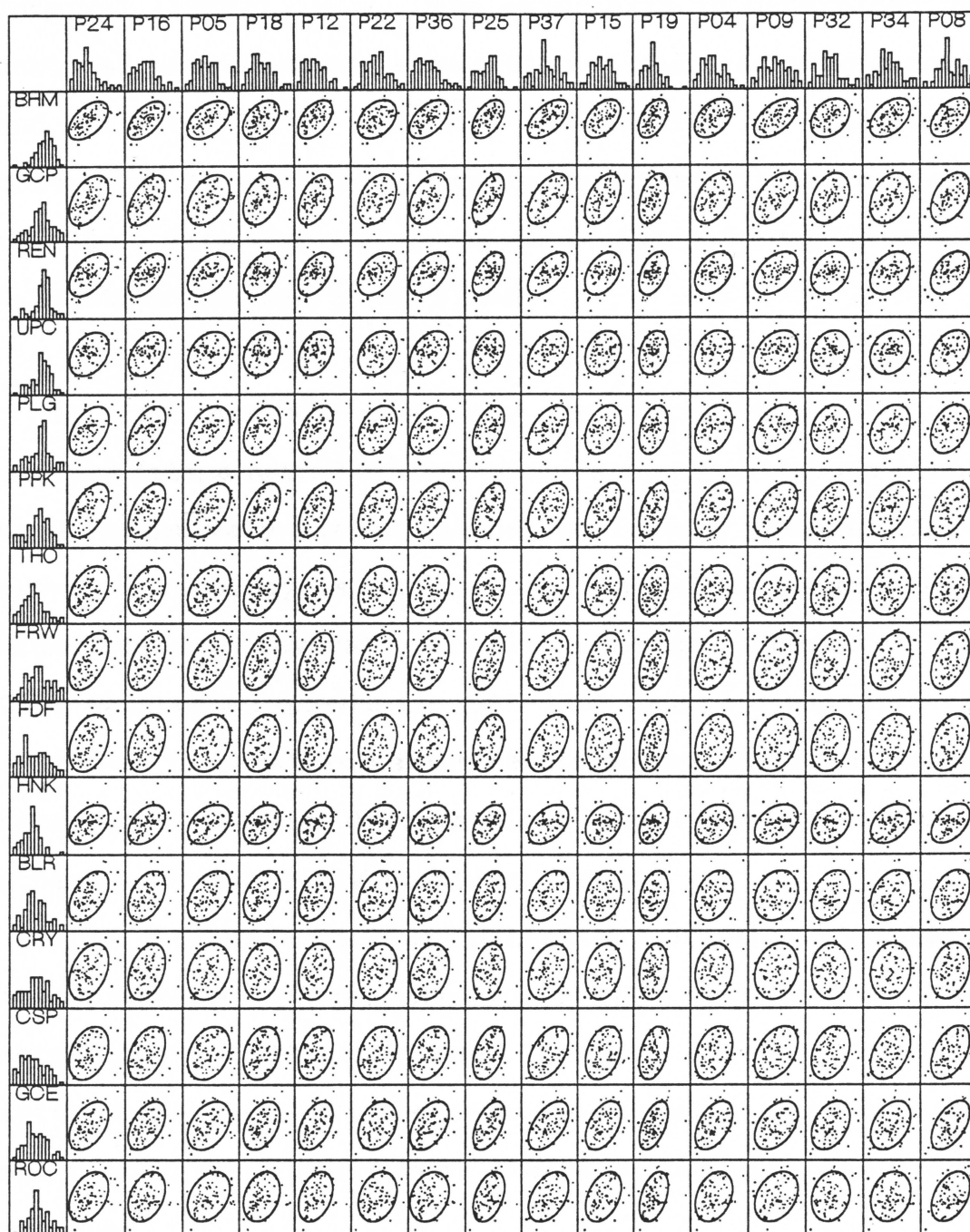


Figure 4-2. Correlation Analysis of Tree-ring Chronology and Precipitation Departure (Apr-Jul). X-axis is climate station, Y-axis is tree-ring sites. Upper part from BHM to PPK is pine; the lower part is oak. Histograms are distributions for each data set.

interval (SYSTAT,1990). The major axis is determined by the unbiased sample standard deviation of the tree-ring chronology and climate data, and the orientation of the axis is determined by the sample covariance between the chronology and climate. From the plots, the following information about the data structure can be obtained:

1) Neither the pine nor the oak chronologies depart greatly from a normal-distribution shape -- although pine tend to be negatively skewed and oak positively skewed. The most skewed chronology is FRW, a result which is associated with high growth in several years on that site. For sites HNK and CSP, suppressed growth in 1930-1950 caused a negative skew.

2) Most temperature series have a normal distribution shape; some precipitation distributions are close to normal, but others are distinctly positive skewed.

3) The 45° incline direction of the ellipses for precipitation shows the positive correlation between chronology and PPT departures. The 135° direction of ellipses for temperature shows the negative correlation of tree growth and temperature departures. These slopes indicate a drought response.

4) All pine chronologies have more significant correlations than the oak chronologies, as exhibited by the narrower shape and steeper slope of the long axis of the scatter ellipse.

Some climate stations, like Pierre (No. 34) and Cottonwood (No.08), have round-shaped ellipses in the scatter (Fig 4-1, T34 vs. UPC; T08 vs. UPC;), or a vertical ellipse (such as T24 vs. CRY). The scatter plots show distinct differences in strength of climate signal among chronologies. For example, the temperature signal in UPC is much weaker than in other chronologies. The relationships between tree-ring chronologies and climate departures shown in Fig 4-1 and Fig 4-2 can help screen data for later processing.

5) Even for the most significant pairs, some points fall outside the ellipse. An outlier will make linear relationships weak between tree-ring chronologies and climate data. Examining outlier behavior can enhance our understanding of the local climate regime and tree response to local climate or non-climate variations. The outlier analysis will be discussed in the next section.

§4.2. Outlier analysis

Outliers from the linear model were screened out by setting the upper-and-lower criterion as two standard deviations of the residuals from the predicted value. If an observed point is outside the upper or lower line, it is considered an outlier from the linear model (Fig 4-3). The method, illustrated in Fig 4-3, was applied to all climate-chronology pairs for 25 climate stations and 15 chronologies. Outliers from each regression were dated and the number that occurred in a given year was counted. These counts are summarized and plotted in Fig 4-4. Outliers outside the upper 2.5σ line were given a positive sign; these represent growth greater than predicted by regression. Likewise, outliers below the level 2.5σ level were given a negative sign; these represent less than the predicted growth. From the results, the two most frequently occurring outlier years were 1932(+) and 1985(-) with more than 130 and 50 occurrences, respectively (Fig 4-4). The direction of the outliers is the same for these two years for temperature and precipitation. Fig 4-5 shows that there are more outliers in the linear models for temperature than for precipitation when use 2σ as the criterion for picking up the outlier-year numbers.

Historical records of the Great Plains show that 1934 was

a very dry and hot year (Lawson & Baker, 1981). Tree-ring data from both pine and oak show a very strong signal for this year, as characterized by narrow or missing rings. The year 1934 does not, however, appear as an outlier. This indicates that even under severe growth conditions, tree growth followed the estimated linear relationship in response to climate. In contrast, the linear relationship was violated in some "ordinary years". Factors other than Apr-Jul climate anomalies must be responsible for non-linear effects. Spatial differences in climatic anomalies between tree sites and climate stations are one possible cause. To study this possibility, climate departure maps for several selected years are plotted in Fig 4-6 to Fig 4-10. The quantile number for each station denotes how severe the climate condition was compared with 75-year records. These maps show that:

- 1) Year 1935 was generally cool and wet, a very 'good' year for tree growth (Fig4-6a,b). The large quantile numbers all denote favorable climatic conditions. A spatial gradient from wet to dry appears from south to north.

- 2) During the severe climate of 1934, both precipitation and temperature produced the conditions that were adverse for tree growth. Very dry, hot conditions are reflected by low-quantile numbers, and wet, cool conditions by high-quantile numbers. In 1934, the Black Hills area, as well as the entire Great Plains's region, was in severe drought, part of a period

known as the 'Dust Bowl' of the 1930s. Many climate stations recorded temperature departures which were the first (or second or third) highest in history. Precipitation was also among the lowest recorded in history. The large circles containing triangles in Fig 4-7a,b denote the severe drought conditions in 1934. Quantile numbers in 1939 are larger than in 1934 at most stations, which means that the drought in 1939 was less severe than in 1934, but the departures of precipitation and temperature have the same direction as in 1934. The small quantile numbers also imply a negative impact on tree growth. From the standpoint of cross-dating, the tree-ring formed in 1939 is a signature year for cross-dating and for model calibration (Fig 4-8a,b).

3) The outlier years of 1985 and 1932 reflect a quite different climatic condition. Year 1932 (Fig4-9a,b) had high temperature and abundant precipitation at most stations, especially at the northern part of the Black Hills, and tree growth was much more than the linear relationship predicted. In contrast, in 1985 (Fig4-10a,b), very low precipitation accompanied slightly high temperature. Tree growth in 1985 was much lower than predicted by the linear methods. According to the relationship between tree growth and climate, higher temperature would reduce the growth and higher moisture will speed the growth, as long as the temperature is higher than the compensation point and the moisture is below the

compensation point (Kramer & Kozlowski, 1979). In the Black Hills area, the arid and semi-arid climate constitutes the growth conditions for both pine and oak with temperature higher above the compensation point and moisture below the compensation point for most of the growing season. The combined two factors may cancel each other and therefore cause only a small change in tree growth. However, tree growth in 1932 was abnormally greater than the linear model predicted. This suggests that there may have been some unknown mechanisms of climatic factors affecting tree growth, or some unknown factors other than climate.

Another possible cause of outlier from the regression models is that the Apr-Jul climate window may not adequately capture the important climate anomaly. To further search for the reason of 1932 outlier, the monthly climate departures from July of the previous year to August of the current year were examined. Fig 4-11 is a plot of precipitation and temperature departures during the 1932 growing season at station No. 15, 25, and 9. It is clear that in March, temperatures were 8°F lower than the mean level at Rapid City and Hot Springs and 6°F at Custer station. At the same time the PPT departure at Custer was as high as 500% above the normal level. This unusual event of a local, intense storm in early spring may be one reason for the greater growing in

1932. Excluding March from the seasonal series may have caused a high number of outliers in linear model.

Reconstruction models based on the assumption of a linear relationship between tree-ring chronology and climate variables should include analysis of potential effects of outliers. The outlier impact may be eliminated by using a more flexible filter to standardize chronologies, but there is a risk of eliminating climate signals. Another approach would be to include the month March in the seasonalization, but that could weaken the linear relationship manifested in non-outlier years.

An alternative approach would be to drop outlier years from both the tree-ring chronology and climate data, but this scenario would benefit only in a mathematical sense by increasing calibration statistics -- unless a tree-ring signature for outlier years exists for eliminating such years from interpretation of reconstructions.

There are four kinds of outlier years, which represent departures from the assumed linear relationship between tree-ring growth and climate. The outlier are divided into two ranges on both positive and negative directions. Outlier numbers around 20 to 40 represent local anomalies of tree-ring

growth from the linear model, while an outlier number of 50 or more indicates a larger-scale spreading of anomalies over the study area. Those outlier years are plotted in Fig 4-4 and listed in Table 4.3 for future analysis.

Table 4.3 Outlier-Year Numbers
(criterion: 2σ)

Year	PPT	TEM									
1900	2	5	1923	4	18	1946	-13	3	1969	10	12
1901	0	-1	1924	13	28	1947	-3	0	1970	-1	1
1902	7	11	1925	15	-23	1948	6	3	1971	0	-1
1903	0	1	1926	-10	-17	1949	-11	-7	1972	4	4
1904	5	6	1927	-8	-3	1950	-10	-22	1973	-4	-1
1905	1	2	1928	-18	-4	1951	-14	-10	1974	2	0
1906	0	-9	1929	-1	-1	1952	-7	-7	1975	8	-9
1907	-6	-9	1930	-14	-14	1953	28	18	1976	-5	-4
1908	-1	-3	1931	-9	-4	1954	-2	-2	1977	-14	16
1909	-7	12	1932	39	50	1955	8	7	1978	17	22
1910	0	-2	1933	5	15	1956	-6	-7	1979	-8	-18
1911	7	-6	1934	4	8	1957	14	15	1980	-3	-5
1912	-9	-16	1935	8	-7	1958	-16	-12	1981	5	2
1913	12	14	1936	-6	8	1959	-12	-22	1982	7	3
1914	20	34	1937	-9	3	1960	-5	13	1983	8	7
1915	3	7	1938	11	-4	1961	10	-20	1984	-7	5
1916	13	-13	1939	-26	-9	1962	10	10	1985	-34	-44
1917	-5	6	1940	-6	-4	1963	4	5	1986	12	47
1918	9	4	1941	-6	-8	1964	9	10	1987	-1	0
1919	-9	3	1942	9	17	1965	4	-5	1988	1	1
1920	-7	-8	1943	-2	9	1966	-2	-5	1989	2	0
1921	-4	-4	1944	4	-8	1967	14	16	1990	13	14
1922	4	9	1945	15	0	1968	3	11			

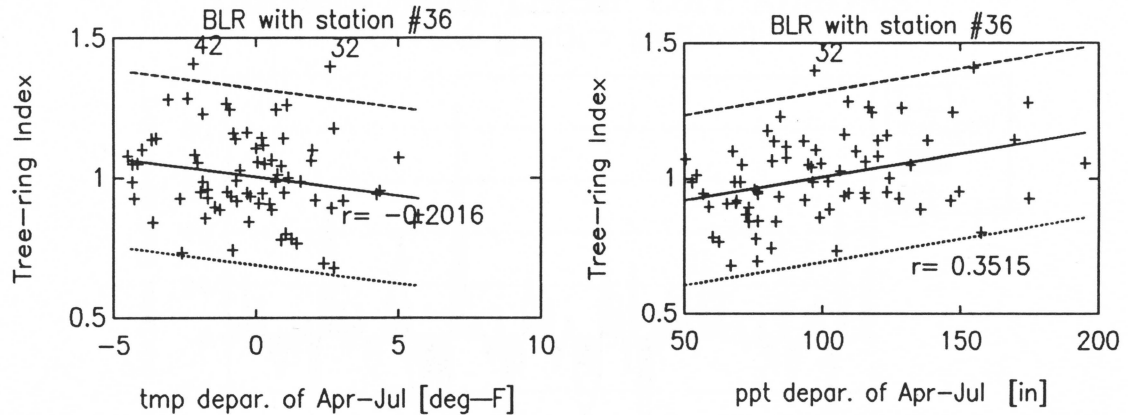


Fig 4-3. Scatter plot of tree-ring chronology with temperature and with precipitation. Solid line is the predicted tree-ring growth by simple regression, the upper and lower dashed line is $\pm 2\sigma$ from the predicted value.

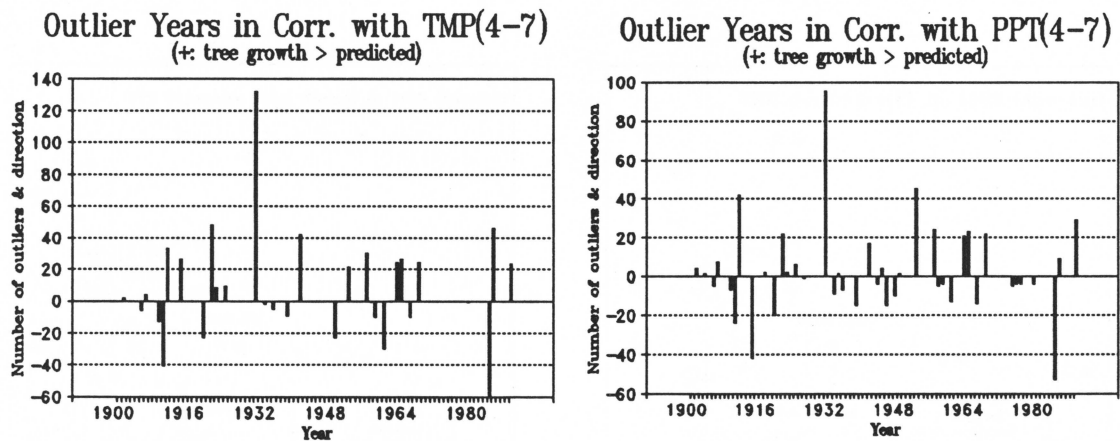


Fig 4-4. Number of outlier-years counted from all linear correlation analysis in Black Hills area using available tree-ring chronologies and climate records. A negative value indicates tree-growth was less than predicted. Both TMP and PPT are departures for Apr-Jul. Criterion for picking up outlier-year number is 2.5σ .

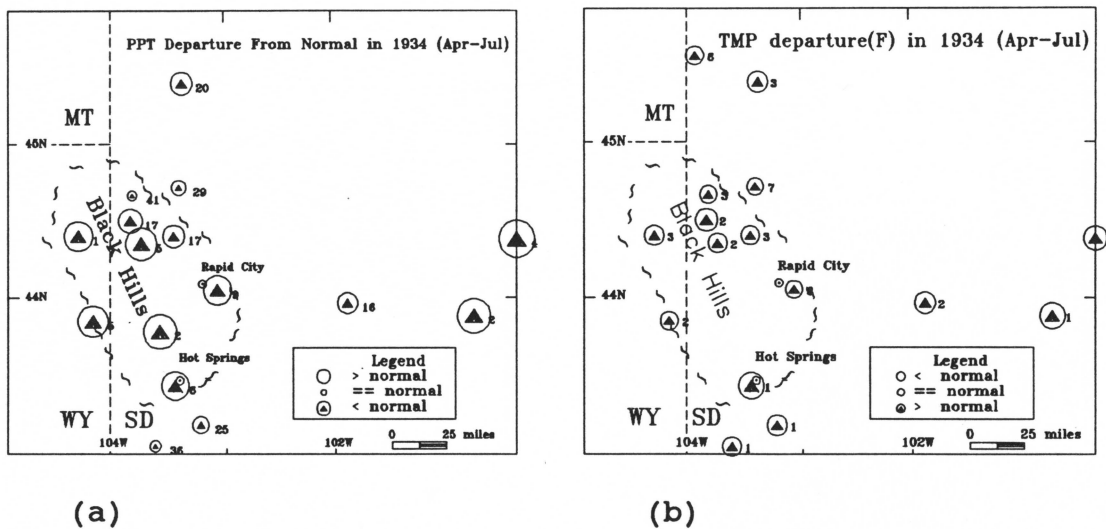


Figure 4-7. Climate pattern in severe dry year 1934.

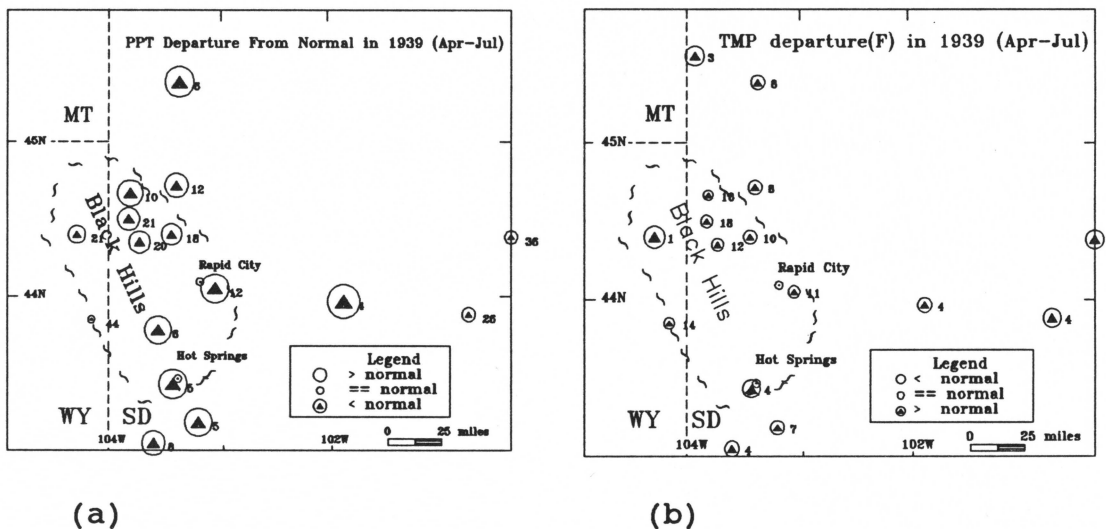
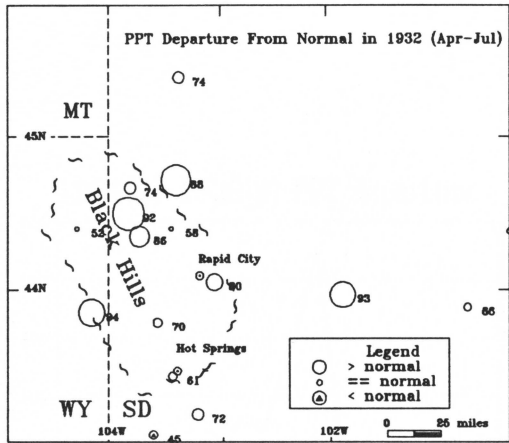
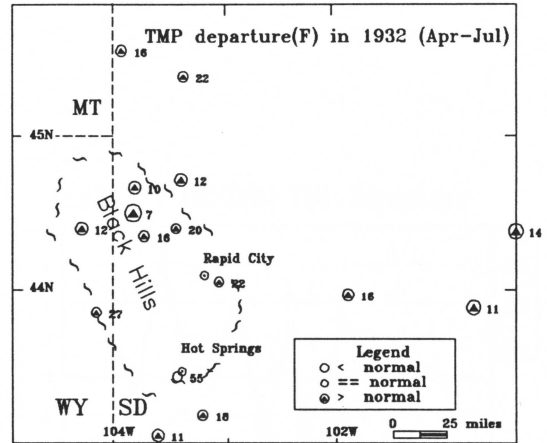


Figure 4-8. Climate pattern in severe dry year 1939.

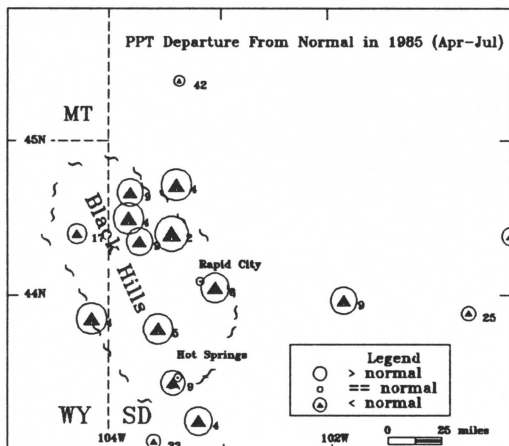


(a)

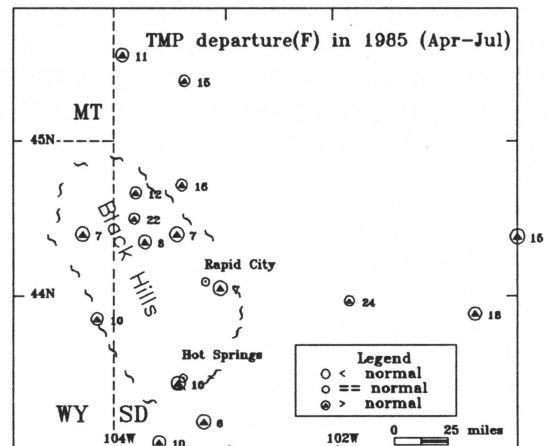


(b)

Figure 4-9. Climate pattern in wet year 1932.



(a)



(b)

Figure 4-10. Climate pattern in dry year 1985.

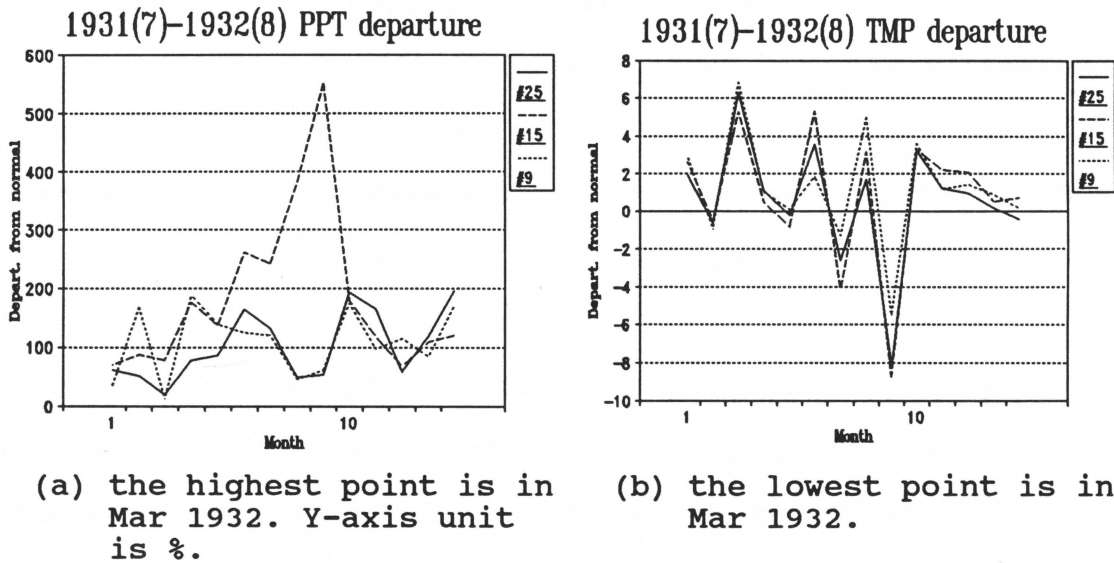


Fig 4-11. Departures of climate variables at three stations in growth year 1932. X-axis is the month number counting from previous July to current August. No.1 refers to previous July, then Aug, ..., and No.10 refers to Apr of current year.

§4.3. Factor analysis and data grouping

The correlation analysis shows a significant relationship between chronology and climate data sets. Principal component analysis (PCA) is generally used to simplify data structure and reduce the number of variables for later analysis. However, a shortcoming of PCA is the difficulty of distinguishing one data group from another (Richman, 1986). PCA results are often also hard to interpret.

As an alternative approach to PCA, factor analysis with varimax rotation was used to identify groups of tree-ring chronologies and climatic stations in the Black Hills. As pointed out by Richman, factor rotation can avoid four major deficiencies (domain shape dependence, sub-domain instability, sampling problems and inaccurate portrayal of physical relationship embedded within the input matrix) which hamper PCA as a method for isolating individual modes of variation. Details of the methods for factor rotation are contained in Richman (1986) and the BMDP (1990) user's manual.

Results of the factor analysis (Table 4.4) show that after the rotation of principle components all chronologies can be divided into four groups: oak from the north; oak from the south; pine group 1 and pine group 2. Because all pine samples are located the in southern part of the Black Hills,

the classification into two pine groups may reflect some factor affecting growth of pine, such as slope direction, or a micro-climatic feature.

For precipitation-departure data, three groups are identified. Stations concentrated in northern and southern sections of the Black Hills are divided into two distinct groups, while stations far from the Black Hills area, most on the eastern side of the Hills, are placed into a separate group by factor rotation. Table 4.5 clearly shows this classification by the rotated factor loadings.

The factor analysis results for temperature (not shown) indicate a strong relationship among all stations. Therefore, all temperature data in the study area can be summarized into one variable.

The chronology factor scores for each group were saved for later analyses. The four groups are coded as:

- i). oak in north, named as Q_n;
- ii) oak in south, named as Q_s;
- iii). pine group1, named as P_1;
- iV). pine group2, named as P_2.

Table 4.4 Chronology Group by Factor Analysis

<u>ID</u>	<u>FACTOR1</u>	<u>FACTOR2</u>	<u>Remarks</u>
FDL	0.885	0.000	
BLR	0.837	0.000	
HNK	0.816	0.000	Q _n
THO	0.792	0.000	Oak, in the north
ROC	0.775	0.253	
GCE	0.769	0.374	
FRW	0.730	0.537	
CSP	0.705	0.267	Q _s
CRY	0.560	0.371	Oak, in the south
GCP	0.000	0.849	
PLG	0.000	0.849	
UPC	0.000	0.811	Pine, group 1
REN	0.294	0.802	
BHM	0.293	0.799	
PPK	0.314	0.714	Pine, group 2
VP	5.657	4.672	

In Table 4.4 and 4.5, the index VP is the variance explained by the factor. It is computed as the sum of squares for the elements of the factor's column in the factor-loading matrix. Generally the larger the VP, the more distinct the characteristics for the group.

Table 4.5 PPT Group by Factor Analysis

ID	<u>FACTOR1</u>	<u>FACTOR2</u>	<u>FACTOR3</u>	
P24	1.010	0.000	0.000	
P16	0.926	0.000	0.000	
P05	0.861	0.000	0.000	
P22	0.848	0.000	0.000	
P18	0.762	0.000	0.000	
P12	0.744	0.000	0.000	
P36	0.725	0.000	0.000	grouped into
P37	0.552	0.416	0.000	PPT_north
P25	0.533	0.389	0.000	and Middle
P15	0.000	0.871	0.000	
P19	0.000	0.867	0.000	
P04	0.000	0.825	0.000	grouped into
P09	0.000	0.775	0.000	ppt_South
P32	0.000	0.000	0.888	
P34	0.000	0.000	0.874	grouped into
P08	0.000	0.325	0.523	ppt_Far_stns
VP	5.681	3.365	1.975	

For climate stations, option DQUART (directly quarti-min rotation) is used for rotation. The correlation coefficients between the three rotated factors for this oblique rotation are shown in Table 4.6:

Table 4.6 Correlation Coefficients Among DQUART Rotation Factors

	FACTOR1	FACTOR2
FACTOR2	0.668	
FACTOR3	0.451	0.422

Even though the three variables are oblique, the rotated structure can give a better view of the data structure in space and make it easier to classify the PPT patterns in the Black Hills area.

By rotation, the chronologies in the study area are optimized into four series, and the climate data sets are also reduced to four series.

§4.4. Running correlation analysis

Because the relationships between climate and tree-growth vary through time, some periods may show a strong response where others will not, or different periods may have reversed relationships. What is the outlook for this relationship through time? Is this relationship consistent over all variables? What is the relationship if we modify the 'screening window' for the running correlation? All these questions may lead to a more detailed understanding of the response of tree-ring growth under certain climate conditions, and the conclusions from the running correlation analysis will help to build a more realistic reconstruction model.

Two aspects of the running correlation are used to investigate the data: A) the response of two tree species on the same site; B) the tree-ring chronology response to climate

variations through the time.

In this study, three windows were selected to investigate the running correlation coefficients (R_r). The window widths are 5-yr, 13-yr, and 23-yr. The 5-yr window is used for examining short period variations; the 23-yr window is used for long period variations; and the 13-yr window is used for intermediate-length variations. The 13-year window is also convenient for studying for periods near the sunspot cycle.

Fig 4-12 displays the running correlation for chronologies GCE and GCP. GCE and GCP are oak and pine, respectively, at the same site. The different window-intervals show the sensitivity of running correlation to time period of analysis. The plot shows:

- 1) As the window interval increases, the sensitivity of the correlation to period of analysis decreases; the wider window which covers a longer segment of the series produces a more stable R_r .

- 2) The R_r curve of 5-year and 13-year windows dips sharply near 1795, 1835, 1890, 1920, 1950 and 1980. Correlation coefficients drop to zero or even change to negative at these times. The practical significance of a drop in correlation is greater if the scale of variations is large. The plot of the running standard deviation (R_{sd}), using the same windows as

with as R_T curve, shows that the variance of pine and oak growth near these 'spike' years is quite dissimilar. For example, in the period centered on 1920, both pine and oak have high variance, but the correlation is negative for this short period (1915-1921 central years). The wider window R_T curve also shows a trough. Historical records show that a serious insect attack called 'small mountain pine beetle' swept through the Black Hills early in this century and caused a lumber loss of 1 to 2 billion board feet (Progulske, 1974). The 1920 trough of R_T may have been caused by the insect attack, since pine would be affected, but not oak.

The combination of troughs in R_T and high standard deviation on pine but low on oak might also reflect periods of insect attack on pine. From this judgment, around year 1840, 1920 and 1950, the downward trend of pine chronologies may carry the signal of insect attack. If enough evidence points to distortion of chronologies from insect attacks, filtering by specially designed flexible splines or other curves might be considered.

3) There are five periods of high R_T in the 13-year and 23-year windows, associated with a sharp jump in the R_T curve for the 5-year window at periods around years 1820, 1850, 1890, 1930 and 1960. In the 1934 drought, both pine and oak

chronologies had a high variance, as shown by both the 5-yr and 23-yr windows of running Stdv. These high variances coincide with a peak in running correlation. These synchronized extreme values on both running correlation and running Stdv happened only in the early 1930s. Does this mean the drought in 1930s was unique at least in the period from 1770 to 1990? Perhaps there may be a way to find such periods of extreme drought by computing running-correlation windows for two species from nearby sites. The question might be answered by collecting more samples and carrying out more research.

Other drought-dominated periods were centered near 1820, 1850 and 1875. These phenomena suggest that there are mechanisms which cause oak and pine to have a similar growth patterns in drought periods. The 1930's was a time of large-scale drought in the Great Plains; the late 1820s may similarly have imposed severe living conditions on trees. These phenomenon also verify the limiting factor concept: during normal periods different species responded differently to environmental factors, the contrast of growth departures in different species can be sharp. In severe climatic years, however, tree growth will be more restricted by limiting factor(s) and all species will respond to the limiting factor simultaneously. If these species are all sensitive to the

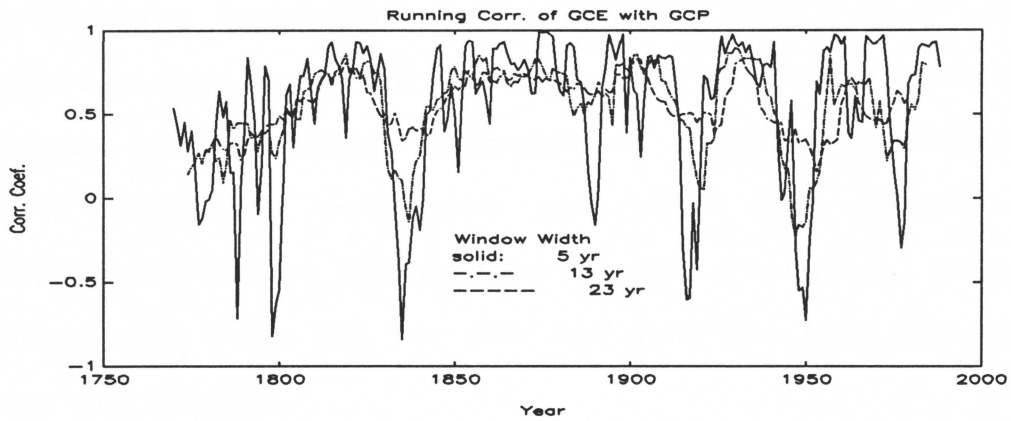


Figure 4-12. Running correlation between pine and oak at same sample site, narrow window show high variation of running r through time.

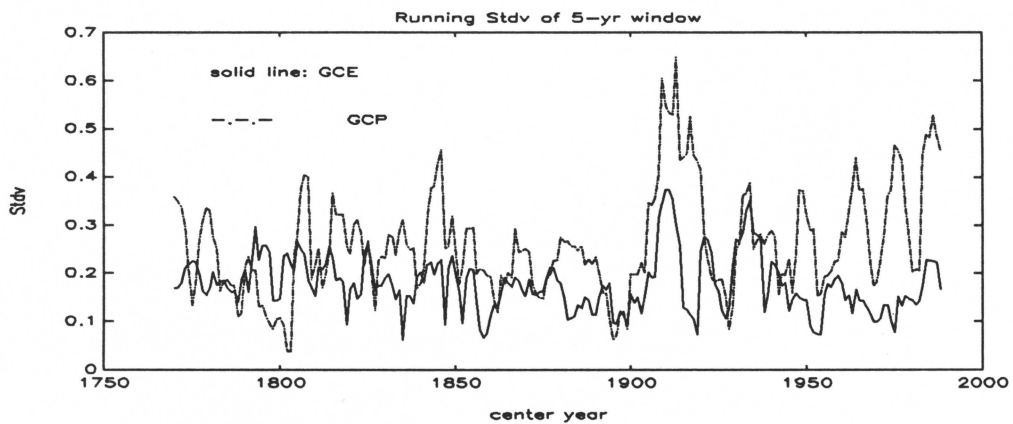


Figure 4-13. Running standard deviation of oak and pine, 5-yr window.

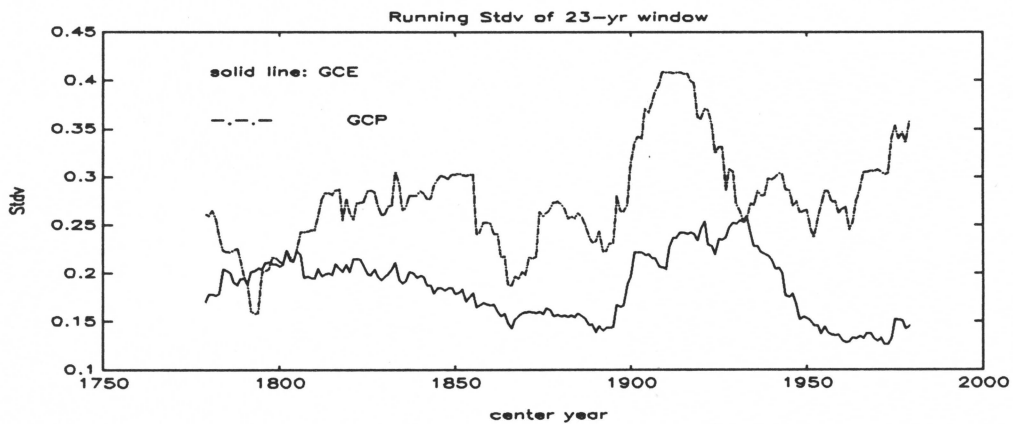


Figure 4-14. Running standard deviation of pine and oak through 23-yr window.

same limiting factor(s), then they will show a very similar response to environmental variation. In the Black Hills area, as shown by the simple correlation analysis discussed in earlier chapters, both oak and pine are sensitive to precipitation during the growing season. Therefore, a high R_r combined with high R_{sd} for oak and pine can help identify a severe dry period.

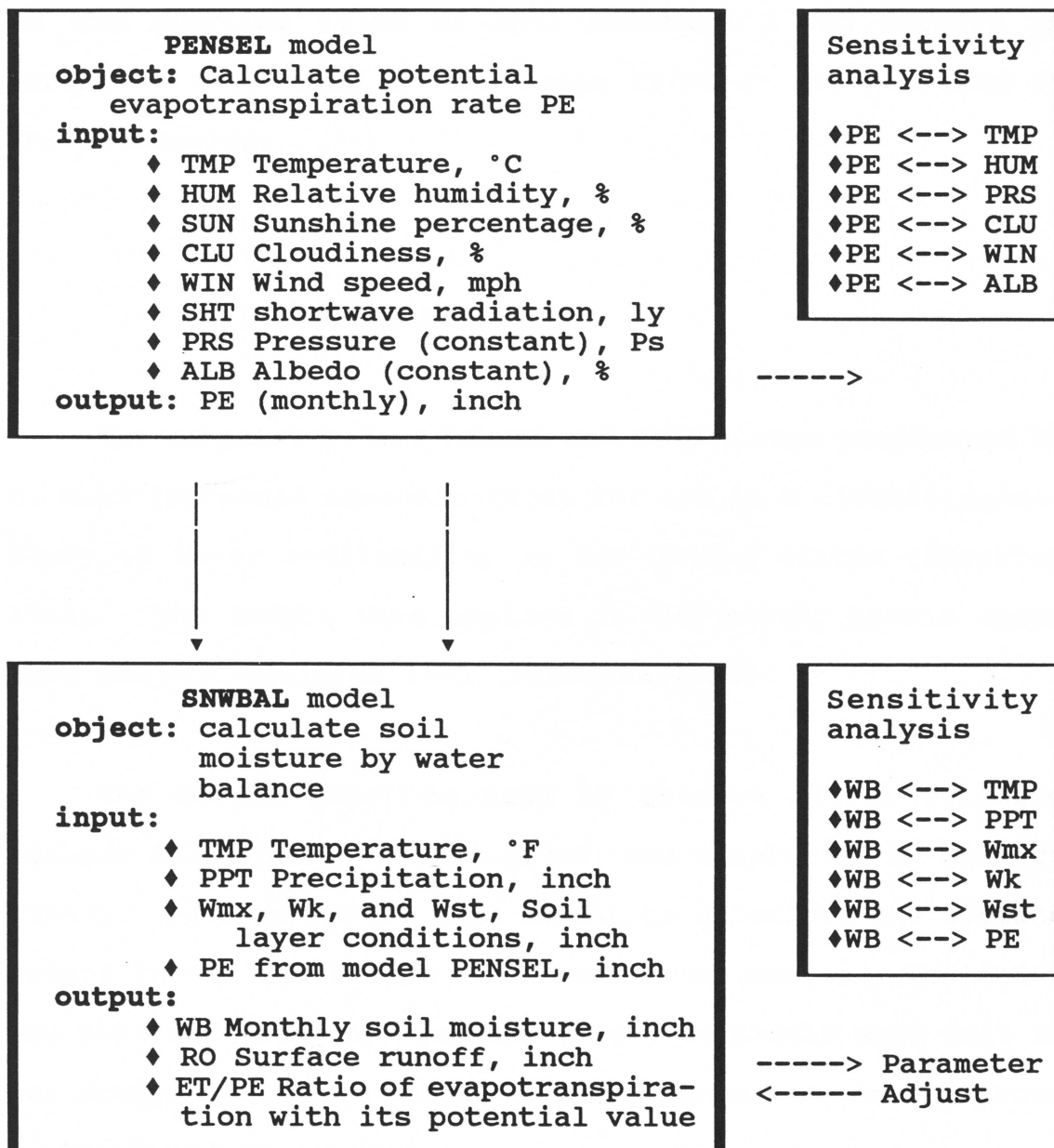
CHAPTER 5.
SOIL MOISTURE SIMULATION AND SEARCH FOR BEST CANDIDATE FOR
CLIMATE RECONSTRUCTION

Because the topographical conditions are different between the northern and southern regions of the Black Hills, climate variables such as precipitation, temperature, relative humidity, wind speed, are not evenly distributed over space.

With the diverse environmental conditions of the Black Hills, it is impossible to develop detailed relations at local levels between tree growth and the climate variables. It is possible, however, to develop a synthetic variable which combines the various climate factors with a single entry, such as potential evapotranspiration (PE). Development of PE is discussed in Appendix I. This synthetic variable can then be input to the climatological water-balance model SNWBAL to calculate local soil moisture availability, \bar{w} . The program PENSEL is used to compute PE. This chapter describe the water-balance model and statistical relationships between tree-ring chronologies and model variables.

A brief flowchat of the variable relations in the PENSEL and SNWBAL models is shown in Table 5.1.

Table 5.1 Process of PENSEL and SNWBAL modeling



In Tab 5.1 WB is the same as \bar{w} in the equations present

later, Wmx is the maximum soil moisture, Wk is the critical

value of soil moisture for unrestricted evaporation and Wst is the starting value of soil moisture. Two outputs in SNWBAL -- the runoff RO and ratio ET/PE -- are not used in the discussion.

§5.1 SNWBAL Model

The computer models PENSEL and SNWBAL were programmed by D. Meko (personal communication) for use in a climatological study of water availability in the United States (Stockton 1984). The models were applied in two master thesis under that project (Quinlan 1982, Flaschka 1984).

The SNWBAL model as used by Quinlan (1982) followed methods described by Budyko (1956) and simplified by Sellers (1965). Quinlan (1982) used SNWBAL to calculate the surface runoff in the Rio Grande and Pecos River Basins. The model was modified later by Flaschka (1984) to handle snow melt in her study of climate variations and surface water resources in the Great Basin Region.

The basic objective of SNWBAL is to convert climatic parameters into estimates of water supply, and to calculate monthly soil moisture. The model uses water balance equation

to calculate the available water content under different climatic and hydrologic conditions during the year. The process is essentially a bookkeeping procedure over monthly time increments. The model takes precipitation as the input component of water in an area. Once precipitation falls on the ground, part of it evaporates; this part is determined as a function of potential evaporation(PE) and water availability. The excess precipitation either forms runoff or is stored in the soil. Ending soil moisture for the month is carried over and taken as the initial value for the next month.

The equation describing the above relationship is taken from Sellers (1965). According to Sellers, to estimate the actual evapotranspiration from climatological data, the water balance in a given region can be described as

$$P = E + S + w_2 - w_1 \quad (5-1)$$

where P --- precipitation during the accounting time interval

E --- evapotranspiration

S --- surplus water

w_1 -- soil moisture in layer at start of month

w_2 -- soil moisture in layer at end of month

This formula assumes that the water for evaporation and transpiration is from the root zone or upper soil layers, and that the surplus water S is the sum of downward percolation and surface runoff.

The value of actual evapotranspiration (E) depends on meteorological factors and the available soil moisture. When soil moisture is above a given critical value w_k , actual evaporation value equals PE ; if moisture falls below that threshold, the rate of evaporation depends on available water within the soil. It is also assumed that the relationship between E and soil moisture is linear. The above relationship can be expressed as

$$E = PE \quad \text{When } \bar{w} \geq w_k \quad (5-2)$$

$$E = (\bar{w}/w_k) PE \quad \text{When } \bar{w} \leq w_k \quad (5-3)$$

where $\bar{w} = (w_1 + w_2)/2 \quad (5-4)$

It is assumed further that the surplus is directly proportional to the precipitation and the soil moisture content, that is,

$$S = b \cdot P \bar{w} / w_{\max} \quad (5-5)$$

where w_{\max} is the maximum possible moisture content and b is

an empirically determined constant of proportionality. Sellers suggested the following formula for calculating b from long-term monthly averages of PE and P ,

$$b = (0.8P)/(PE + P) \quad (5-6)$$

This will give good results in both arid and semi-arid sections of the United States.

Combining equations (5-1) to (5-6), the average monthly soil moisture can be calculated as

$$\bar{w}_{(1)} = \frac{P+2w_1-PE}{2+b\frac{P}{w_{\max}}} \quad (5-7)$$

when $\bar{w} \geq w_k$, and

$$\bar{w}_{(2)} = \frac{P+2w_1}{2+b\frac{P}{w_{\max}} + \frac{PE}{w_k}} \quad (5-8)$$

when $\bar{w} \leq w_k$.

In applying model, w_1 is unknown for the first month. If the accounting period begins in January of the first year,

soil can be assumed to be saturated (i.e. $w_1 = w_{\max}$) at the start of the model. This value is entered into equation (5-7), along with P , PE , w_{\max} and w_k to get $\bar{w}_{(1)}$ for January. The following discussion will show that soil moisture in the starting month has negligible effect on the model results.

If $\bar{w}_{(1)}$ is greater than or equal to w_k , $\bar{w} = \bar{w}_{(1)}$; otherwise $\bar{w} = \bar{w}_{(2)}$. After that, the value of w_2 for the period is obtained from equation (5-4) and is used as w_1 for the following period. The process is repeated and the average soil moisture is obtained from month to month.

There are some restrictions for the soil moisture capacity: if \bar{w} is greater than $(w_1 + w_{\max})/2$, then w_2 is assumed to equal w_{\max} , and \bar{w} is set equal to $(w_1 + w_{\max})/2$. If, on the other hand, \bar{w} is less than $w_1/2$, then w_2 is set to zero and \bar{w} is set to $w_1/2$.

In the early application of the model, it was recognized that the accumulation of snow changes the albedo, and snow melt consumes more energy in the Penman equation (Appendix I), causing \bar{w} to be biased (Quinlan, 1982). Two alternative methods for handling snow are taken into consideration. The first method was suggested by Thornthwaite and Mather: when

actual temperature $T < -1^{\circ}\text{C}$, all precipitation is assumed to fall as snow and is treated as storage to be carried to the next month. When monthly mean temperature increases above -1°C , water in the snowpack is allowed to run off at a pre-determined rate. The second method is to treat snow as ordinary rainfall which runs off in the same month in which it falls. To reduce the error, potential evaporation never drops to zero (Flaschka, 1984).

In this project, the first alternative method described above was used in the model to handle the snowpack problem. Analysis of the mean temperature, maximum temperature and minimum temperature in the study area, shows that the minimum temperatures are constantly below -1°C from December to February of most recorded years. In March the temperature fluctuates around 2°C , and is still less than 10°C during April of most years. May is the first month with temperature above 20°C . Taking into consideration the energy needed to melt the snowpack and after trial and error with the model, the weights were subjectively selected as 25%, 50% and 100% for remaining percentage of snow melted in each succeeding month after monthly mean temperature exceeds -1°C .

Rapid City (station #25) is the only climate station in the Black Hills with long-term climatological data required

for developing the Penman model. The 1916-1979 data for Rapid City were used in the SNWBAL model to calculate the soil moisture \bar{w} . Due to the long modeling period (64 years) downward percolation of water could be ignored, and the surplus water component S in equation 5-1 could be considered the same as monthly surface runoff.

Settings for maximum soil moisture capacity W_{\max} and critical value W_k are somewhat arbitrary because of the lack of field measurements and the likelihood that any particular settings will not be representative of conditions at several tree locations within a site. Thornthwaite and Mather (1955) suggest that the soil moisture capacity is 10 to 16 inches in a closed, mature forest and 6 inches in pastures. In her study of the Great Basin, Flaschka (1984) used a soil moisture capacity of 4.0 inches.

About 14% of the yearly total precipitation for 1940-1990 fell in the winter season and probably was snow released as snowmelt in the spring (Fig 5-1). Therefore, the treatment for snowmelt is probably important in sorting out the tree growth - climate relationship.

Mean Precipitation in the Black Hills period: (1940-1990)

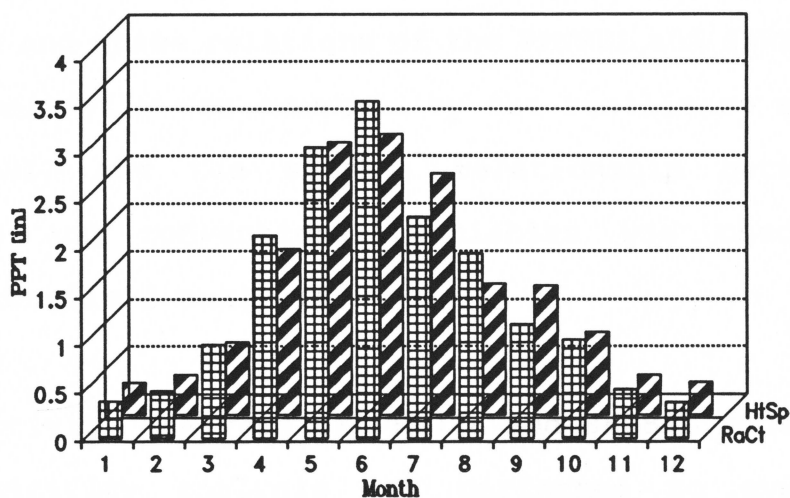


Figure 5-1. Precipitation distribution at Rapid City(RaCt) and Hot Springs(HtSp).

From previous studies mentioned above, a range of 1.5 to 5.0 inches was initially selected for w_{max} . The model was run with different combinations of w_k and w_{max} . The 'best' combination was chosen, based on a sensitivity analysis to be discussed later in this chapter. The sensitivity analysis identified 3.15 inches as an appropriate value for w_{max} and w_k . Because there were no field measurements available to refine the model results, the 'best' choice also came from the model sensitivity analysis.

§5.2 Characteristics analysis of the model

Two methods were used to investigate the sensitivity, stability and space relations of the PENSEL and SNWBAL models. Model sensitivity was examined by the resilience sensitivity index (RSI) and the spatial relationship between model variables and conventional variables was checked using correlation field analysis.

A. Sensitivity analysis of PENSEL and SNWBAL model

Sensitivity analysis was performed to evaluate the effects of parameter estimation on model predictions and indicate where new data can be used to improve the parameter estimation. Sensitivity analysis also plays an important role in surveying the stability of the model output along with input parameter variations (Gardner, 1984).

Two basic methods have been used in sensitivity analysis: the analytical method and numerical (or statistical) approaches. The former is only applied to simple mathematical formulations and the latter requires complete information about the attributes of the model parameters.

Because the PENSEL and SNWBAL models describe complex meteorological and hydrological processes, it is difficult to

use mathematical sensitivity tests. Statistical analysis can provide an efficient way to check the sensitivity of the model, as long as the distribution of the parameters can be delineated.

The SNWBAL model input includes potential evaporation rate (PE), which comes from the Penman equation (PENSEL model) and is a key variable in water balance calculation. The scenarios for testing key parameters are listed in Table 5.1.

Sensitivity of the PENSEL and SNWBAL models was determined by resilience sensitivity index analysis. According to Gardner (1984), the resilience sensitivity of Y with respect to X_j is the percentage change in Y divided by the percentage change in X_j . It is calculated at the point of means of each of the independent variables as

$$S_j = \frac{\partial Y / Y_m}{\partial X_j / X_{jm}} = b_j \frac{X_{jm}}{Y_m} \quad (5-12)$$

Where the m denotes the mean series of that variable.

The values of resilience sensitivity are unbounded and may be positive or negative. Resilience sensitivity values

are unit-free so they are independent of units in which the variables are measured. The resilience sensitivity of PE in model PENSEL and \bar{w} in SNWBAL when checked against with their input variables is listed in Table 5.1 and the results are shown in Table 5.2 and Table 5.3.

The sensitivity of PE in model PENSEL shows that potential evapotranspiration is most sensitive to changes in temperature, then to relative humidity, then to wind speed; and finally to albedo. Table 5.2 lists the variability of PE with each input variable, under the condition that variables other than the one being tested were kept constant.

Table 5.2 Sensitivity Test for Main Input Factors of Model PENSEL

dx	A) PE <--> Windspeed					
	Jan	Feb	Mar	Apr	May	Jun
0.800	-0.253	-0.233	-0.220	-0.220	-0.205	-0.201
0.820	-0.244	-0.225	-0.212	-0.212	-0.198	-0.194
0.850	-0.229	-0.211	-0.199	-0.199	-0.185	-0.182
0.900	-0.195	-0.180	-0.169	-0.170	-0.158	-0.155
1.020	0.098	0.090	0.085	0.085	0.079	0.078
1.050	0.160	0.147	0.139	0.139	0.129	0.127
1.080	0.209	0.192	0.181	0.181	0.169	0.166
1.100	0.238	0.220	0.207	0.207	0.193	0.190

dx	Jul	Aug	Sep	Oct	Nov	Dec
0.800	-0.202	-0.221	-0.233	-0.250	-0.259	-0.275
0.820	-0.195	-0.214	-0.224	-0.242	-0.249	-0.265
0.850	-0.182	-0.200	-0.210	-0.226	-0.234	-0.248
0.900	-0.156	-0.171	-0.179	-0.193	-0.199	-0.212
1.020	0.078	0.086	0.090	0.097	0.100	0.107
1.050	0.127	0.140	0.147	0.158	0.163	0.174
1.080	0.166	0.183	0.192	0.207	0.213	0.227
1.100	0.190	0.209	0.219	0.236	0.244	0.259

B) PE <--> Relative humidity						
dx	Jan	Feb	Mar	Apr	May	Jun
0.800	0.426	0.367	0.295	0.240	0.211	0.210
0.820	0.411	0.355	0.284	0.231	0.204	0.203
0.850	0.385	0.332	0.267	0.217	0.191	0.191
0.900	0.329	0.284	0.228	0.185	0.163	0.163
1.020	-0.165	-0.143	-0.115	-0.093	-0.082	-0.082
1.050	-0.270	-0.233	-0.187	-0.152	-0.134	-0.135
1.080	-0.353	-0.304	-0.244	-0.199	-0.176	-0.176
1.100	-0.403	-0.348	-0.279	-0.227	-0.201	-0.201

B) PE <--> Relative humidity						
dx	Jul	Aug	Sep	Oct	Nov	Dec
0.800	0.163	0.161	0.199	0.258	0.361	0.449
0.820	0.158	0.155	0.193	0.249	0.348	0.434
0.850	0.148	0.146	0.181	0.234	0.327	0.407
0.900	0.127	0.125	0.155	0.200	0.279	0.347
1.020	-0.065	-0.064	-0.078	-0.101	-0.140	-0.175
1.050	-0.105	-0.104	-0.128	-0.165	-0.229	-0.285
1.080	-0.138	-0.136	-0.167	-0.215	-0.299	-0.372
1.100	-0.158	-0.156	-0.191	-0.246	-0.342	-0.426

C) PE <--> Temperature						
dx	Jan	Feb	Mar	Apr	May	Jun
0.800	-0.283	-0.298	-0.318	-0.339	-0.346	-0.354
0.820	-0.274	-0.288	-0.308	-0.327	-0.334	-0.341
0.850	-0.257	-0.270	-0.289	-0.307	-0.313	-0.320
0.900	-0.220	-0.232	-0.248	-0.263	-0.267	-0.274
1.020	0.112	0.118	0.125	0.133	0.134	0.138
1.050	0.183	0.192	0.205	0.216	0.219	0.226
1.080	0.240	0.252	0.268	0.283	0.286	0.295
1.100	0.274	0.288	0.307	0.324	0.327	0.338

dx	Jul	Aug	Sep	Oct	Nov	Dec
0.800	-0.355	-0.355	-0.354	-0.350	-0.331	-0.306
0.820	-0.342	-0.343	-0.342	-0.338	-0.320	-0.296
0.850	-0.321	-0.322	-0.320	-0.318	-0.301	-0.278
0.900	-0.275	-0.275	-0.274	-0.272	-0.258	-0.239
1.020	0.139	0.139	0.138	0.138	0.131	0.122
1.050	0.227	0.227	0.226	0.226	0.215	0.199
1.080	0.298	0.298	0.296	0.295	0.281	0.261
1.100	0.341	0.341	0.339	0.338	0.322	0.298

D)		PE <--> Cloudiness				
dx	Jan	Feb	Mar	Apr	May	Jun
0.800	0.304	0.273	0.223	0.194	0.178	0.190
0.820	0.294	0.264	0.215	0.187	0.172	0.184
0.850	0.275	0.247	0.201	0.175	0.161	0.172
0.900	0.235	0.211	0.172	0.149	0.137	0.147
1.020	-0.118	-0.106	-0.086	-0.075	-0.069	-0.074
1.050	-0.192	-0.172	-0.141	-0.122	-0.112	-0.120
1.080	-0.251	-0.225	-0.184	-0.160	-0.147	-0.157
1.100	-0.287	-0.258	-0.210	-0.183	-0.168	-0.179

D)		PE <--> Cloudiness				
dx	Jul	Aug	Sep	Oct	Nov	Dec
0.800	0.195	0.211	0.221	0.246	0.268	0.319
0.820	0.188	0.203	0.213	0.238	0.259	0.308
0.850	0.176	0.191	0.200	0.223	0.242	0.288
0.900	0.151	0.163	0.171	0.190	0.207	0.246
1.020	-0.076	-0.082	-0.086	-0.095	-0.104	-0.123
1.050	-0.123	-0.133	-0.140	-0.156	-0.169	-0.201
1.080	-0.161	-0.174	-0.182	-0.203	-0.221	-0.263
1.100	-0.184	-0.199	-0.208	-0.232	-0.253	-0.301

E)		PE <--> Pressure				
dx	Jan	Feb	Mar	Apr	May	Jun
0.800	0.329	0.320	0.304	0.274	0.247	0.223
0.820	0.315	0.307	0.291	0.263	0.237	0.214
0.850	0.292	0.284	0.270	0.245	0.221	0.200
0.900	0.244	0.238	0.227	0.206	0.186	0.169
1.020	-0.118	-0.115	-0.110	-0.100	-0.091	-0.083
1.050	-0.190	-0.186	-0.178	-0.163	-0.148	-0.135
1.080	-0.246	-0.240	-0.230	-0.211	-0.192	-0.175
1.100	-0.279	-0.273	-0.262	-0.240	-0.219	-0.200

dx	Jul	Aug	Sep	Oct	Nov	Dec
0.800	0.204	0.208	0.232	0.261	0.297	0.319
0.820	0.196	0.200	0.223	0.251	0.285	0.305
0.850	0.183	0.187	0.208	0.233	0.264	0.283
0.900	0.155	0.158	0.176	0.197	0.222	0.237
1.020	-0.077	-0.078	-0.086	-0.096	-0.107	-0.114
1.050	-0.124	-0.127	-0.140	-0.156	-0.174	-0.185
1.080	-0.162	-0.165	-0.182	-0.202	-0.226	-0.239
1.100	-0.184	-0.188	-0.207	-0.230	-0.256	-0.272

dx	F) PE <--> Albedo					
	Jan	Feb	Mar	Apr	May	Jun
0.800	0.182	0.178	0.167	0.158	0.159	0.162
0.820	0.176	0.172	0.161	0.153	0.153	0.156
0.850	0.165	0.161	0.151	0.143	0.144	0.147
0.900	0.140	0.138	0.129	0.122	0.123	0.125
1.020	-0.071	-0.069	-0.065	-0.061	-0.062	-0.063
1.050	-0.115	-0.113	-0.106	-0.100	-0.100	-0.102
1.080	-0.150	-0.147	-0.138	-0.131	-0.131	-0.134
1.100	-0.172	-0.168	-0.158	-0.149	-0.150	-0.153

dx	F) PE <--> Albedo					
	Jul	Aug	Sep	Oct	Nov	Dec
0.800	0.162	0.158	0.158	0.159	0.165	0.178
0.820	0.156	0.153	0.152	0.153	0.159	0.172
0.850	0.146	0.143	0.143	0.144	0.149	0.161
0.900	0.125	0.122	0.122	0.123	0.127	0.137
1.020	-0.063	-0.061	-0.061	-0.062	-0.064	-0.068
1.050	-0.102	-0.100	-0.100	-0.100	-0.104	-0.112
1.080	-0.133	-0.131	-0.130	-0.131	-0.136	-0.147
1.100	-0.152	-0.149	-0.149	-0.150	-0.156	-0.167

Table 5.3 Sensitivity Test of SNWBAL Model

dx	A) Wmax <--> WB, Wmax(0) = 3.00					
	Jan	Feb	Mar	Apr	May	Jun
-0.5	-0.088	-0.090	-0.127	-0.273	-0.320	-0.261
-0.1	-0.051	-0.042	-0.045	-0.084	-0.114	-0.115
0.10	0.038	0.026	0.038	0.051	0.081	0.087
0.50	0.024	0.023	0.030	0.045	0.063	0.067

dx	Jul	Aug	Sep	Oct	Nov	Dec
-0.5	-0.218	-0.109	-0.081	-0.085	-0.089	-0.093
-0.1	-0.091	-0.042	-0.026	-0.034	-0.048	-0.032
0.10	0.075	0.036	0.033	0.030	0.030	0.036
0.50	0.052	0.023	0.019	0.023	0.023	0.028

B)		Wk <--> WB, Wk(0) = 2.25				
dx	Jan	Feb	Mar	Apr	May	Jun
-0.56	1.116	1.131	0.815	0.824	0.906	0.898
-0.20	1.180	1.270	0.811	0.758	0.879	0.890
-0.12	1.194	1.295	0.796	0.743	0.873	0.887
1.00	1.216	1.381	0.822	0.585	0.711	0.789

dx	Jul	Aug	Sep	Oct	Nov	Dec
-0.56	0.939	0.953	0.925	0.940	0.972	1.108
-0.20	0.946	0.990	0.888	0.917	0.958	1.113
-0.12	0.953	0.996	0.884	0.919	0.963	1.097
1.00	0.912	1.137	0.955	0.889	0.898	1.091

C)		Wstart <--> WB, Wstart(0) = 1.81				
dx	Jan	Feb	Mar	Apr	May	Jun
1.00	0.070	0.057	0.015	0.002	0.000	0.000
0.17	0.062	0.041	0.010	0.002	-0.001	0.000
-0.18	0.062	0.043	0.011	0.001	0.000	0.000
-0.50	0.061	0.042	0.011	0.001	0.000	0.000

dx	Jul	Aug	Sep	Oct	Nov	Dec
1.00	0.000	0.000	0.000	0.000	0.000	0.000
0.17	0.000	0.000	0.000	0.000	0.000	0.000
-0.18	0.000	0.000	0.000	0.000	0.000	0.000
-0.50	0.000	0.000	0.000	0.000	0.000	0.000

D)		PE <--> WB, PE(0) = 1.0 (assumed)				
dx	Jan	Feb	Mar	Apr	May	Jun
-0.50	2.275	2.589	0.501	1.032	1.249	1.364
-0.20	1.465	1.618	0.974	0.781	0.936	0.981
0.20	0.563	0.581	0.399	0.394	0.437	0.436
1.00	0.978	1.044	0.659	0.593	0.692	0.697

dx	Jul	Aug	Sep	Oct	Nov	Dec
-0.50	1.617	2.114	1.773	1.637	1.655	2.025
-0.20	1.090	1.278	1.093	1.074	1.110	1.340
0.20	0.462	0.473	0.454	0.466	0.482	0.552
1.00	0.760	0.811	0.725	0.751	0.779	0.907

The results also show that all of the input variables listed in Table 5.1 of PENSEL model have a significant influence on calculation of PE. For example, a 10% increase in wind speed will induce about 19-25% increase in PE for different months of the year. Also, a 10% increase in relative humidity will cause the PE to decrease more than 30% in winter and 15-20% in the summer. Considering all input variables, temperature has the greatest effect on PE: a 10% increase in temperature during May, will cause PE to increase 34.6%.

The scope of sensitivity in the PENSEL model varies from month to month. For most variables, except temperature, the sensitivity of PE is higher in winter than in summer. However, all effects are significant. PE is therefore a good representation or 'synthesis' of all the input variables.

There

Table 5.2 also indicates that variables such as wind speed, relative humidity, and temperature have greater weight in calculating PE than cloudiness, surface pressure and albedo.

Similar sensitivity tests were run for the SNWBAL model, with the input variables w_{max} , w_k , w_{st} , PE, being oscillated around their individual 'mean' value as discussed by Flaschka (1984). Table 5.3 lists the results of the sensitivity test for \bar{w} with changes of w_{max} . Main results are as follows:

a) The starting value of soil moisture in the model does not have any significant effect on \bar{w} . Because of the long period covered by the model (64 years), soil moisture content is largely determined by the succeeding climatic and hydrologic conditions rather than the initial conditions;

b) The variation of w_k proportionally affects \bar{w} . In other words, reducing w_k results in less time for PE to reach the potential rate PE_0 , causing greater evapotranspiration and resulting in reduced soil moisture \bar{w} . Therefore, choosing the appropriate w_k values is very important for the SNWBAL model.

c) Like w_k , PE also causes large changes in \bar{w} , but this depends on the season of the year. In winter, the ground is covered by snow, vegetation is dormant, and soil moisture is higher than in summer when evapotranspiration is active. Therefore, the small changes in PE will cause high oscillations of \bar{w} .

d) \bar{w} is very sensitive to the changes in w_{\max} , especially when the value of w_{\max} is reduced. A 35% increase of w_{\max} may cause 80-90% increase of \bar{w} . A 18% w_{\max} decrease will cause almost twice the decrease in soil moisture \bar{w} .

The model shows that taking measures which decrease surface evaporation will augment the water supply for vegetation. From the sensitivity analysis, the SNWBAL model

appears relatively insensitive to changes in w_{\max} , and more sensitive to potential evaporation. The starting month soil moisture, which sets the initial conditions, does not affect the model.

Summarily, \bar{w} , which reflects the availability of soil moisture in a given month, also reflects the combinations of climatic and environmental conditions, and can be used as a synthesis factor to study the relationship between climate-environmental variations and tree growth.

B. Correlation field analysis

Correlation field analysis investigates the simple correlation coefficients of related or potentially related variables over space with the target variable at a check point. Using the correlation contour map, it is possible to recognize and identify the internal or external relationship between space variables and target variables. To check the site relationship with other climate factors for model SNWBAL, the simulated monthly mean soil moisture, \bar{w} at Rapid City, determined from the model, is entered into the correlation field analysis with monthly precipitation and temperature data from other stations in the Black Hills area. The most consistent relationship is in the spring-summer period. Fig

5-2 and Fig 5-3 show the correlation field of \bar{w} with July precipitation and temperature for the period of April through July. Correlations are generally low for precipitation, higher for temperature. The difference reflects the greater spatial inhomogeneity of precipitation than temperature. It is found that there are two high precipitation correlations in the west-central part of the Black Hills. Low correlations are on the far north side, near the North Dakota/South Dakota boundary, and on the eastern side of the area.

April to July temperature for all climate stations is strongly negatively correlated with \bar{w} in Rapid City. The correlation pattern is similar to precipitation. These phenomena indicate that the early spring and late summer storms have relatively common characteristics affecting the whole Black Hills area. Temperature, as a continuous field, has a more stable pattern than precipitation over a large area, and thus has a stronger relation to \bar{w} at the target site. Accordingly, soil moisture calculated for Rapid City can be used as synthetic data for environmental conditions -- especially for available water content combined with temperature conditions -- for the Black Hills area.

As discussed in Chapter 3, the tree-ring chronologies have a significant positive response to precipitation and a

Corr. Field of WB vs. PPT(Jul)

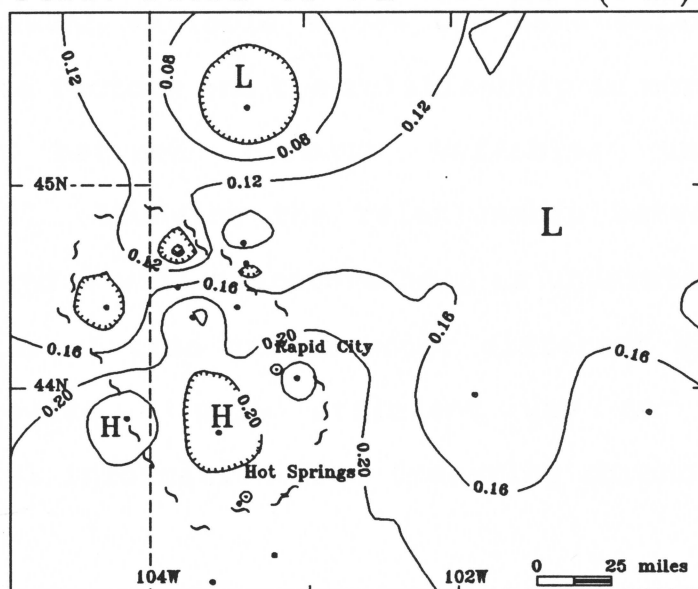


Figure 5-2. Correlation field of soil moisture \bar{w} (Apr-Jul) at Rapid City with precipitation at various stations.

Corr. Field of WB vs. TMP(4-7)

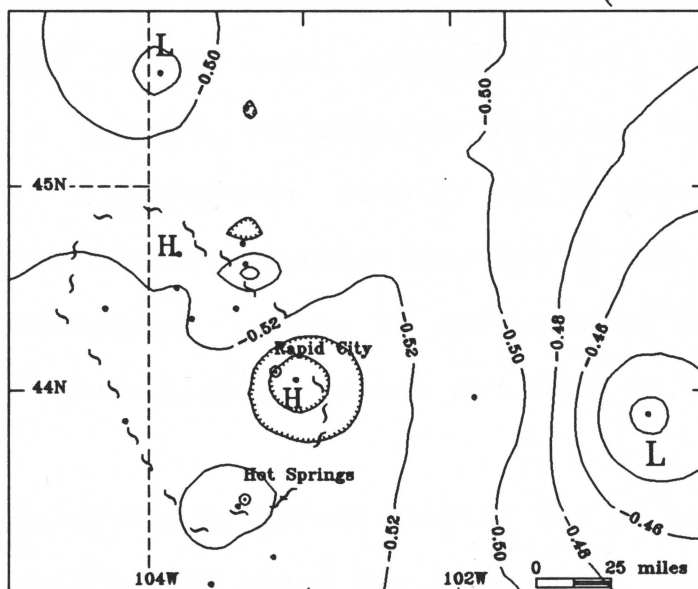


Figure 5-3. Correlation field of soil moisture \bar{w} (Apr-Jul) at Rapid City with temperature at various stations.

negative response to temperature during April-July. The simulated SNWBAL variable \bar{w} has the same relationship with these climate factors and the relationship is more significant than that between climate variables and tree-ring chronologies. Studying the relationship between tree-ring chronology and \bar{w} will therefore help us understand more about the mechanism of tree growth under different situations and further provide a more efficient way to extract past environmental information from tree-ring chronologies.

§5.3 Running correlation analysis of \bar{w} against tree rings

To investigate the response of tree-growth to climate variables, the SNWBAL model simulated soil moisture \bar{w} is applied in a running correlation analysis with tree-ring chronologies. Fig 5-4(a-d) display the R_T curve of 5, 13 and 23 year window running correlations for \bar{w} and GCE, GCP, REN and ROC chronologies. These R_T curves show that the 23-yr window can produce high R_T values for most of the sites.

The 5-yr window R_T curves display low or negative values near 1928, and the mid 1940s for pine sites REN and GCP, and in the early 1970s for REN. These dips in R_T may be

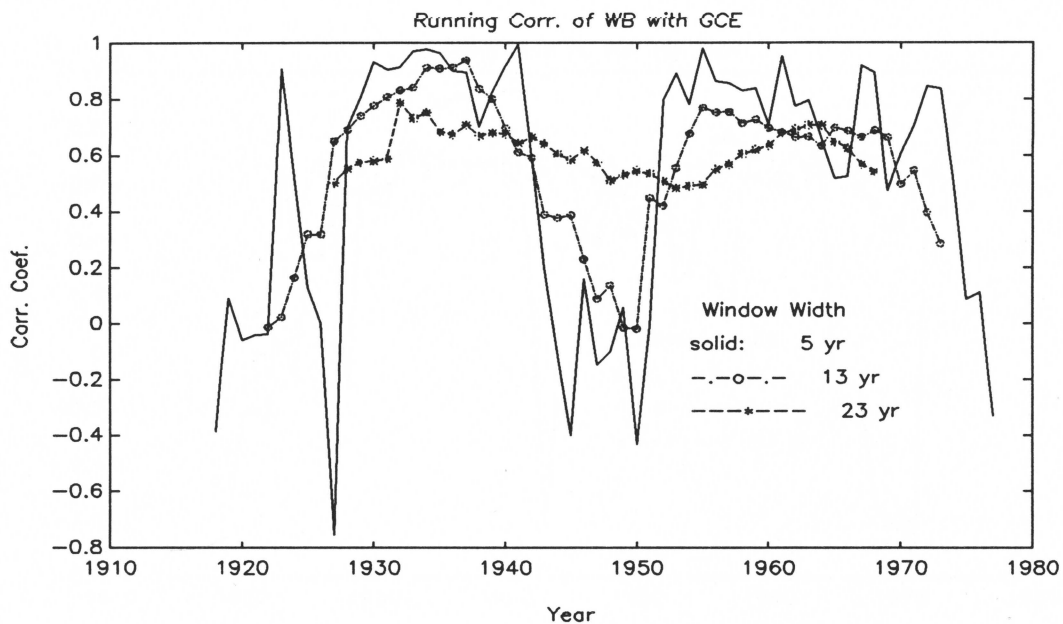


Figure 5-4a. R_T plot of \bar{w} and oak chronology

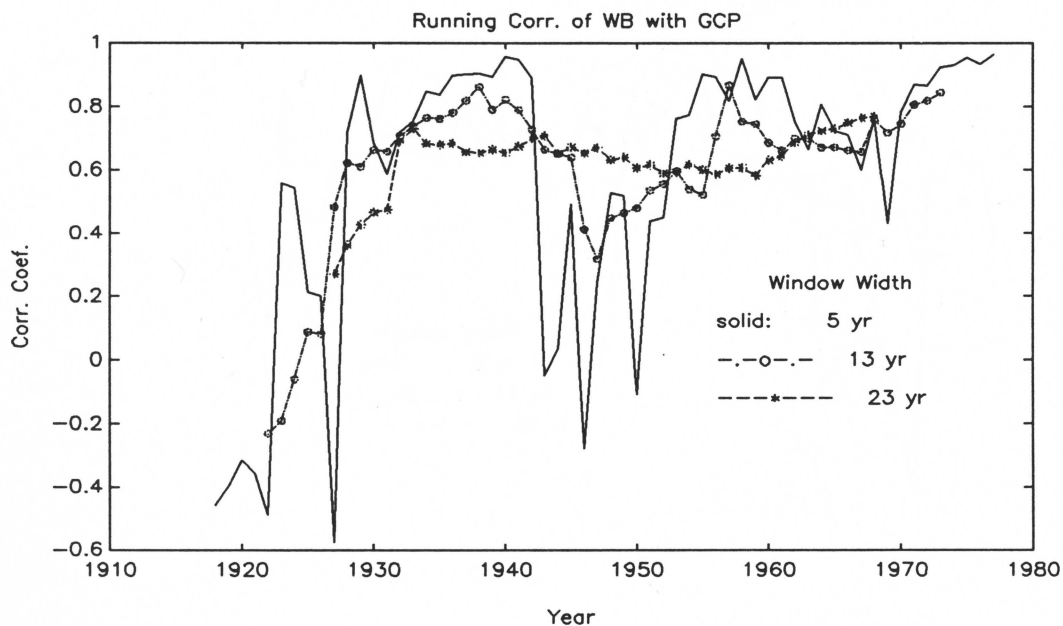


Figure 5-4b. R_T plot of \bar{w} and pine chronology

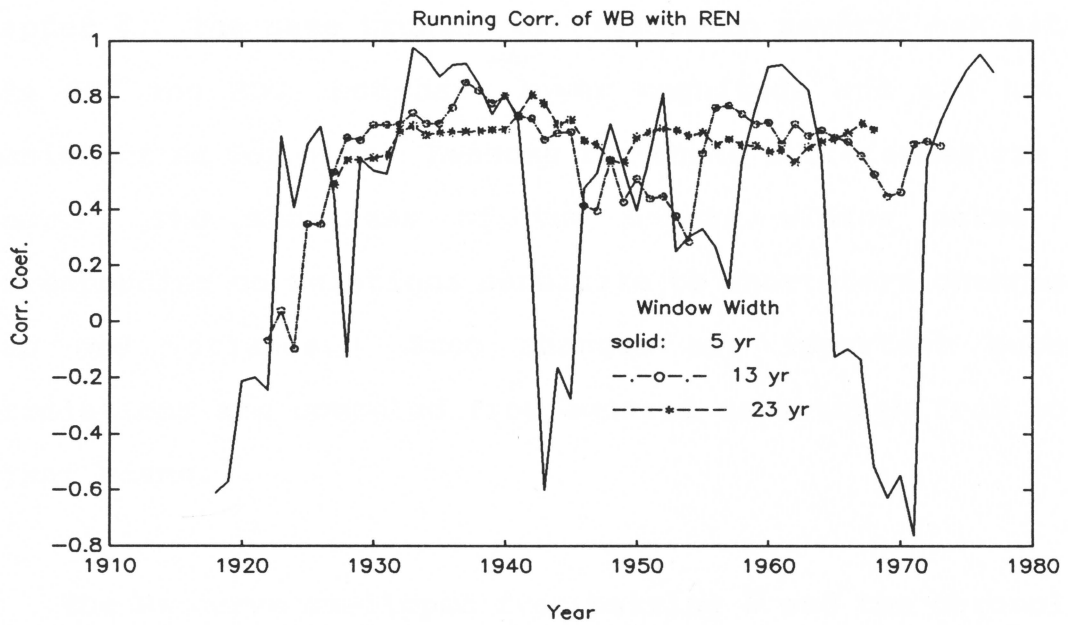


Figure 5-4c. Rr plot of \bar{w} with pine chronology.

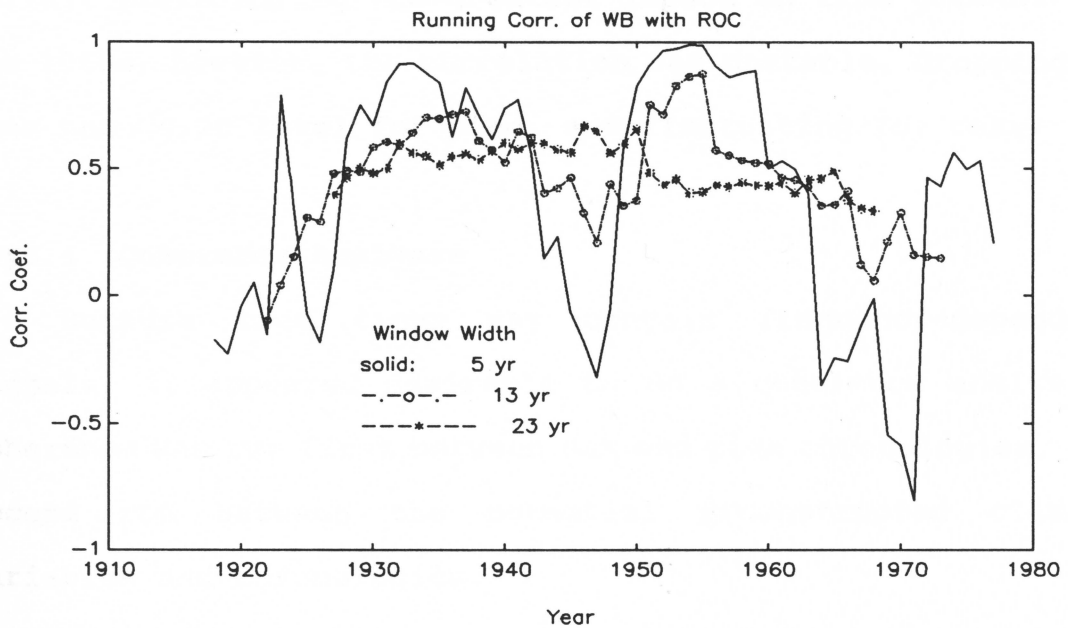


Figure 5-4d. Rr plot of \bar{w} with oak chronology.

associated with insect attacks on the trees, as discussed in Chapter 4. The same troughs of R_T show in several oak sites, like GCE and ROC, but have lower magnitude and are not as consistent as for pine. Reasons for these differences are not clear. The shortness of the 5-year window makes the corresponding correlations sensitive to short-term changes in mean and variance. Such changes are important because correlations are computed from squared departures from local 5-year means.

The R_T curve developed from pairing \bar{w} and the chronology data show good relationship between tree-growth and soil moisture during 1930s, 1950s, and 1970s; with large water deficit years having the greatest impact on tree growth. In the 1960s, however, the correlation was unstable, dropping to less than 0.20 level for pine, and fluctuating for oak.

§5.4 Coherence analysis

Because tree rings may contain frequency-dependent signals, it appeared desirable to do a coherence analysis. Coherence was run first between oak and pine chronologies, and second run between the potential reconstructed climate variables and chronologies.

Spectra and cross-spectra were estimated by smoothing the

periodogram or cross-periodogram with low-pass filters (Bloomfield, 1976). The FIR (Finite Impulse Response) low-pass filters were designed by using matlab function `filtfilt`, which filters data in both forward and reversed directions (Oppenheim, 1975). The frequency response curve for the different filters are plotted in Fig 5-5. In order to examine the long period variations, a year low-pass filter was selected for the analysis.

The null hypothesis of zero squared coherence was tested by the method described by Bloomfield (1976). By letting $s_{x,y}(\omega)^2$ be the sample squared coherence and $\tau_{x,y}(\omega)$ be the theoretical coherency, then the probability of a given level p is given by:

$$\sigma(p)^2 = 1 - (1-p)g^2/(1-g^2)$$

The quantity g^2 in the equation simply equals the sum of the squares of the filter weights. In this analysis, for an 11-weight polygon filter (Tab 5.4), the 95% and 99.99% confidence limits for squared coherency are

$$\sigma(0.95) = \sqrt{1 - (1-0.95)^{0.333/(1-0.333)}} = 0.23$$

$$\sigma(0.9999) = \sqrt{1 - (1 - 0.9999)^{0.3333 / (1 - 0.3333)}} = 0.90$$

The coherence spectrum between oak(CGE) and pine(GCP) at the same site (Fig 5-6) indicates that there is a common low-frequency signal in these two species. A common low-frequency signal also shows in plots for chronologies REN-GCE, and BHM-BLR.

The coherence spectra between the climate variables (seasonal precipitation, seasonal mean temperature) and chronologies are significantly different from zero($p=0.05$) at wavelengths near 2.0, 5.0 and 22.0 years for most of the pairs(Fig 5-7 , Table 5.4). Climate reconstructed from tree-ring chronologies should therefore reflect the mid-range(5.0 - 50 years) frequency variations.

Table 5.4 **Low-pass Filter Weights**

Type	95%	99%	Filter Weights
F4	0.1510	0.2224	.02, .03, .10, .15, .4,
F6	0.0864	0.1297	.08, .123, .1561, .2816, ...

Note: because of the symmetry of the weights, only half are listed.

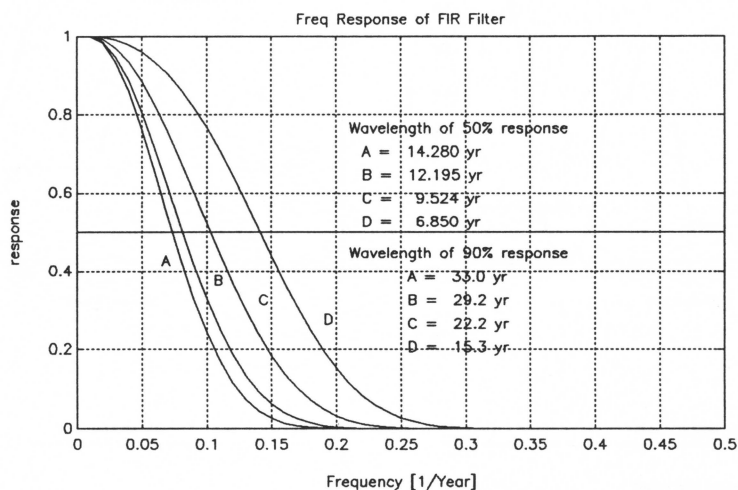


Figure 5-5. Frequency response of designed filters.

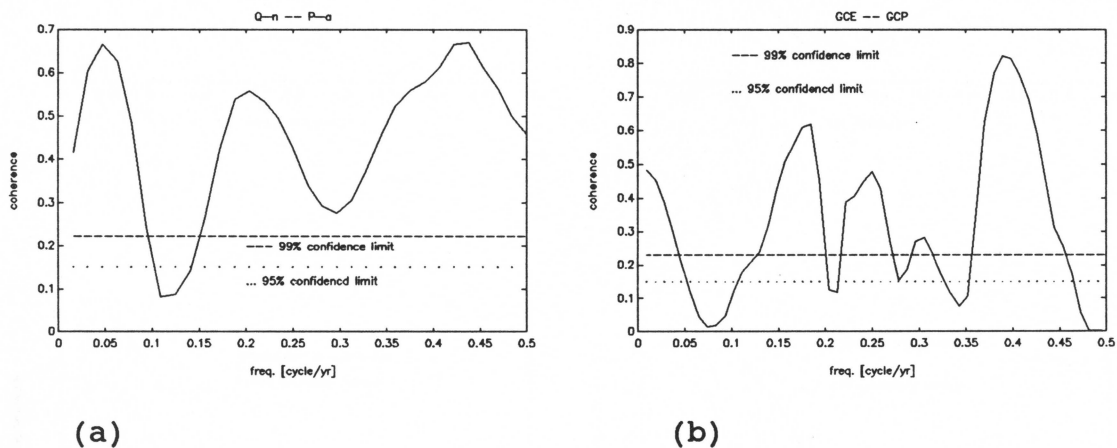
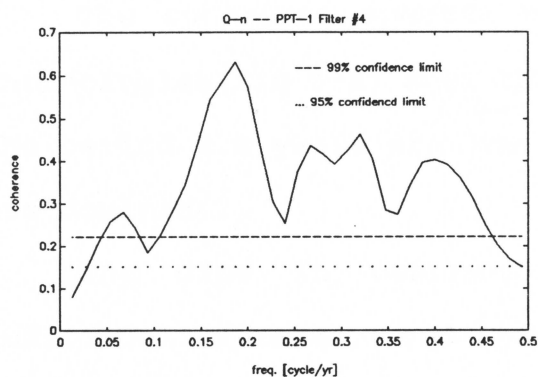
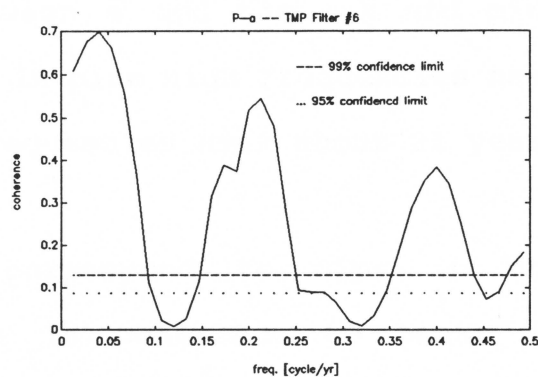


Figure 5-6. Coherence analysis of oak-pine on the basis of factor scores (a); site chronologies (b).

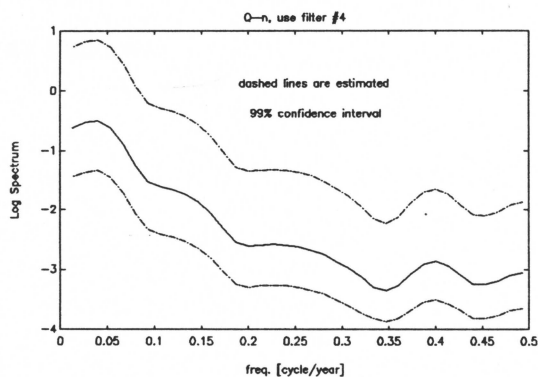
(3)
Fig
[(1)]
are used



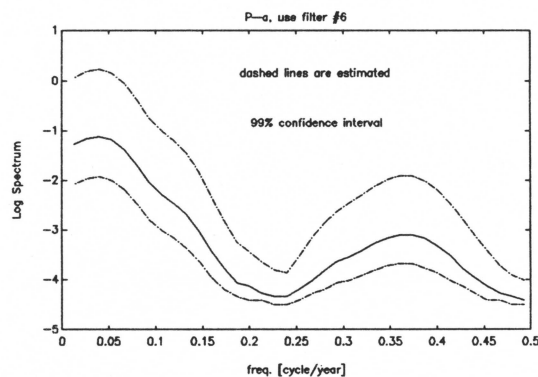
(1)



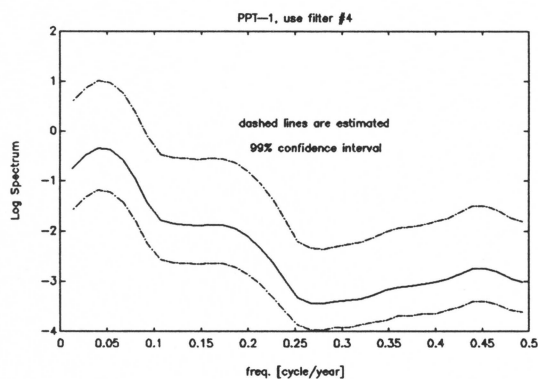
(4)



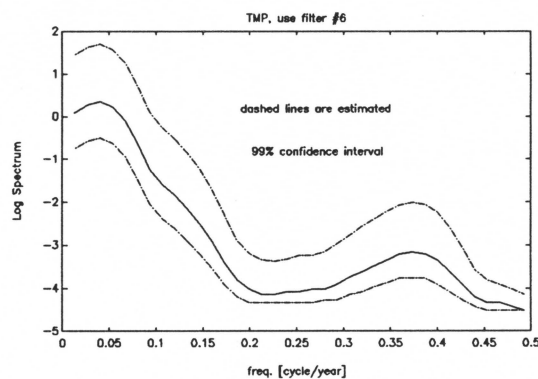
(2)



(5)



(3)

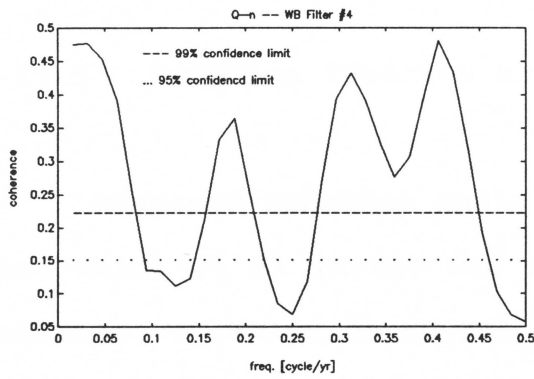


(6)

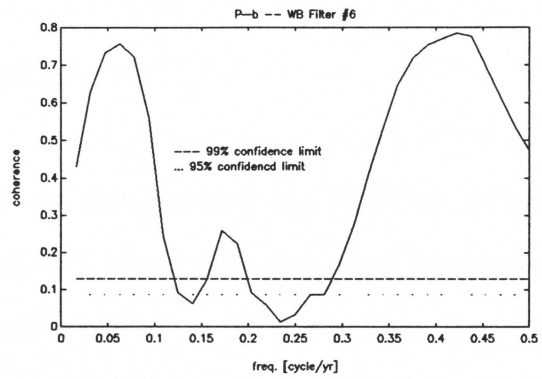
Fig 5-7. Coherence and spectrum of pair oak(n)-PPT_1 [(1),(2),(3)]; pair pine(a)-TMP [(4),(5),(6)]. The filters are described in Tab 5.4.

The coherence spectra between \bar{w} and the oak and pine chronologies (Fig 5-8) show that in pine high frequencies near the period 2.8 years and low frequencies near about 21 years are dominant.

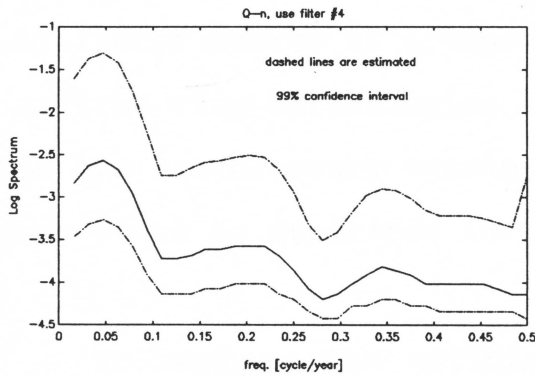
The dips in coherence correspond to dips in the individual spectra, and peaks in coherence to peaks in spectra. This result is reasonable in that the tree-growth response is stronger at frequencies where the climate is more variable.



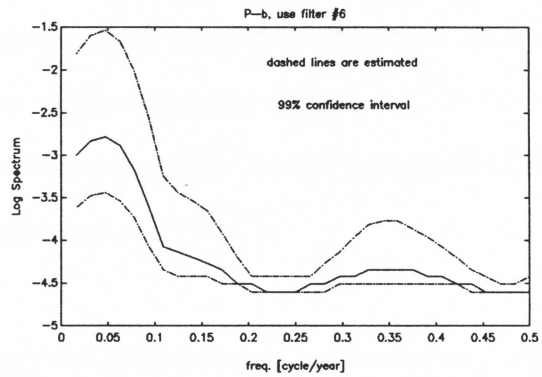
(1)



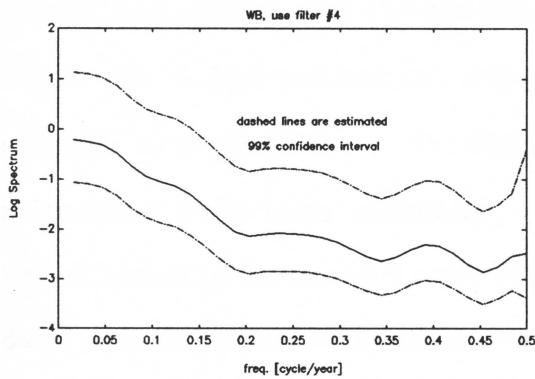
(4)



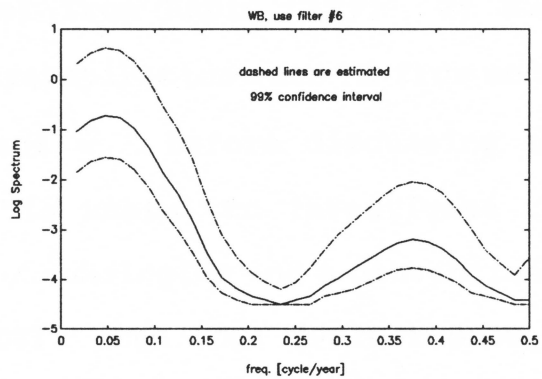
(2)



(5)



(3)



(6)

Figure 5-8. Coherence and spectrum of pair oak(n)- \bar{w} [(1), (2), (3)]; pair pine(b)- \bar{w} [(4), (5), (6)]. The filters are described in Tab 5.4.

§5.5 Response function analysis

Response function analysis as described by Fritts (1976) and Guiot et al (1982) was used to analyze the influence of climate variables on annual tree growth. The matlab program RESPO1 written by D. Meko was used in the calculation. The predictand for the regression equation was chosen as:

- 1) factor scores of grouped tree-ring chronologies.
- 2) tree-ring chronologies from each sample site.

For the factor-score version, chronologies were grouped into four sites as described in Chapter 4.

To compare the efficiency of variable selection, the predictor pairs were chosen as: 1) climate observations (precipitation and temperature) from Rapid City; 2) soil moisture \bar{w} and potential evapotranspiration rate PE from model PENSEL and SNWBAL; 3) PDSI and \bar{w} . Before discussing the response function results, it is useful to investigate the relationship between tree-ring chronologies and a conventional derived drought variable -- PDSI. The PDSI (Palmer Drought Severity Index, Palmer, 1965) has been widely used by climatologists to describe drought severity using a simplified water balance. Palmer originally designed his drought

computations for monthly average data, using the principle of a balance between moisture supply and demand (Karl, 1983). The classification of PDSI is divided from -6 to +6 to denote the soil moisture range from very severe drought(-6) to very wet(+6).

Table 5.5 lists the correlation of Apr-Jul PDSI from five climate stations with tree-ring chronologies. The chronologies for UPC and CRY have low and insignificant correlation coefficients with PDSI, except the pair for CRY with Hot Springs. Oak chronologies generally have correlation coefficients of 0.3 to 0.4, except for CRY which has an insignificant correlation.

Table 5.6 compares the correlation coefficients of two tree-ring chronologies (pine and oak) with different climate variables. PDSI shows lower correlation with tree growth than other variables.

Although PDSI correlates well with most tree-ring chronologies, there are still some problems in its use as the sole index. One is that snow cover is not included in the model. Another is that no lag is incorporated in runoff calculation. PDSI uses the Thornthwaite water balance, and assumes that runoff does not occur until the water capacity of the soil is satisfied in a monthly total. This is an unrealistic approximation because surface runoff will take

place just after the ponding process while the underlying soil may be still far from saturated (Hawkins,1975). Another shortcoming is that PDSI uses the Thornthwaite method for estimating PE. PE is considered to be solely a function of temperature. In reality, wind speed, relative humidity, and other factors bear on PE.

Table 5.5 Correlation Coefficients of Tree-ring Chronologies with Seasonal PDSI (April -- July)

site spe.	A	B	C	D	E
BHM pine	0.236	0.308	0.404	0.258	0.401
GCP pine	0.242	0.275	0.412	0.221	0.345
REN pine	0.311	0.288	0.479	0.301	0.417
UPC pine	0.032	0.079	0.144	0.193	0.199
PLG pine	0.183	0.138	0.309	0.190	0.303
PPK pine	0.316	0.297	0.398	0.313	0.429
THO oak	0.327	0.257	0.284	0.258	0.226
FRW oak	0.403	0.431	0.545	0.401	0.504
FDF oak	0.335	0.414	0.444	0.297	0.396
HNK oak	0.336	0.370	0.387	0.282	0.355
BLR oak	0.275	0.275	0.258	0.244	0.302
CRY oak	0.268	0.132	0.197	0.087	0.162
CSP oak	0.338	0.338	0.287	0.239	0.362
GCE oak	0.466	0.395	0.429	0.349	0.390
ROC oak	0.382	0.423	0.381	0.283	0.298

Note: the station ID represent,

A--- Hot Spring

B--- Rapid City

C--- Murdo

D--- Pierre FAA

E--- Cottonwood

Table 5.6 Correlation Coefficients of Two Chronologies with Climate Parameters

ID	\bar{w}	PPT	TEMP	PDSI
GCE (oak)	0.53	0.42	-0.42	0.40
REN (pine)	0.59	0.59	-0.34	0.29

The periods used for response functions analysis were Jan-Sep, and Apr-Jul, respectively. The response results for various combinations of predictands and predictors are listed in Table 5.7 and Table 5.8. Three typical response functions are plotted in Fig 5-9, 5-10 and 5-11.

The results show that:

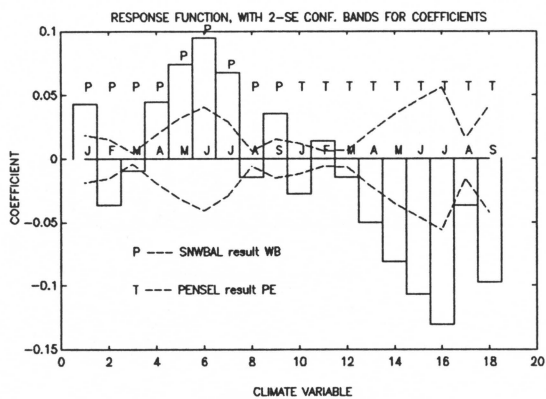
A. When \bar{w} and PE are used as the predictors in the multiple regression model (ID_Type # is P_b-C), instead of precipitation and temperature (ID_Type # is P_b-A), the former (\bar{w} and PE) has less variables enter but has a higher explained variance (0.6389 than 0.5277, also shown in Figure 5-9a_b). A similar improvement was found for oak in the southern region (Q_s). Here the variables \bar{w} and PE increased the explained variance from 0.4704 to 0.5304 as compared to variables PPT and TMP. (Table 5.7, ID_Type # Q_s-A and ID_Type # Q_s-C).

B. When PDSI and \bar{w} are the predictors, the response

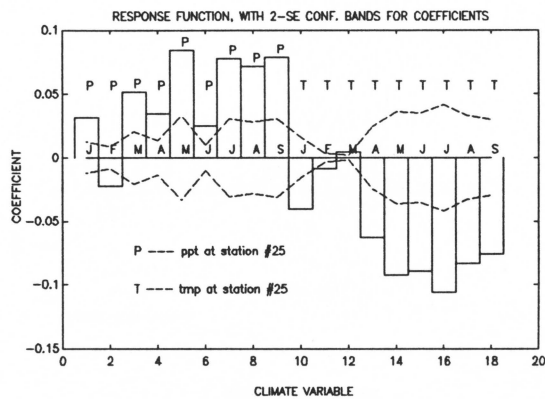
function shows that \bar{w} acts like precipitation while PDSI acts like temperature. Figure 5-10a_b shows GCE and Figure 5-11a_b shows REN response to \bar{w} and PDSI, respectively. It is shown that this pine chronology is more sensitive to soil moisture (\bar{w}) variations. Table 5.8 shows that pine chronologies GCP, REN, PPK and oak chronologies FRW, GCE possess stronger climate signals than other chronologies.

C. When precipitation and temperature are the predictors, the explained variances are close to those for scenarios A and B, but more variables enter the regression models (Figure 5-9c_d, 5-10c_d and 5-11c_d).

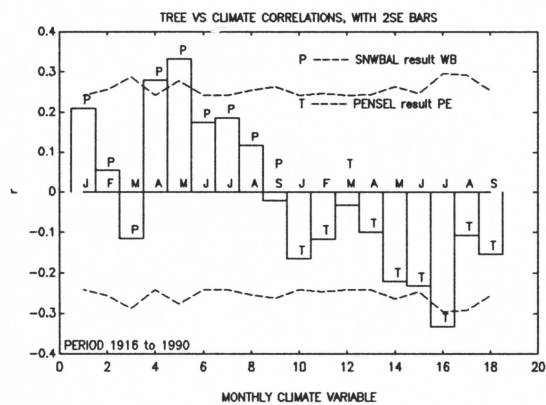
The advantage of using \bar{w} and PE as proxy data for local climate conditions, was discussed earlier. According to the principles of plant physiology, tree growth depends on a number of factors. The conventional variables for response analysis are temperature and precipitation. In traditional analysis, factors such as wind speed, previous soil moisture, and hours of sunshine, which interact with each other and with other climatic factors to form a complex cause-and-effect chain that affects tree growth, are rarely considered. Synthetic factors like model-output soil moisture may possess a more direct connection with tree growth and represent the



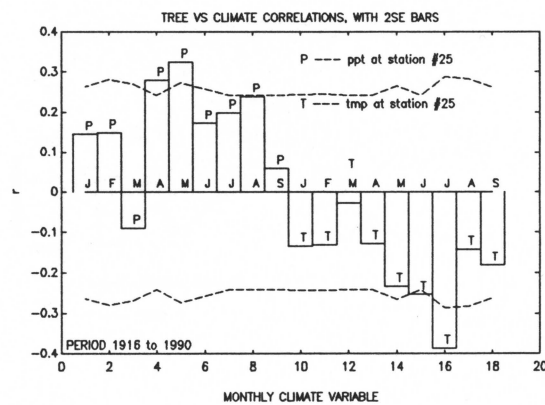
(a)



(c)

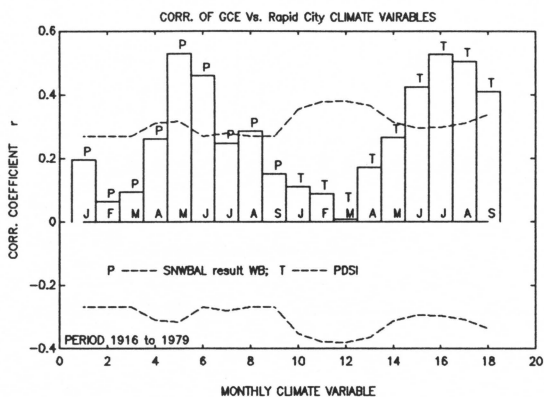


(b)

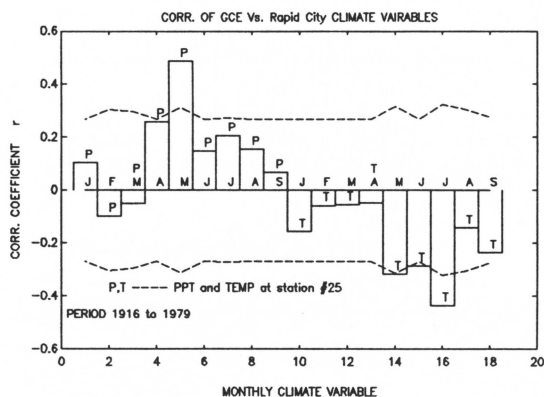


(d)

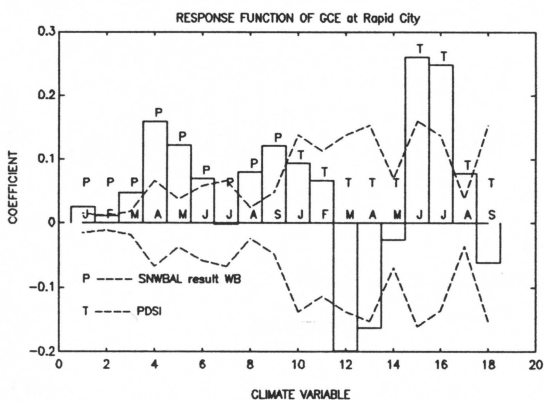
Figure 5-9. Response functions for different variable combinations. WB is same as \bar{w} . The chronology is P_a. The chronology factor score from pine group_a (see Table 4.4). a) and b) corresponds to Table 5.7, type C, c) and d) corresponds to Table 5.7, type A.



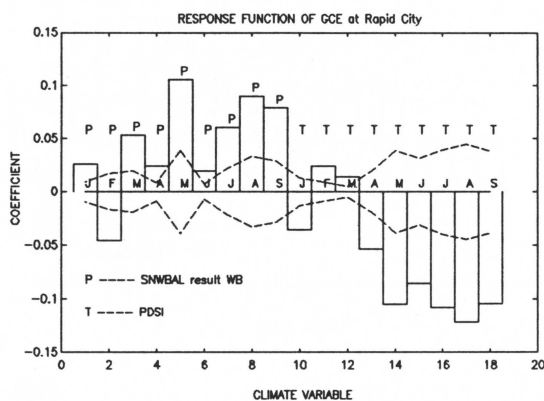
(a)



(c)

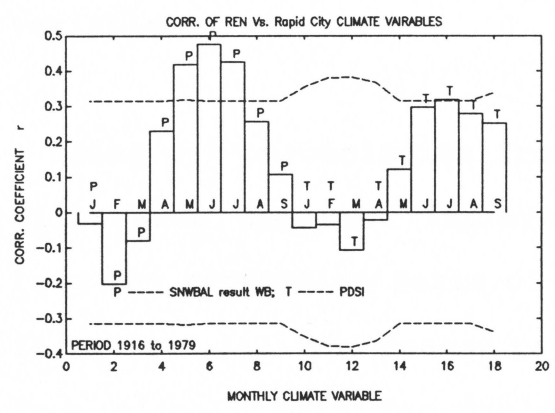


(b)

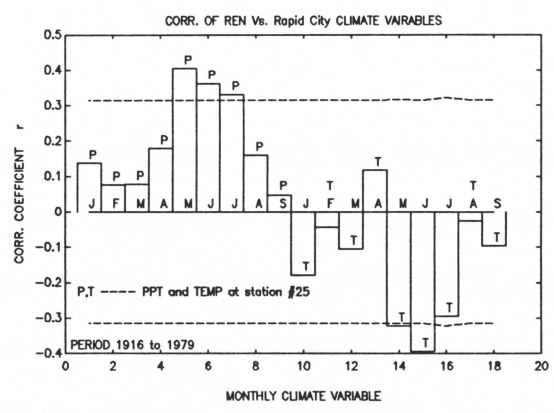


(d)

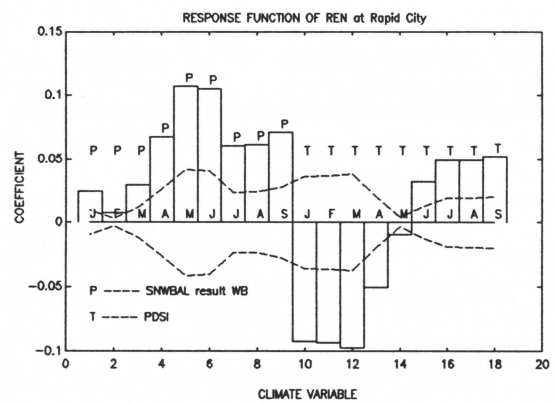
Figure 5-10. Response functions for different variable combinations. Tree-ring site is GCE (oak), and WB is the same as \bar{w} . The dash lines denote the 2-SE bars.



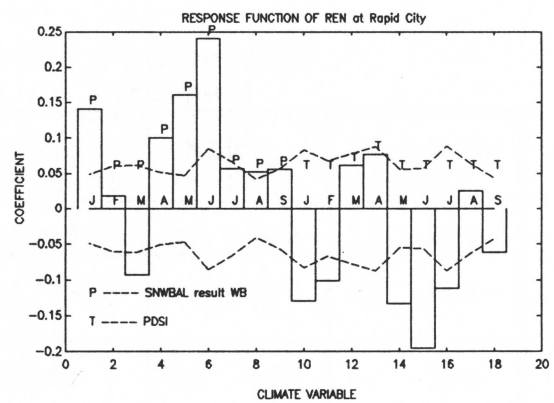
(a)



(c)



(b)



(d)

Figure 5-11. Response functions for different variable combinations. Tree-ring site is REN (pine), WB is same as \bar{w} . The dash lines denote the 2-SE bars.

comprehensive functions better than the conventional variables.

Using oak chronologies from the northern part of the Black Hills area does not improve the response functions much. (see the regression pairs of Q_n-A and Q_n-C, Q_n-B and Q_n-D in Table 5.7). The reason may be that \bar{w} and PE were developed from climate data for Rapid City, which is located in the southern part of the Black Hills.

Table 5.7 Comparison of Variable Selection in Response Function (grouped)

ID**	T*	Significant Variables	Expld ¹ Variance	MLR ² #--PC ³	Expld by #--PC ³
Q _n	A	4p, 5p, 6t, 7t;	0.4078	9; .389	1; .200
Q _s	A	4p, 5p, 7p, 8p, 5t, 7t;	0.4704	6; .430	2; .309
P _a	A	(3-5)p; (7-9)p; (4-9)t;	0.5261	9; .501	4; .386
P _b	A	(3-4) ⁴ p, 8p, 7t;	0.5277	8; .512	5; .435
Q _n	B	4p, 5p, 6t, 7t;	0.2690	4; .267	1; .235
Q _s	B	4p, 5p, 7p, 5t, 7t;	0.3854	4; .363	2; .369
P _a	B	(5-7)p, 7t;	0.3670	7; .365	1; .249
P _b	B	(4-7)p, 5t, 7t;	0.4244	6; .423	1; .332
Q _n	C	(4-6)p, 8p, 7t;	0.3751	5; .289	1; .155
Q _s	C	5p, 6p, 8p, (5-7)t	0.5304	8; .508	2; .303

ID**	T*	Significant Variables	Expld ¹ Variance	MLR ² #--PC ³	Expld by #--PC ³
P_a	C	(5-7)p; (4-7)t; 9t	0.4615	7; .415	2; .225
P_b	C	(3-4)p, 7t;	0.6389	9; .613	7; .588
Q_n	D	(4-6)p, 7t;	0.2353	2; .219	1; .190
Q_s	D	5p, 6p, 6t, 7t;	0.3663	1; .301	1; .190
P_a	D	5p, 6p, 7t;	0.3546	5; .354	4; .484
P_b	D	(4-7)p, 7t;	0.5134	/ ⁵	/

ID** ---- ID for grouped chronologies, same as in Table 4.4.

T* ---- Variable combinations:

A: p-- ppt #25, t-- tmp #25, Jan-Sep input;

B: same as A, Apr-Jul input;

C: p-- \bar{w} , t-- PE, from SNWBAL, Jan-Sep input;

D: same as C, Apr-Jul input;

1 ---- explained

2 ---- multiple linear regression

3 ---- number of eigenvectors and explained variance;

4 ---- (4-7)p means 4p, 5p, 6p, and 7p;

5 ---- regression not available in response function;

Table 5.7 also shows that choosing a "season" of Apr-Jul is reasonable for the data analysis. Increasing the number of predictors (months) generally increases the explained variance, but generally only for pine response models. In the Black Hills, pine chronologies are more sensitive in response than oak to climatic variations.

Table 5.8 shows that using the combination of PDSI and \bar{w} as the predictors, and the individual site chronology as the predictand, the number of significant variables and explained variance varies among different site locations.

Table 5.8 Comparison of Variable Selection in Response Function (separated)

ID	Significant Variables	MLR #--PC	Expld by #--PC
GCP	(5-7)p, (7-8)t	4, 0.3500	0.4239
REN	(5-7)p, 7t	6, 0.4028	0.4470
UPC	/	4, 0.1929	/
PLG	(6-8)p	6, 0.3449	0.4137
PPK	(4-7)p, (7-9)t	8, 0.5037	0.5685
THO	8p, 7t, 8t	5, 0.2773	/
FRW	4p, 6p, 8p, (5-9)t	4, 0.4298	0.5059
FDF	5p, (5-8)t	3, 0.2862	0.4088
HNK	5p, 6p, (5-8)t	4, 0.3535	0.4183
BLR	5p, 6p, 7t, 8t	4, 0.2123	/
CRY	8p	4, 0.2162	/
CSP	5p, 6p, (6-8)t	3, 0.2377	/
GCE	5p, 6p, 8p, (6-9)t	8, 0.5606	0.5992
ROC	5p, 6p, (5-9)t	5, 0.3205	0.3772

Note:

p ----- SNWBAL \bar{w} ;

t ----- PDSI;

the others are same as Table 5.7.

The quality of the tree-ring chronology at an individual site can be evaluated by the explained variance and the number of significant variables in the regression model. Generally, the higher the quality, the higher the variance explained by principal components (PC). Fig 5-12 illustrates this relationship. The explained variance usually increases as the number of significant variables increases. FRW, HNK and GCP are good sites to develop a climate signal because high variance is concentrated on few variables. GCE, PPK and REN also contain a strong climate signal but more variables are needed to describe it. UPC and THO need to be improved to enhance the climatic signals. PLG and BHM are marginal in quality.

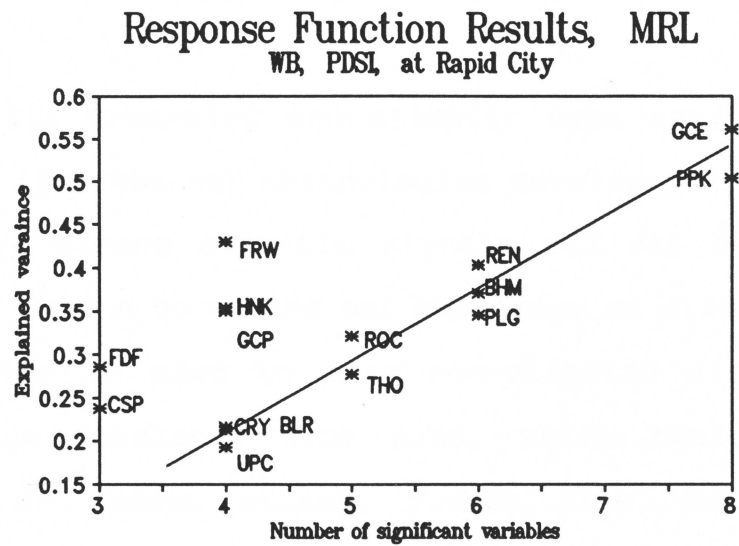


Fig 5-12. Relationship number of significant variables to explained variance in response function analysis.

§5.6 Conclusions and suggestions

From the tree-ring and climatic data analysis, it has been shown that the oak chronologies developed from the Black Hills carry strong climatic signals and can be used as a dependable source to extend our knowledge on climate changes. Oak can also be used to flag non-climatic distortions in chronologies developed from pine, which could have been subjected to insect attack, forest fire, or some other influences. The main problem with using oak in climate-related research in the Black Hills is the need for older living trees or older stumps or remnants, so that chronologies can be extended farther into the past.

Pine samples collected from the Black Hills area in this study display a good connection with climate records and oak chronologies. Longer series like REN could provide long-term information on the history of drought in the Black Hills area. Additional samples from older trees would greatly benefit future studies, especially at sites CRY, CSP, THO and UPC.

The potential evaporation rate PE and soil moisture \bar{w} , calculated from PENSEL and SNWBAL models, reflects local

climatic and environmental conditions. In future studies, the reconstructed long term \bar{w} for each tree-ring site or for larger area, such as the northern or southern Black Hills, may provide more direct and detailed information about drought history.

To reconstruct past climate and keep as close as possible to reality, the following suggestions are made:

i) Understand the outlier years and their possible distortions of reconstructions. Some unusual years, like 1915, 1932, and 1985, need to be identified before using them in calibration or reconstruction models. Methods used in this study will provide efficient ways to identify these anomalies, especially when used on overlapping periods for different species.

ii) Calculate \bar{w} and PE for more climate stations to provide clearer spatial patterns and help in reconstructing past climate conditions and soil moisture. The dilemma is the lack of adequate climate records to run the PENSEL model. Collecting more data, finding some way to simplify the PENSEL model, or use of alternative methods to calculate PE, may make it possible to develop \bar{w} for more stations.

iii) Use the tree-ring chronologies developed from the Black Hills in combination with chronologies from a wider area, such

as the northern Great Plains, to provide a better understanding of broad climatic regimes.

APPENDIX

I. Penman Formula Calculation

H.L. Penman (1956) proposed an empirical method for estimating the potential evaporation from weather observations data. By his definition, the potential evaporation is 'the amount of water transpired in a given time over a short green crop, completely shading the ground, of uniform height never short of water. In Penman's equation, the potential evaporation can be expressed as,

$$PE * LE_o = \frac{R_n * \gamma + \Delta * LE_a}{\Delta + \gamma} \quad (1)$$

- where, PE -- potential evaporation [mm·min⁻¹]
 R_n -- net radiation [cal·cm⁻²·min⁻¹]
 Δ -- slope of saturation vapor pressure-
 temperature curve at T_a [mm·K⁻¹];
 γ -- psychrometric constant [mm·K⁻¹];
 LE_o -- latent heat of water evaporation,
 E_o = 590 [cal·g⁻¹]
 LE_a -- wind evaporation parameter
 [cal·cm⁻²·min⁻¹]
 E_a -- drying power of air [mm·day⁻¹]

where in equation(1), Δ and γ are obtained by

$$\Delta = \frac{0.622 * E_o}{R_d} * e_{sair} * \frac{1}{T^2} \quad (2)$$

where, R_d -- gas constant of dry air,

$$R_d = 0.068592 \text{ [g} \cdot \text{cc}^{-1}]$$

e_{sair} -- saturated vapor pressure of air at air
temperature T

T -- temperature [$^{\circ}$ K]

The Psychometric constant, γ , is computed from

$$\gamma = \frac{C_p * P}{0.622 * e_o} \quad (3)$$

where, C_p -- Specific heat, at constant pressure,

$$C_p = 0.24 \text{ [cal} \cdot \text{g}^{-1} \cdot \text{K}^{-1}]$$

P -- Atmospheric (or air) pressure;
if not available for actual
value, use values for standard
atmosphere [760 mm]

In equation (2), the saturated vapor pressure of air can be derived from the well-known Clausius-Clapeyron equation for a

given temperature T [$^{\circ}$ K]:

$$e_{sair} = e_0 * EXP \left[\frac{M_v * LE_0}{R^*} \left(\frac{1}{273.15} - \frac{1}{T} \right) \right] \quad (4)$$

where, e_0 -- saturated vapor pressure at T=273 $^{\circ}$ K,
from Clausius-Clapeyron equation.

At the intersection of evaporation and
sublimation, $e_s = 6.11$ mb, the relation
is 1013.25 mb = 760 mm. Therefore,
 $e_0 = 4.582876883$ mm;

M_v -- molecular weight of water,
18.016 [g \cdot mol $^{-1}$]

R^* -- universal gas constant,
(1.98624 [cal \cdot mol $^{-1}\cdot$ $^{\circ}$ K $^{-1}$])

In equation (3), the actual vapor pressure of air can be
obtained by:

$$e_{air} = e_{sair} * \frac{Rh}{100} \quad (5)$$

where, Rh -- relative humidity, in percentage.

From the calculated results of e_{sair} and e_{air} , wind evaporation

parameter LE_a can be determined by:

$$LE_a = \frac{0.622D_w * \rho}{P} LE_o (E_{sair} - e_{air}) \quad (6)$$

where D_w -- vapor transfer coefficient, it is derived from equation (7).

ρ -- density of atmosphere
(0.001205 g/cm³)

It is assumed that D_w is almost linearly related to the wind speed u [Sellers, 1965, p159], that is,

$$D_w = a + bu \quad (7)$$

where a is 0.45 for a standard Class A pan, b is 0.2 for 'all types of water surface', D_w is in [cm·sec⁻¹] and u is in [m·sec⁻¹] at a height of 2m above the ground. To obtain the proper units for LE_a , D_w needs to be converted into [cm·min⁻¹] before applying (6).

The net radiation can be calculated as short wave radiation and long wave radiation. Taking incoming radiation as

positive and outgoing radiation as negative, it is

$$R_n = R_{short}(1 - \alpha) - R_{long} \quad (8)$$

where R_{short} -- incoming short wave radiation;
 α -- albedo, assume to be 0.18;
 R_{long} -- net outgoing long wave radiation;

When measurements are not available, R_{short} can be estimated by the following equation (Tanner 1960):

$$R_{short} = R_A(a + bF) \quad (9)$$

where R_A is the extra-terrestrial radiation defined as solar radiation flux density that would arrive at a horizontal surface if attenuating atmosphere is not present. For a given latitude the value R_A can be checked out from Brunt (1932) or Smithsonian Meteorologic Tables (List, 1958). In our study site, a and b take the values of 0.25 and 0.54, respectively. In equation (9), F is the possible percentage of duration of sunshine expressed on a fractional basis. When measurement of F is not available but the daily cloud cover have been measured, then F can be substantially acquired by,

$F = (1 - C)$, where C is the cloud cover in percentage.

For outgoing long wave radiation R_{long} , there is also an empirical equation:

$$R_{long} = \sigma T^4 (0.56 - 0.09 \sqrt{e_{air}}) (0.10 + 0.90F) \quad (10)$$

where $\sigma = 0.8128 * 10^{-10}$ [$ly \cdot ^\circ K^{-4} \cdot min^{-1}$], Stefan-Boltzman constant.

Summary

To calculate Penman potential evaporation, the input data of temperature, relative humidity, wind speed, and cloudiness are needed. For the formula described above, if the constant and coefficients are in the consistent units shown, the input data will be in units of $^\circ K$, percentage, m/sec, and percentage respectively. The results for PE will be [in/min] and can be easily transferred into [in/mon] or other units.

II. Tree-ring Sample Site Name List

No	ID	Site	Name
01	CRW	Crowley	
02	CSP	Custer State Park	
03	SNY	Dean Snyder	
04	MFH	Middle Fork H Creek,	WY
05	HNK	Hankins	
06	ORD	Ordahl	
07	ORC	Oak Ridge Cent.	
08	HRV	Jerome Harvey	
09	WIL	Wils. Jim & Don.	
10	PPK	Parker Park Lookout	
11	PLG	Pilger Mount	
12	FDF	Frawley D. Farm	
13	FRW	Frawley	
16	CRY	Crystal Cave	
17	GCE	Grace Creek E	
18	THO	Wes Thompson Ranch	
25	ROC	Rockverville	
26	BHM	Buckhorn Mount	
27	BLR	Geoge Blair	
28	VET	Veteran's Point	
29	REN	Reno Gulch	
30	HTL	Horse Thief Lake	
31	BTD	Big Tree Draw	
38	UPC	Upper Pine Creek	NA

Note: The number is identical with the Great Plains collection.

Except MFH, all sites are in South Dakota.

LIST OF REFERENCES

- Baumgartner, T.R., J. Michaelsen, L.G. Thompson, G.T. Shen, A. Soutar & R.E. Casey 1989 : The recording of interannual climate change by high-resolution natural systems: tree-rings, coral bands, glacial ice-layers and marine varves. In "Aspects of Climate Variability in the Pacific and Western Americas". (ed by D.H. Peterson), Geographic Monograph 55, pp 1-14.
- Biondi, F. & T.W. Swetnam, 1987 : Box-Jenkins models of forest interior tree-ring chronologies. Tree-ring Bulletin, Vol 47, pp 71-96.
- Blasing T.J., D.N. Duvick & D.C. West, 1981 : Dendroclimatic Calibration and Verification Using Regional Averaged and Single Station Precipitation Data. Tree-ring Bulletin, Vol 41, pp 37-43.
- Bloomfield, P., 1976 : Fourier Analysis of Time Series: An Introduction. New York, Wiley, pp 258.
- Borchert, J.R., 1971 : The Dust Bowl in 1970s. Annals of the Association of American Geographers. Vol 61 No.1 pp 1-22.
- Box, G.E. & G.M. Jenkins, 1976 : Time Series Analysis, Forecasting and Control. Holden-day, San Francisco.
- BMDP, 1990: Factor Analysis. BMDP Statistical Software Manual, University of California Press, Vol 1, pp 311-37.
- Brunt, D., 1932 : Notes on Radiation in the Atmosphere. Quart. J. Roy. Meteorol. Soc. Vol 58, pp 389-420.
- Budyko, M.I., 1956 : The Heat Balance of the Earth's Surface. Leningrad.
- Cook, E.R., 1982 : A long-term drought sequence for the Hudson Valley, New York. Climate From Tree Rings, edited by Hughes et al. pp 163-64.
- Cook, E.R. 1985 : A Time Series Analysis Approach to Tree-rings Standardization. Ph.D. Thesis, Univ. of Arizona, Tucson.
- Cook, E.R., 1990 : A Comparison of Some Tree-ring Standardization Methods. In "Methods of Dendrochronology: Applications in Environmental Science". (ed. E.R. Cook,

- L.A. Kairiukstis) Int. Inst. for applied system analysis. Kluwer Academic Publishers, Boston MA pp 153-62.
- Currie, R.G. 1981 : Evidence for 18.6-year Mn Signal in Temperature and Drought Conditions in North American since A.D. 1800. *Journal of Geophysical Research* 86 (C11), pp 11055-64.
- Currie, R.G. 1989 : Comments on 'Power spectra and coherence of drought in the interior plains by E.O. Oladipo', *Journal of Climatology*, 9, 91-100.
- Douglass, A.E. 1914 : A method of estimating rainfall by the growth of trees. In "The Climate Factor" (ed by E. Huntington), Carnegie Inst. Wash Publ. 192, pp 101-22.
- Eckstein D. and E. Frisse, 1982 : The influence of temperature and precipitation on vessel area and ring width of oak and beech. *Climate From Tree Rings*, edited by Hughes et al.
- Flaschka, I.M., 1984: Climate Change and Water Supply In the Great Basin. Master thesis, University of Arizona.
- Fritts, H.C., 1976 : Tree rings and climate. Academic Press, London.
- Fritts, H.C., and T.W. Swetnam, 1989 : Dendroecology: a tool for evaluating variations in the past and present forest environments. Advances in Ecological Research 19, pp 111-89.
- Fritts, H.C., 1991: Reconstructing Large-scale Climatic Patterns from Tree-Ring Data, A Diagnostic Analysis. University of Arizona Press.
- Gardner, R.H., 1984 : A unified approach to sensitivity and uncertainty analysis. In "Applied simulation and modeling. Proce. of the IASTED". (ed. by M. H. Hamza). Int. Symp., June 4-6, San Francisco, CA. p. 155-57.
- Graumlich, L.J., 1987: Precipitation Variation in Pacific Northwest(1675-1975) as Reconstructed from Tree Rings. Annals of the Association of American Geographers. 77(1), pp 19-29.
- Graybill D.A. 1982: Chronology Development and Analysis. Climate From Tree rings. Cambridge University Press, pp 21-30.

- Guiot, J., A.L. Berger, A.V. Munaut et al, 1982 : Response functions. In "Climate From Tree Rings" (ed. by M.K. Hughes et al). Cambridge University Press. pp 38-50.
- Hawkins R.H., 1975 : The importance of Accurate curve numbers in the estimation of storm runoff. Water Resources Bulletin Vol.11, No5. pp 887-91.
- Holmes, R.L., R.K. Adams, and H.C. Fritts, 1986 : Tree-ring chronologies of Western North America: California, Eastern Oregon and Northern Great Basin with procedures used in the Chronology development work including users manuals for computer programs COFECHA and ARSTAN. Laboratory of Tree-Ring Research, Tucson, Arizona.
- Hughes, M.K., P.M. Kelly, J.R. Pilcher and V.C. LaMarche Jr. 1982 : Climate From Tree Rings. Cambridge University Press.
- Karl T.R., 1983 : Some Spatial Characteristics of Drought Duration In the United States. J. Climate and Appl. Meteorolo. 22: 1356-66.
- Karl T.R., C.N. Williams Jr., F.T. Quinlan and T.A. Boden, 1990 : United States Historical Climatology Network (HCN) Serial Temperature and Precipitation Data: QRNL/CDIAC-30, NDP-019/R1, Carbon Dioxide Information Analysis Center, Oak Ridge National Lab., Oak Ridge, TN, 377p.
- Kramer, P.J. and T.T. Kozlowski, 1979 : Physiology of Woody Plants. Academic Press, New York. pp 189-199.
- Lawson, M.P., R. Heim Jr. and J.A. Mangimeli, 1978 : Dendroclimatic Analysis of Bur Oak in Eastern Nebraska.
- Lawson, M.P., and M.E. Baker, 1981 : The Great Plains Perspectives and Prospects. Center for Great Plains Studies, Univ. of Nebraska-Lincoln. pp 11-34.
- List, R.J., (ed) 1958 : Smithsonian Meteorological Tables. Smithsonian Institution, Washington.
- Meko, D.M., 1981 : Applications of Box-Jenkins Methods of Time Series Analysis to the Reconstruction of Drought from Tree Rings. Ph. D Dissertation, University of Arizona.
- Meko, D.M., 1992 : Dendroclimatic evidence from the Great Plains of the United States. In "Climate Since A.D.

- 1500" (ed. by R.S. Bradley and P.D. Jones), Routledge London.
- Miller, J.R. Jr., 1986 : Rapid City Climate. South Dakota School of Mines and Technology Foundation.
- Mitchell, J.M., C.W. Stockton, and D.M. Meko, 1979 : Evidence of a 22-year rhythm of drought in the Western United States related to the hale solar cycle since the 17th century. In: Solar-terrestrial influences in climate. B.M. McCormac and T.A. Seliga (eds). Reidel Publ. Co. Holland. pp 125-43.
- Oladipo, E.O., 1987 : Power Spectra and Coherence of Drought in the Interior Plains. Journal of Climatology. Vol 7, pp 477-91.
- Oppenheim, A.V., 1975 : Digital Signal Processing. Bell Telephone Laboratories, Inc. pp 237-69.
- Penman H.L., 1956 : Estimating Evaporation. Trans. Am. Geophys. Union vol 37, pp 43-50.
- Palmer, W.C., 1965 : Meteorological Drought. U.S. Weather Bur. Res. Pap. 45, U.S. Government Printing Office, Washington, D.C.
- Perry, C.A., 1980 : Preliminary Analysis of Regional Precipitation Periodicity. USGS Water Resources Investi. 80-74. Lawrence, Kansas.
- Progulske, D.R. and Shideler, F.J, 1974 : Following Custer. Bulletin 647. Agricultural experiment station, south Dakota State University, Brookings.
- Quinlan, P.T. 1982 : Climatic Change and Water Availability in the Rio Grand and Pecos River Basin. Master thesis, University of Arizona.
- Richman, M.B., 1986 : Review Article, Rotation of Principal Components. J. of Climatology, Vol. 6, 293-335(1986).
- Schulman, E. 1951 : Tree-ring indices of rainfall, temperature and river flow. In "Compendium Meteorology", American Meteorology Soc, Boston. pp 1024-29.
- Schulman, E. 1956 : Dendroclimatic changes in semiarid America, University of Arizona Press, Tucson, AZ, USA.

- Schweingruber, F.H., 1988 : Tree Rings : basics and applications of dendrochronology. Reidel Publishing Company, pp 276.
- Sellers William D. 1965, Physical Climatology. The University of Chicago Press, Chicago & London. pp 156-180.
- Stockton, C.W., and D.M. Meko, 1983 : Drought recurrence in the Great Plains as reconstructed from long-term tree-ring records. J. Cli. App. Meteo. 22(1), pp 17-29.
- Stockton, C.W. 1984 : Projected effects of climatic variation upon water availability in western United States. Final Reports, Grant No. ATM 79-24356.
- Stokes, M.A., and T.L. Smiley 1968 : An introduction to tree-ring dating. Univ. of Chicago Press, Chicago.
- Tanner, C.B. & W.L. Pelton, 1960 : Potential Evapotranspiration Estimates by the Approximate Energy Balance Method of Penman. J. Geophys. Res. Vol 65, pp3410.
- Thomas, H.E. 1962 : The Meteorological Phenomenon of Drought in the Southwest. USGS Prof. Paper 872-A.
- Thorntwaite, C.W. & J.R. Mather, 1955 : The Water Balance. Drexel Inst. of Tech. Publications in Climatology, 8(1).
- Will G. F. 1946 : Tree Ring Studies in North Dakota. Agricultural Experimental Station, North Dakota Agricultural College, Bulletin 338 Fargo, ND. pp 2-24.
- Willeke G.E., N.B. Guttman and W.O. Thomas, 1991 : A National Drought Atlas for the United States of America. USGS Open-File Report 91-244, pp 45-50.